



UNIVERSITA' POLITECNICA DELLE MARCHE
FACOLTA' DI INGEGNERIA

Corso di Laurea magistrale in Ingegneria Edile

**MODELLAZIONE DI ORDINE RIDOTTO DI UNA STRUTTURA DI PROVA PER
INVOLUCRO EDILIZIO**

REDUCED ORDER MODELLING OF A BUILDING ENVELOPE TEST STRUCTURE

Relatore: Chiar.mo

Prof. **Giretti Alberto**

Tesi di Laurea di:

Valentina Malorni

Correlatori : Chiar.mi

Prof. **Carbonari Alessandro**

Dr. **Hajdukiewicz Magdalena**

A.A. 2021 /2022

TABLE OF CONTENTS

ABSTRACT.....	5
SOMMARIO.....	6
ACKNOWLEDGEMENT.....	7
LIST OF ACRONYMUS.....	8
LIST OF FIGURES.....	9
LIST OF TABLES.....	11
1. INTRODUCTION	12
1.1. Background	12
1.2. Energy policies.....	15
1.2.1. IRISH CONTEXT.....	16
1.3. METABUILDING Labs	16
1.4. Building Energy Modelling	18
1.4.1. Urban Building Energy Model	18
1.4.2. Building Energy Model.....	19
1.5. Project goal	21
2. LITERATURE REVIEW.....	23
2.1. Overview	23
2.2. Physical environment.....	23
2.3. Digital environment	23
2.3.1. Reduced Order Model	24
2.3.2. Digital Twin	26
2.4. Model calibration.....	27
3. METHODOLOGY.....	28
3.1. Model procedure	29
3.1.1. Collecting data	30
3.1.2. Parameter estimation	31
3.1.3. Reduced order modelling	31
3.1.4. Simulation and scenario analysis.....	33
3.2. Case study	34

3.2.1.	Collecting data	36
3.2.2.	parameter estimation	38
3.2.3.	reduced order modelling	41
3.2.4.	Simulation and scenario analysis	76
4.	RESULT AND DISCUSSION	84
5.	CONCLUSIONS	88
	REFERENCES.....	90

ABSTRACT

The focus on the energy efficiency of buildings is increasing exponentially as they are responsible for about 40% of total final energy consumption and 36% of greenhouse gas emissions. One of the ways to achieve sustainability goals in buildings is to improve the energy performance of their envelope. Boundary between indoor and outdoor environments, the facades of buildings are responsible for a large part of heat loss in winter and overheating in summer.

The objective of this thesis is the application of a Reduced Order Model, through the grey box modelling technique, to a building envelope test structure, located in Anglet, France, belonging to the European Metabuilding Labs project. The ROM, through the combination of data from sensors installed in the test structure with local meteorological information and the application of physical equations, will be able to calculate thermal loads and the main parameters describing the building's response to the thermal loads to which it is subjected.

The final intention is to use the ROM subject of this study as a digital twin to perform analysis scenarios for the optimisation of the design phase of other similar test structures. For this reason, the final output of this work will be a sensitivity analysis of the reduced order model to the input parameters.

SOMMARIO

L'attenzione per l'efficienza energetica degli edifici sta aumentando in modo esponenziale, poiché essi sono responsabili di circa il 40% del consumo finale di energia e del 36% delle emissioni di gas serra. Uno dei modi per raggiungere gli obiettivi di sostenibilità negli edifici è quello di migliorare le prestazioni energetiche del loro involucro. Confine tra ambienti interni ed esterni, le facciate degli edifici sono responsabili di gran parte delle perdite di calore in inverno e del surriscaldamento in estate.

L'obiettivo di questa tesi è l'applicazione di un Modello di Ordine Ridotto, attraverso la tecnica della modellazione a scatola grigia, ad una struttura di prova dell'involucro edilizio, situata ad Anglet, in Francia, appartenente al progetto europeo Metabuilding Labs. Il ROM, attraverso la combinazione di dati provenienti da sensori installati nella struttura di prova con informazioni meteorologiche locali e l'applicazione di equazioni fisiche, sarà in grado di calcolare la risposta termica della struttura di prova.

L'intenzione finale è quella di utilizzare il ROM oggetto di questo studio come gemello digitale per eseguire scenari di analisi per l'ottimizzazione della fase di progettazione di altre strutture di prova simili. Per questo motivo, l'output finale di questo lavoro sarà un'analisi di sensibilità del modello di ordine ridotto considerate ai parametri di input.

ACKNOWLEDGEMENT

The complete success of this internship and project would not have been possible without the support of a number of persons. The cooperation and time availability shown was essential.

First of all, I would like to thank the engineering department of the National University Ireland of Galway for welcoming me and providing me with the facilities to conduct my research.

In particular, I would like to thank NUIG in the person of Prof. Jamie Goggins for hosting me into the “Sustainable & Resilient Structures” research group.

A great thanks goes to my co-supervisor Dr. Magdalena Hajdukiewicz who followed my work during the entire period abroad and also once back in Italy. Her guidance and confrontations with her were the keystone for the completion of the work.

Also, a word of thanks to Dr. Alessandro Piccinini who provided me with advice and instructions on reduced order modelling.

Lastly, I would like to acknowledge the Università Politecnica delle Marche, and particularly my supervisor Prof. Alberto Giretti and co-supervisor Prof. Alessandro Carbonari, for allowing me to live this experience of study, work and life.

LIST OF ACRONYMUS

ASHRAE: AMERICAN SOCIETY OF HEATING, REFRIGERATING AND AIR-CONDITIONING ENGINEERS

BEM: BUILDING ENERGY MODEL

BET: BUILDING ENVELOPE TESTBED

BIM: BUILDING INFORMATION MODEL

DT: DIGITAL TWIN, 28

EPBD: ENERGY PERFORMANCE OF BUILDINGS

EPC: ENERGY PERFORMANCE CERTIFICATES

EPDM: ETHYLENE-PROPYLENE DIENE MONOMER

FMI: FUNCTIONAL MOCKUP INTERFACE

FMU: FUNCTIONAL MOCKUP UNIT

IPMVP: INTERNATIONAL PERFORMANCE MEASUREMENT AND VERIFICATION PROTOCOL

M&V: MEASUREMENT & VERIFICATION

MBLABS: METABUILDINGLABS

NZEB: NEAR ZERO ENERGY BUILDING

OBS: ORIENTED STRAD BOARD

PUR: POLYURETHANE

RC: RESISTANCE CAPACITOR

ROM: REDUCED ORDER MODEL

SME: SMALL MEDIUM ENTERPRISE

UBEM: URBAN ENERGY MODELLING

UNFCCC: UNITED NATIONS FRAMEWORK CONVENTION ON CLIMATE CHANGE

LIST OF FIGURES

FIG. 1 GLOBAL ENERGY USE BY SECTOR, 2020 [2].....	12
FIG. 2 RESIDENTIAL ENERGY CONSUMPTION BY END USE,2019.....	13
FIG. 3 GLOBAL ENERGY-RELATED CO2 EMISSIONS BY SECTOR, 2020.....	13
FIG. 4 PERCENTAGE BREAKDOWN OF HEAT LOSS IN THE BUILDINGS[4]	14
FIG. 5 BUILDING ENVELOPE TESTBED (BET) AS A PHYSICAL ASSET EMPOWERED BY DIGITAL DEVELOPMENTS.....	18
FIG. 6 METHODOLOGICAL APPROACHES FOR THE ENERGY MODELLING	21
FIG. 7 LINK BETWEEN THE DIGITAL ENVIRONMENT AND THE PHYSICAL ONE TROUGH DT AND ROM, ADAPTED FROM [24] ...	22
FIG. 8 2R1C MODEL OF A MULTILAYER WALL [37].....	25
FIG. 9 PARAMETRIC MODELLING.....	29
FIG. 10 OVERVIEW OF THE WHOLE PROCEDURE.....	30
FIG. 11 MAIN COMPONENTS OF THE ROM.....	31
FIG. 12 BUILDING COMPONENT OF THE ROM [61]	32
FIG. 13 EXCHANGE OF INFORMATION BETWEEN THE PHYSICAL BET AND ITS DIGITAL TWIN	34
FIG. 14 EXISTING BET IN ANGET, FRANCE	35
FIG. 15 BET CONFIGURATION.....	35
FIG. 16 ARCHITECTURE OF THE MONITORING OF THE BET	36
FIG. 17 WEEKLY AND ANNUAL LIGHTING PROFILE GENERATED	40
FIG. 18 WEEKLY AND ANNUAL HEATING PROFILE GENERATED.....	41
FIG. 19 REPRESENTATION OF THE STANDARD CELL	43
FIG. 20 REPRESENTATION OF THE SMALL CELL	44
FIG. 21 REPRESENTATION OF THE LARGE CELL	44
FIG. 22 TESTED WALL NUMBER 1.....	45
FIG. 23 COMPARISON BETWEEN MEAN RADIANT TEMPERATURE AND AIR TEMPERATURE	47
FIG. 24 ANNUAL TRENDS IN ELECTRICITY AND FOSSIL ENERGY DEMAND	48
FIG. 25 ANNUAL TREND OF THE AIR TEMPERATURE	49
FIG. 26 ANNUAL TREND OF THE MEAN RADIANT TEMPERATURE	49
FIG. 27 COMPARISON BETWEEN MEAN RADIANT TEMPERATURE AND AIR TEMPERATURE	50
FIG. 28 ANNUAL TRENDS IN ELECTRICITY AND FOSSIL ENERGY DEMAND.....	50
FIG. 29 ANNUAL TREND OF THE AIR TEMPERATURE	51
FIG. 30 ANNUAL TREND OF THE MEAN RADIANT TEMPERATURE	52
FIG. 31 COMPARISON BETWEEN MEAN RADIANT TEMPERATURE AND AIR TEMPERATURE.....	52
FIG. 32 ANNUAL TRENDS IN ELECTRICITY AND FOSSIL ENERGY DEMAND	52
FIG. 33 TESTED WAL NUMBER 2.....	53
FIG. 34 ANNUAL TREND OF THE AIR TEMPERATURE	55
FIG. 35 ANNUAL TREND OF THE MEAN RADIANT TEMPERATURE	55
FIG. 36 COMPARISON BETWEEN MEAN RADIANT TEMPERATURE AND AIR TEMPERATURE.....	55
FIG. 37 ANNUAL TRENDS IN ELECTRICITY AND FOSSIL ENERGY DEMAND	56
FIG. 38 ANNUAL TREND OF THE AIR TEMPERATURE	57
FIG. 39 ANNUAL TREND OF THE MAIN RADIANT TEMPERATURE.....	57
FIG. 40 COMPARISON BETWEEN MAIN RADIANT TEMPERATURE AND AIR TEMPERATURE	58
FIG. 41 ANNUAL TRENDS IN ELECTRICITY AND FOSSIL ENERGY DEMAND	58

FIG. 42 ANNUAL TREND OF THE AIR TEMPERATURE	59
FIG. 43 ANNUAL TREND OF THE MAIN RADIANT TEMPERATURE.....	60
FIG. 44 COMPARISON BETWEEN MEAN RADIANT TEMPERATURE AND AIR TEMPERATURE	60
FIG. 45 ANNUAL TRENDS IN ELECTRICITY AND FOSSIL ENERGY DEMAND	60
FIG. 46 TESTED WALL NUMBER 3	61
FIG. 47 ANNUAL TRENDS OF THE AIR TEMPERATURE.....	62
FIG. 48 ANNUAL TRENDS OF THE MAIN RADIANT TEMPERATURE	63
FIG. 49 COMPARISON BETWEEN THE MAIN RADIANT TEMPERATURE AND THE AIR TEMPERATURE.....	63
FIG. 50 ANNUAL TRENDS IN ELECTRICITY AND FOSSIL ENERGY DEMAND	63
FIG. 51 ANNUAL TREND OF THE AIR TEMPERATURE	65
FIG. 52 ANNUAL TREND OF THE MAIN RADIANT TEMPERATURE.....	65
FIG. 53 COMPARISON BETWEEN MEAN RADIANT TEMPERATURE AND AIR TEMPERATURE	65
FIG. 54 ANNUAL TRENDS IN ELECTRICITY AND FOSSIL ENERGY DEMAND	66
FIG. 55 ANNUAL TREND OF THE AIR TEMPERATURE	67
FIG. 56 ANNUAL TREND OF THE MAIN RADIANT TEMPERATURE.....	67
FIG. 57 COMPARISON BETWEEN MEAN RADIANT TEMPERATURE AND AIR TEMPERATURE	68
FIG. 58 ANNUAL TRENDS IN ELECTRICITY AND FOSSIL ENERGY DEMAND	68
FIG. 59 TESTED WALL NUMBER 4	69
FIG. 60 ANNUAL TREND OF THE AIR TEMPERATURE	70
FIG. 61 ANNUAL TREND OF THE MAIN RADIANT TEMPERATURE.....	70
FIG. 62 COMPARISON BETWEEN MEAN RADIANT TEMPERATURE AND AIR TEMPERATURE	71
FIG. 63 ANNUAL TRENDS IN ELECTRICITY AND FOSSIL ENERGY DEMAND	71
FIG. 64 ANNUAL TREND OF THE AIR TEMPERATURE	72
FIG. 65 ANNUAL TREND OF THE MAIN RADIANT TEMPERATURE.....	73
FIG. 66 COMPARISON BETWEEN MEAN RADIANT TEMPERATURE AND AIR TEMPERATURE	73
FIG. 67 ANNUAL TRENDS IN ELECTRICITY AND FOSSIL ENERGY DEMAND	73
FIG. 68 ANNUAL TREND OF THE AIR TEMPERATURE	75
FIG. 69 ANNUAL TREND OF THE MAIN RADIANT TEMPERATURE.....	75
FIG. 70 COMPARISON BETWEEN MEAN RADIANT TEMPERATURE AND AIR TEMPERATURE	75
FIG. 71 ANNUAL TRENDS IN ELECTRICITY AND FOSSIL ENERGY DEMAND	76
FIG. 72 STATISTICAL ANALYSIS OF RESULTS FOR THE STANDARD CELL	77
FIG. 73 AIR TEMPERATURE TREND	78
FIG. 74 MEAN RADIANT TEMPERATURE TREND.....	78
FIG. 75 STATISTICAL ANALYSIS OF RESULTS FOR THE SMALL CELL	79
FIG. 76 AIR TEMPERATURE TREND	80
FIG. 77 MEAN RADIANT TEMPERATURE TREND.....	80
FIG. 78 STATISTICAL ANALYSIS OF RESULTS FOR THE LARGE CELL	81
FIG. 79 AIR TEMPERATURE TREND	82
FIG. 80 MEAN RADIANT TEMPERATURE TREND.....	82
FIG. 81 FOSSIL ENERGY DEMAND PER SQM.	83
FIG. 82 ANALYSIS OF PERCENTAGE VARIATION IN FOSSIL ENERGY DEMAND.....	86
FIG. 83 ANALYSIS OF PERCENTAGE VARIATION IN STANDARD DEVIATION OF MAIN RADIANT TEMPERATURE.....	86
FIG. 84 ANALYSIS OF PERCENTAGE VARIATION IN STANDARD DEVIATION OF AIR TEMPERATURE	87

LIST OF TABLES

TABLE 1 PROPERTIES OF THE CELL CEILING	36
TABLE 2 PROPERTIES OF THE CELL WALLS.....	37
TABLE 3 PROPERTIES OF THE CELL FLOOR.....	37
TABLE 4 TESTED WALL NUMBER 1.....	45
TABLE 5 MODELLING OUTPUT.....	76
TABLE 6 MODELLING RESULTS FOR SCENARIO NUMBER 1	77
TABLE 7 AIR TEMPERATURE REFERENCE PARAMETERS	78
TABLE 8 MEAN RADIANT TEMPERATURE REFERENCE PARAMETERS.....	79
TABLE 9 MODELLING RESULTS FOR SCENARIO NUMBER 2	79
TABLE 10 AIR TEMPERATURE REFERENCE PARAMETERS	80
TABLE 11 MEAN RADIANT TEMPERATURE REFERENCE PARAMETERS.....	81
TABLE 12 MODELLING RESULTS FOR SCENARIO NUMBER 3	81
TABLE 13 AIR TEMPERATURE REFERENCE PARAMETERS	82
TABLE 14 MEAN RADIANT TEMPERATURE REFERENCE PARAMETERS.....	83

1. INTRODUCTION

1.1. Background

People spend most of their time inside buildings. Over the years, people's needs have changed, as have the characteristics of buildings. This process has led the buildings and the construction industry to become one of the largest consumers of energy and greenhouse gas emitters, both factors strongly linked to climate change. Despite a small decrease during the COVID-19 pandemic period the energy consumption of the built environment continues to grow, in 2020 it was estimated that the total demand from the entire construction sector was 36 [1] % of the global final energy consumption, as shown in Fig. 1.

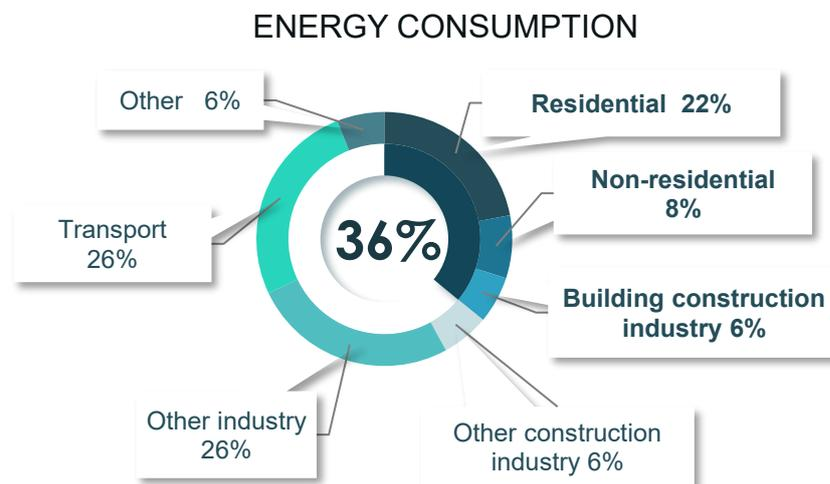


Fig. 1 Global energy use by sector, 2020 [2]

In the analysis of energy consumption, reference is made to the concept of embodied energy, that is, not only the energy linked to the use of buildings, but to their entire life cycle. The numerous construction processes require large amounts of energy in various forms. The transport of materials, the excavation of the ground, the hoisting of loads and demolitions of buildings are just some of the processes requiring energy that are considered talking about building construction industry. From beginning to end, each construction project requires energy sources.

On the other side the energy demand of buildings during their operational phase is closely related to their use. Focusing on residential buildings, energy consumption is closely linked to the satisfaction of occupant comfort conditions and evolves together with their requests. As shown in Fig.2, the most important energy demand in residential

buildings is related to their heating, followed by the use of appliances, by the heating of domestic water and finally the lighting that requires a minimum content.

RESIDENTIAL ENERGY CONSUMPTION BY END USE

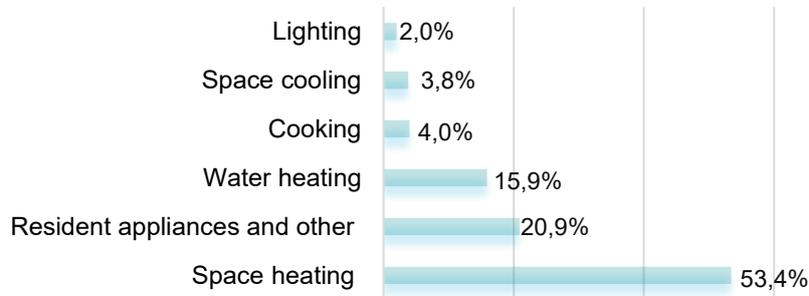


Fig. 2 Residential energy consumption by end use, 2019

Notes: adapted from “Shares of residential energy consumption by end use in selected IEA countries, 2019” [3]

In addition to being responsible for one third of total energy consumption buildings are responsible of one tenth of direct CO₂ emissions, as shown in Fig. 3. Where indirect emissions mean emissions related to power generation for electricity and commercial heat. In general, the built environment is responsible for the 37% of the global CO₂ emissions.

ENERGY-RELATED CO₂ EMISSIONS

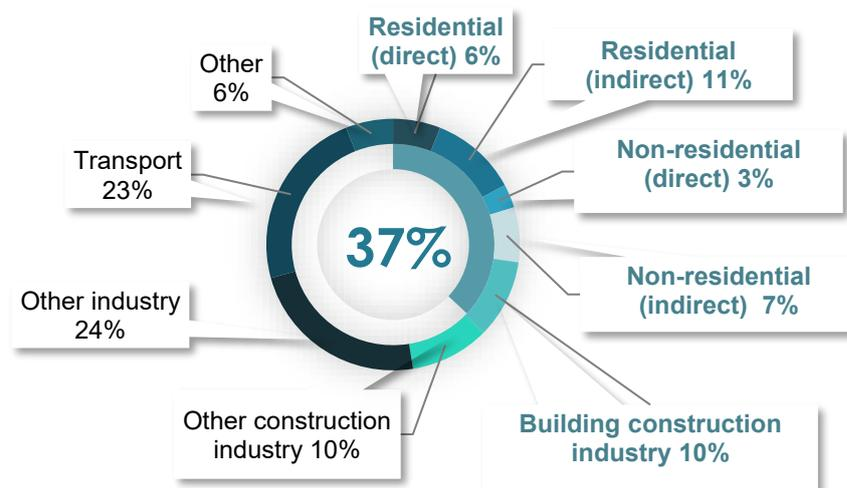


Fig. 3 Global energy-related CO₂ emissions by sector, 2020

Notes: “Other construction industry” in Fig 1 and Fig.3 refers to the share of industry that manufactures materials for the construction of other infrastructure. Sources: (IEA 2020d; IEA 2020b) [2].

The strong population growth and the relative demand for floor area bring the energy consumption of the built environment and the associated emissions with it to be constantly increasing. This trend is not in line with the sustainability objectives set at global and European level. Hence, the growing focus on energy efficiency in buildings plays a critical role in achieving the sustainability objectives, for combating climate change. First of these, the European goal of achieving carbon neutrality by 2050 [2]. Certainly, one of the most efficient ways to make an impact on the energy consumption of buildings is to intervene where consumption is highest, i.e., in space heating, thus limiting heat loss. The main causes of heat loss in residential buildings are ventilation, air infiltration and, most importantly, heat loss through the building envelope. The heat loss through the elements that make up the entire building envelope is significantly higher than that through ventilation as shown in Fig. 4.

PERCENTAGE BREAKDOWN OF HEAT LOSS

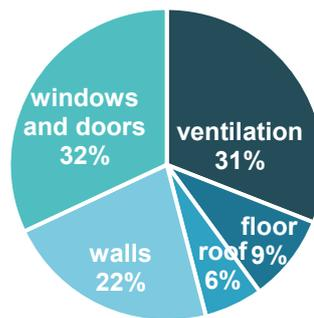


Fig. 4 Percentage breakdown of heat loss in the buildings[4]

Boundary between the indoor and outdoor environments, among which energy transfer occurs in terms of lighting and heat exchange, the building envelope is an essential element regarding the reduction of operational energy consumption. It has been estimated that the building envelope is accountable of 40% of winter heat loss and summer overheating in the building. [5]. Nowadays, a large part of the investment in the building sector consists of technologies that lead to an improvement in the performance of the building envelope, fundamental for energy performance[6]. In addition, the interest in innovative research applied to building envelopes is growing more and more [7].

1.2. Energy policies

Over the years, directives taken at all levels, from international to national, have assumed a fundamental role in combating climate change and its effects. Starting with the main international treaty on combating climate change, the United Nations Framework Convention on Climate Change[8], agreed in 1992, followed by Kyoto Protocol[9], one of the most important documents at global level to reduce greenhouse gas emissions before 2020 and finally the Paris Agreement adopted by all UNFCCC Parties in December 2015, [10] the very first legally binding universal climate agreement.

The EU has shown great dedication to combating climate change. One of the ways to achieve the EU's energy and climate goals is through energy-efficient buildings. To boost energy performance of buildings, the EU has established a legislative framework that includes the Energy Performance of Buildings 2010/31/EU [11]that aims to improve the energy performance of building, taking into account various climatic and local conditions, setting out a common framework for calculating energy performance and the Energy Efficiency Directive 2012/27/EU [12]that defines energy saving goals to be achieved for central government buildings in all European countries.

These energy policies introduced new concepts that are key respond effectively to the problems that, particularly in the last decades, are affecting the environment: pollution, resource depletion, global warming. First of all, the concept of a near zero-energy building (NZEB), they are considered to be the ultimate solution for mitigating the negative impacts of future building energy consumption. NZEBs are energy-efficient buildings with a minimal, almost zero energy demand, which is usually covered by renewable resources. The objectives set by the EPBD are different: all new buildings in European countries must be NZEB from 2020 and ZEB from 2030. The revolution must obviously start with public buildings, which must be NZEB by 31 December 2018, and for communal buildings the goal is set for the end of 2020. From 2027 all new buildings serving public authorities must be ZEB, from January 2030 this requirement must be met by all new buildings. The EPBD also defines the requirements for the production of Energy Performance Certificates (EPC), an important instrument that contributes to the enhancement of the energy performance of buildings. In order to accurately measure the results obtained in terms of energy efficiency, for the M&V (Measurement and

Verification), many tools have been provided. These include the International Performance Measurement and Verification Protocol (IPMVP) a guideline to verify the results of energy efficiency, water efficiency and renewable energy projects in any field, from civil buildings to industrial sites.

1.2.1. IRISH CONTEXT

Ireland as a European country is aiming to achieve the targets set by the e green deal through national policies. Project Ireland 2040[13] sets out the investment priorities that will underpin the successful implementation of the new National Planning Framework in Ireland. This will guide national, regional and local planning and investment decisions in Ireland over the next two decades and is designed to cater for an expected population increase of over 1 million people in Ireland. The Plan sets out a very substantial commitment of resources and is expected to move Ireland close to the top of the international league table for public investment, demonstrating the Government's commitment to meeting Ireland's infrastructure and investment needs over the next ten years. Transition to a Low-Carbon and Climate Resilient Society remains the single largest investment priority under Project Ireland 2040 in order to ensure Ireland's delivery of climate action objectives, including decarbonisation pathway to 2030 and net zero target in Ireland by 2050. The Climate Action Plan sets a target of reducing the greenhouse gas emissions from the residential sector from 6Mt CO₂e in 2017 to 3-4Mt CO₂e in 2030, as well as the targets of 500,000 retrofits to Building Energy Rating B2/Cost Optimal Equivalent or carbon equivalent; and the installation of 400,000 heat pumps in existing homes will be achieved. A modern, innovative and resilient construction sector is central to delivering on the Project Ireland 2040 Plan and to ensuring maximum value for money. Introducing lean construction methods and Building Information Modelling (BIM) plays an important role in driving productivity and enabling innovation.

1.3. METABUILDING Labs

The European path towards a twin green and digital transitions that can make our communities greener and less polluting pass also - and above all - through the research programmes in the construction sector, which is responsible for a considerable share of

environmental impact. Small medium enterprises, SMEs, embody 99,9% of companies in the construction sector in Europe and produce 80% of the output of the whole sector. It is in this perspective that EU innovation project METABUILDING Labs, (MBLabs) strives to unleash the innovation potential of the SMEs of the Construction sector by lowering the entry barriers to test innovative solutions in a network of testing facilities in RTOs (real-time operating system) and Living Labs in 13 countries, allowing direct feedback from the end-users during the final development stages. MBLabs is a 5-year project started in January 2021 and is linked to another project called METABUILDING [14]. These two sister projects aim to create a digital platform that consists of several digital tools and services to help SMEs and other stakeholders engage in successful innovation. One of the innovation pillars of the MBLabs is the construction of a network of O3 Building Envelope Testbenchs (standardized, replicable, affordable, Digital Twin enabled): first fully replicable, standardised, cost-effective Open Source/Open Data/Open Access Building Envelope



Testbeds enabling virtual testing and made available (co-funded) to some of the project partners. The O3BET is perfectly adapted for the development of smart envelope systems where real conditions, real scale and easy access are key to ensure fast, agile and effective development of new technologies. The smart envelope systems studied will include curtain walls, advanced windows (e.g., windows with thermal mass), innovative glazing, solar thermal panels for walls / roofs, photovoltaic thermal collectors, coatings for cool roofs, light reflector connections, heat-reflective and vacuum insulation panels, green roofs and light redirection systems in windows. It uses the open access 7D Building Information Model (BIM), the digital twin model and the Parametric Building Energy Model (pBEM), which will be linked to the Open Innovation Test Bed platform for data collection, exchange, performance simulation (virtual testing) and monitoring. By combining the real-time data of the physical BET with digital developments, it is possible to implement testing and performance analysis of new systems and envelope solutions, as shown in Fig. 5. Furthermore, the full-scale controlled BET bridges the gap between the small-scale laboratory testing and installation in operating buildings, providing building product developers with additional quality assurance checks before bringing their products to market

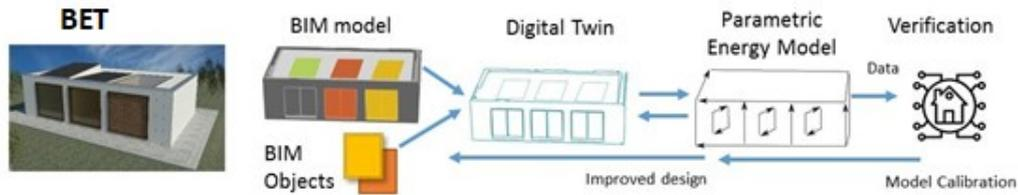


Fig. 5 Building Envelope Testbed (BET) as a physical asset empowered by digital developments

1.4. Building Energy Modelling

The energy consumption of the construction industry and its products represents one third of the world's energy consumption and 15% [15] of carbon dioxide emissions. Urban areas are responsible for the majority of greenhouse gas emissions. Existing urban settlements must be updated and constructed in such a way that their resource consumption is minimized. In this process, energy modelling and optimising of the urban environment will be critical. In addition to the implementation of energy efficiency policies, energy modelling has become widespread in recent years to regulate energy consumption and related emissions.

The modelling can be used as an evaluation tool in decisions concerning buildings, both existing and planned [16]. This allows through consumption estimation, impact prediction or retrofit analysis to make decisions calibrated to the actual situation and consistent with existing energy limitations and policies, both in the case of new construction and in the case of modifications or demolitions of existing buildings.

The applications of building energy model are manifold, for instance, energy planning, energy supply-demand calculation, retrofit analysis, forecasting, renewable energy impact, emission reduction. Another important application of building energy models is the optimisation and analysis of various design scenarios in order to increase the building's energy efficiency. Depending on the level at which energy modelling is done, we talk about Urban Building Energy Modelling (UBEM) if it's at urban level, or Building Energy Modelling (BEM) if the modelling object is the single building.

1.4.1. URBAN BUILDING ENERGY MODEL

Energetic modelling on urban scale takes into account not only the performance of the individual building but analyses the effects and relationships between the building and the group of buildings to which it belongs, taking into account the urban microclimate

[17]. There are two types of techniques used for urban energy modelling, “top-down” and “bottom-up”. The name of the techniques comes from the approach they follow; one deductive, top down, which uses as input the estimated total energy consumption of the building sector, the other inductive, bottom up, which starts from the consumption of the individual building[18].

Top-down models use large amounts of data that can come from different sources, such as institution archives or building energy certification reports [19]. This is a large-scale analysis of the system without going into detail. An interesting aspect of the top-down approach is the possibility of assessing the relationship between energy use at urban level and technological, demographic and macroeconomic effects. The relationship between the energy sector and the economy is assessed. We distinguish two applications of top-down models that are econometric and technological models[20].

Econometric model connects the energy sector to quantifiable parameters to represent the results (fuel price, income).

Technological model instead considers those parameters that affect the use of energy (technological growth, structural changes).

1.4.2. BUILDING ENERGY MODEL

The "bottom-up “modelling has as object the single building, carrying out a detailed analysis. The outputs of this type of modelling can be called Building Energy Models (BEM). What is a BEM is well explained by the definition provided by the U.S. energy department. “BEM is physics-based software simulation of building energy use. A BEM program takes as input a description of a building including geometry, construction materials, and lighting, HVAC, refrigeration, water heating, and renewable generation system configurations, component efficiencies, and control strategies. It also takes descriptions of the building’s use and operation including schedules for occupancy, lighting, plug-loads, and thermostat settings. A BEM program combines these inputs with information about local weather and uses physics equations to calculate thermal loads, system response to those loads, and resulting energy use, along with related metrics like occupant comfort and energy costs. BEM programs perform a full year of calculations on an hourly or shorter basis. They also account for system interactions like the ones between lighting and heating/cooling”[21]. Three different approaches can be followed for modelling a BEM: physics-based, data-driven and reduced-order modelling.

1.4.2.1. White box model

White boxes, which are physical energy models, model the thermal behaviour of the building on the basis of heat balance equations. To analyse the heat balance between the building and the outdoor environment, all methods of heat transmission, from convection to irradiation, are considered. This modelling technique requires a large amount of information about the building as geometric characteristics, materials used, occupant flow, data about weather conditions, information about the systems used. [22] Detailed specifications that are often difficult to find, especially for historic buildings or when designing. Knowledge of all these details can be a problem, along with the long computational times this technique requires. The pro of this approach is the possibility of having a clear link between inputs and outputs.

1.4.2.2. Black box model

Black-box models are data driven models that are viewed in terms of their inputs and outputs without any knowledge of their internal mechanism. These are models that make forecasts based on time series of historical data. This allows the application even in cases where physical characteristics are not known in detail. Data collection is a fundamental moment, as the entire modelling of this type is based on data, which must be cleaned and processed before it can be used[19].

1.4.2.3. Grey box model

Grey box models are hybrid models obtained by combining numerical methods and physical approaches. Models of this type are also defined reduced order models. The main benefit of the hybrid method is that it allows one to consider only a limited amount of data. In addition, you have the possibility of not having to set the input data from the beginning, but only limits on the parameters. It's possible to start with a description of the main geometric and energetic characteristics of the building [23].

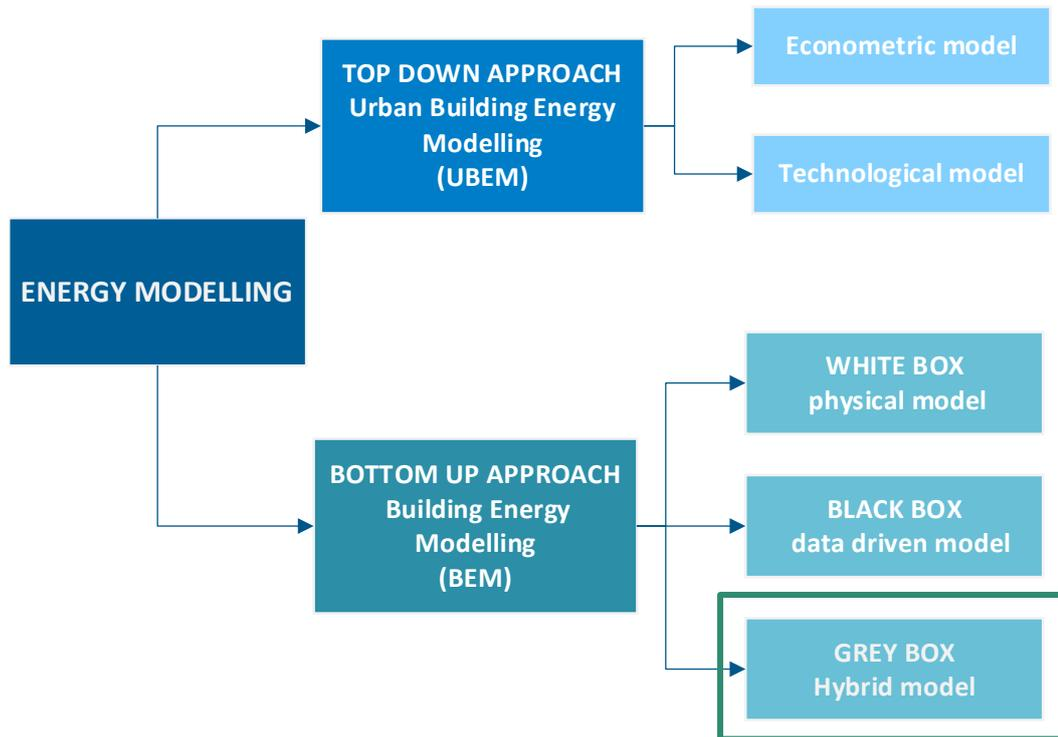


Fig. 6 Methodological approaches for the energy modelling

The modelling possibilities as shown in Fig. 6 are different, it all depends on the model's overall design (top-down vs. bottom-up) and degree of transparency (black-box vs. white box)

1.5. Project goal

The objective of this work is to produce a reduced-order model (ROM), following the grey-box model approach for the energy modelling of a test bed already built and operating in France. In particular, the modelling will concern one of the three identical cells of the test facility.

The model, combined with a system of sensors and related data processing algorithms, will enable the precise detection and evaluation of the building's main environmental and energy parameters. It creates a real link between the physical environment, the subject of the model, and the digital environment. As illustrated below (Fig. 7), an information exchange cycle between the physical and digital environment will be created, leading to the improvement and efficiency of both existing assets and those under construction (optimisation of the design phase). The obtained model can be used to simulate the response of the existing test structure when the tested envelope

changes. In addition, the ROM will be used to analyse different design scenarios in order to design the test structure to be built in Ireland. The ROM will be used as an alter ego of the structure to be built, a digital twin that will enable scenario analysis to optimise the design phase. It will be analysed how variation in the size of the test cell will affect the thermal response of the entire structure. A sensitivity analysis of the model to the input parameters will be performed. The digital twin of the test bench will improve the set of additional test procedures, ensure better real-time monitoring services, better data integration and cohesion. It will also guarantee a complete description of the context in which the façade panels are tested.

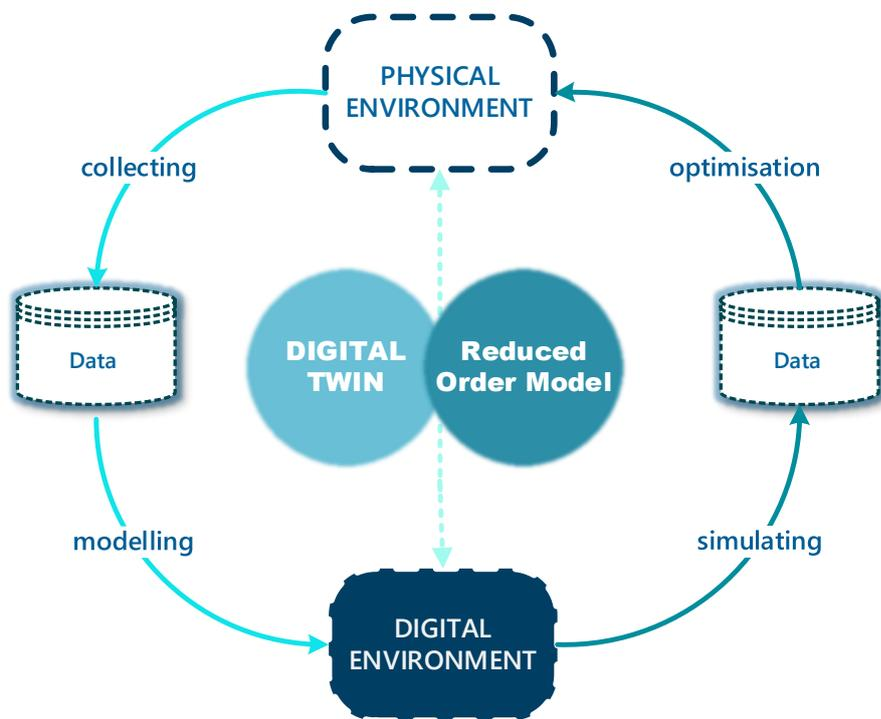


Fig. 7 Link between the digital environment and the physical one through DT and ROM, adapted from [24]

2. LITERATURE REVIEW

2.1. Overview

The building is a complex system, the energy phenomena that develop inside it are different and in continuous relationship with each other. These issues concern the characteristics of the envelope, the systems, the use of the rooms, the presence of a large number of people or machinery producing heat. The design of energy-efficient buildings requires advanced tools that allow the correct evaluation of thermophysical phenomena. Over the years, several researches have been carried out to achieve different sustainability goals and improve the performance of buildings.

2.2. Physical environment

Energy modelling as a tool to improve the efficiency of buildings and to achieve the performance required by energy policies has been applied and studied in different scenarios. Numerous models have been developed to model various contexts with different data availability. Building modelling is nowadays used at different scales. Starting from urban modelling, where city model based on large dataset can be used as instrument to for energy planning and city development[25][26], then moving to a lower level, energy modelling has also been applied to a set of buildings [27]. There are many studies focus on studying the thermal behaviour of individual buildings and analysing the ability of thermal models to predict their thermal demand and temperature. The behaviour of several type of buildings such as offices [28], residential buildings and commercial buildings[29] is studied. And finally, modelling is also applied at a level of detail where the focus of the study is on a single room[30] or test facility[31][32].

2.3. Digital environment

The simulation of the energy behaviour of buildings is a theme of investigation much followed. Great progress has been made in forecasting the energy needs of the building and assessing its thermal response. The application of grey box model for the energy simulation of buildings in recent years has spread widely, as it is more interpretable than

black-box model and more computationally efficient and simpler than the white-box model.

2.3.1. REDUCED ORDER MODEL

2.3.1.1. Applications

There are numerous applications of the ROM in the buildings, as model-reduction of non-linear thermal dynamics of multi-zone buildings[33], modelling to predict the thermal behaviour of occupied buildings [28], prediction and estimation of thermal loads in building [34]. Also heat dynamic analysis focusing on investigating heat transfer properties of building elements [35], the estimation of the energy saving, and of course, simulation control and optimisation of thermal conditions [36]. By simulating the energy performance of the building, ROM can be associated to what we call digital twins, virtual copies of a real world.

2.3.1.2. Modelling technology

To model a reduced order model there are several approaches, starting from the union of white-box and black-box methods, one to estimate the physical parameters and the other to implement the model using statistics. Different combinations of the two approaches can be applied, such as the combination of genetic algorithms and nodal methods[37], thermal models and regression techniques or nodal approach with the artificial neural network. But surely the most used method is the RC network model, based on the electrical analogy. Since the 1980s [38] , when a multi-layer wall was shaped by two resistances and a capacitor(2R1C), as show in the Fig. 8, the method of energy modelling by the electric analogy has been widely spread and evolved over time.

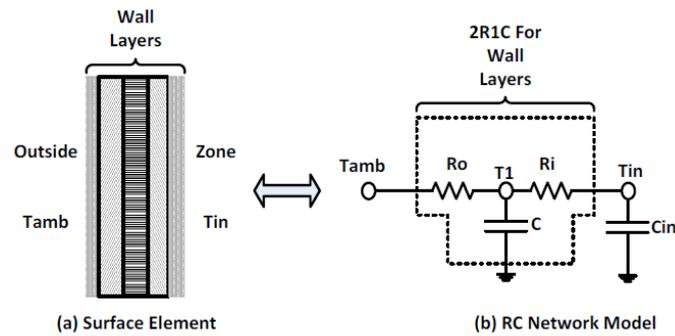


Fig. 8 2R1C model of a multilayer wall [37]

In general, an $RxCy$ model has x resistances and y capacitances. The capacitances discretise the thermal mass of the building and the number of capacities gives the order of the diagram. Starting with the first-order model, numerous other types of models have been used to model buildings, even up to fifth. But it has been demonstrated that increasing the model order beyond 2 does not imply in a substantial increase in simulation outcomes [39]. The most widely used are the second and the third-order models. There are multiple applications of RC modelling starting from the study of heat dynamics, thermal load estimation to urban/district energy modelling, and building grid integration demonstrate that RC modelling is a viable choice.

2.3.1.3. Parameter estimation

One of the most important issues in reduced order modelling is the estimation of the parameters to be used as input. The ROM makes it possible to switch from a continuous system to a discrete one, and thus to switch to a system with concentrated parameters. Consequently, the estimation of the parameters on which to base this process is fundamental. Two approaches to parameter estimation can be followed[40]: the forward approach, the parameters are calculated directly from the physical model and the inverse approach, resistance and capacitance values are obtained through data-driven algorithms. Automated parameter estimation was introduced in the 1990s to minimise the level of error and since then various tools have been developed and applied. The many tools that have been developed have different features and use different software such as MatLab plugin[41] for parameter estimation in FMUs, or Python[42] tool for parameter estimation in FMI-compliant models[43]. Others make use of modelling techniques such as using continuous time stochastic modelling in R

programming language that uses the maximum likelihood estimation and automates the estimation procedure[44]. Tools have also been developed that do not necessarily require the use of specific software and knowledge of certain languages such as MatLab[45] and Modelica[46]. These include the RomPar tool[47], which allows parameters to be estimated using an Excel spreadsheet starting from information obtained through data collection and on-site surveys.

2.3.1.4. *Simulating tool*

Energy modelling of buildings in general is based on heat balance equations. In order to study the dynamic behaviour of buildings, it is necessary to solve these equations, which can be done using various software and tools. Three groups of toolboxes used for ROMs and in particular RC circuits can be identified[48], the models developed using the MatLab language, an environment for numerical calculation and statistical analysis written in C, useful for writing statistical models and for numerical mathematical analysis. Useful for writing models and for analysis from a numerical-mathematical point of view, they are very fast in simulations. Modelling using MatLab takes less time due to the high computational power but at the same time can take longer to calibrate the model as each component has to be modelled by the user[49]. In contrast, the second group of toolboxes, the one developed with Modelica, offers an approach that is easier to use and understand [50]. Object-oriented modelling makes it possible to obtain models that can be reused in different solutions, and the Modelica libraries provide a great deal of help with modelling containing ready-made models for certain parts of the building such as the envelope or the HVAC equipment and heating system. The third group consists of general-purpose free programming languages. These are toolboxes that use other languages that are still in the development phase and have not been as widely applied and studied as those described above.

2.3.2. DIGITAL TWIN

The concept of Digital Twin as a physical mirror date back to the 1960s. This approach was first applied by NASA, which used the digital twin to map and simulate the status of its devices during missions [51]. The Digital Twin consists of three main components: the physical model, the digital model and data transmission. Digital Twin is a system that

connects a physical project to its digital representation, and that monitors its state through sensors that send data from the real environment to the digital one [52]. In the past, DT has been mainly used for production, prognosis and diagnosis, predictive maintenance of the product. Today it could play an important role in the optimisation of the design phase through virtual simulation. The application of the DT as a verification tool allows to obtain very reliable simulations on which to refine the design process. The results of DT modelling enable scenario analysis and timely results. Implementing thoughtful choices and avoiding physical tests and the consequent waste of money and time [53].

There are more studies focusing on DT in the production design phase. From design production lines, taking a glass production line as an example, the digital twin model is used for production line design (including functionality and information needed in each phase/step) in the preproduction phase and later inherited for inspection preparation and process control, [54] to the design of a longitudinal fuselage joint, DT allows not only to determine the response to different design scenarios, but also to evaluate the behaviour as some parameters vary, in this case it is evaluated as the overlap length affects the failure rate. Though there are not many cases related to DT applications for designing a new project in the civil engineering sector, DT for design has a great potential, it can assist in planning and task clarification, conceptual design, preliminary design, detailed design, and virtual verification[55]. Several studies have shown the potential to support the identification of optimal design decisions and that approximately 20% of design decisions made in the early design stage account for 80% of the total impact on the final building energy performance [56].

2.4. Model calibration

At the end of modelling, the completed model must be calibrated in order to be used as a valid simulation tool. The aim is to obtain results from the simulation that are in line with reality, by acting on what are defined as key parameters. Commonly, the parameters that are subject to calibration in BEMs are energy demand, cooling or heating system heat load, and indoor air temperature[57]. The objective is to correlate the simulated values with those measured in a specific time period. The reference period depends on the availability of data and the final purpose of the calibration. Either a manual calibration can be made, which requires practical experience on the part of

the user, or an automatic calibration, which is based on functions that match the simulation results with the measured data and automatically act on the parameters. Some calibration methods are also involved in estimating the parameters and determining the uncertainty related to the input parameters in the final model.

The issue of calibration of simulation models of the energy behaviour of buildings is still evolving and being studied. One of the first approaches to calibration was the simple comparison of measured data and simulation results. With this method there was a risk of offsetting, the overestimates cancelled out the underestimates [58], for this reason, a switch was made to the use of standardised indices. With regard to statistical indices, guidelines have been published to help the user assess the accuracy of the calibration process, including the ASHRAE and IPMVP guidelines. These guidelines provide threshold values to consider the model calibrated, these values depend on the monthly calibration interval considered, either hourly or monthly.

3. METHODOLOGY

In this study, a grey box model will be applied to control and predict the thermal response of a test building envelope structure. The thermal response of the modelled test structure when different wall types are tested will be analysed. The simulations will be carried out on 4 sample walls. Such ROM-based simulations with different wall types serve to verify that the variations in the behaviour of experimental cells are significantly different depending on the type of wall being tested. During the simulations, the model inputs related to the dimensions of the test cell will be varied. The input parameters will be changed by varying the test scenarios. The ultimate goal is to assess the sensitivity of the model to the input parameters. To conduct this parametric analysis, the same simulation outputs will be taken as reference for each combination of cell size and wall type tested. The output parameters that will be taken as reference for analysis and evaluation are, as shown in the graph beneath:

- Time for simulation
- Air temperature
- Main radiant air temperature
- Demand for electrical energy
- Demand for fossil energy

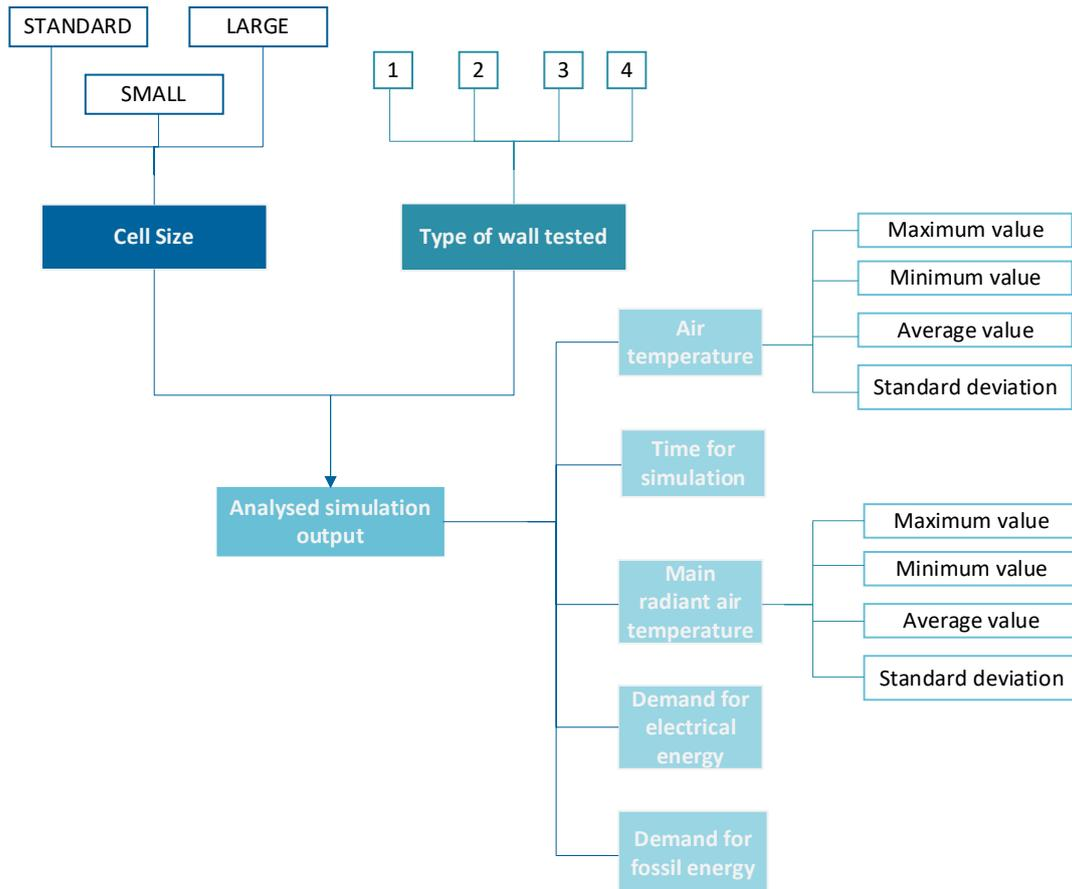


Fig. 9 Parametric modelling

All this is being done with a view to using the ROM as a tool for the design of another test facility, belonging to the MBLabs project's network of test facilities, to be built in Ireland. Use of the ROM as a digital twin for the optimisation of the design phase in the preliminary phase.

3.1. Model procedure

The whole procedure is divided into 4 steps as described in the following workflow.

1. Initially, information about the characteristics of the test structure and its location will be collected for ROM parameter estimation.
2. Once all the information is collected, the parameters to be used as input for the modelling are estimated through a special tool, RomPar.
3. After obtaining the inputs, the reduced order modelling is carried out. Three different scenarios will be simulated. This will be repeated for four sample walls. In total, the results of twelve simulations will be analysed.

4. The model will be used as a scenario analysis tool for optimising the design phase of other test structures. In this phase, it will be analysed how the different parameters influence the final response of the ROM. Following a test protocol, the study will focus on the sensitivity of the model's final response to the variation of the input relative to the size of the test cell. Once all the data have been collected, marginalisation will be carried out in order to obtain results on the sensitivity of the model.

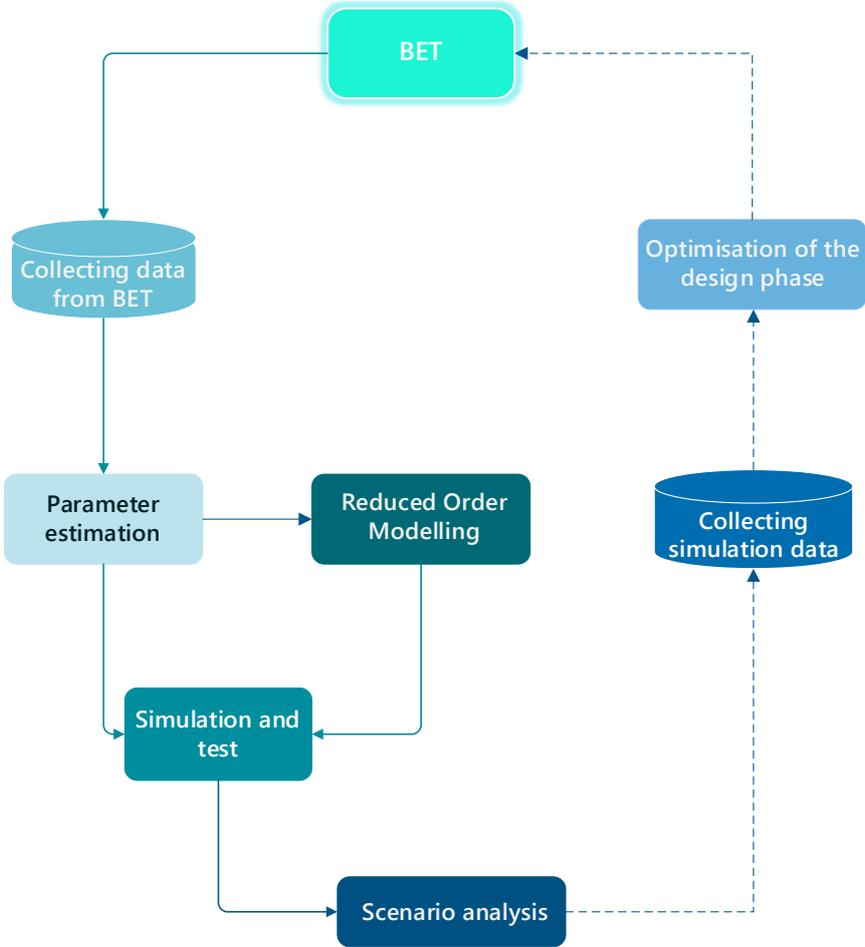


Fig. 10 Overview of the whole procedure

3.1.1. COLLECTING DATA

The initial information needed is related to the geometric characteristics of the building, therefore the dimensions and the properties of the different elements that compose it. This information is supplemented by data on the installations thus the heating and cooling systems used. Information about the use of the building and occupancy profiles. Collection of information related to the building site, such as location and weather data.

3.1.2. PARAMETER ESTIMATION

In order to simulate the behaviour of the study object, it is necessary to estimate the parameters to be used as input for the reduced-order model. The tool used to estimate the parameters is an excel tool, RomPar [59], which uses the formulas and guidance provided by the relevant standards to calculate the thermal resistances and capacities. The use of this tool makes it possible to calculate the resistances and heat capacities to be included in the building component of the ROM. Also, by means of excel, schedules will be generated concerning the profiles for switching the system on and off and the use of the different equipment and lighting. No occupancy data will be collected since, as this is a test facility, no human activities are carried out in it.

3.1.3. REDUCED ORDER MODELLING

A RC network is adopted for energy modelling of the examined structure. In particular, a model using the Modelica language, built in the dymola environment, is used. The ROM structure used is a development by Piccinini et al. [47] of the model proposed by Bacher and Madsen, [59] and Giretti [60], that has already been applied to other case studies [61]. As shown in Fig.10, the model discretises the entire continuous system into a discrete system consisting of four main components.

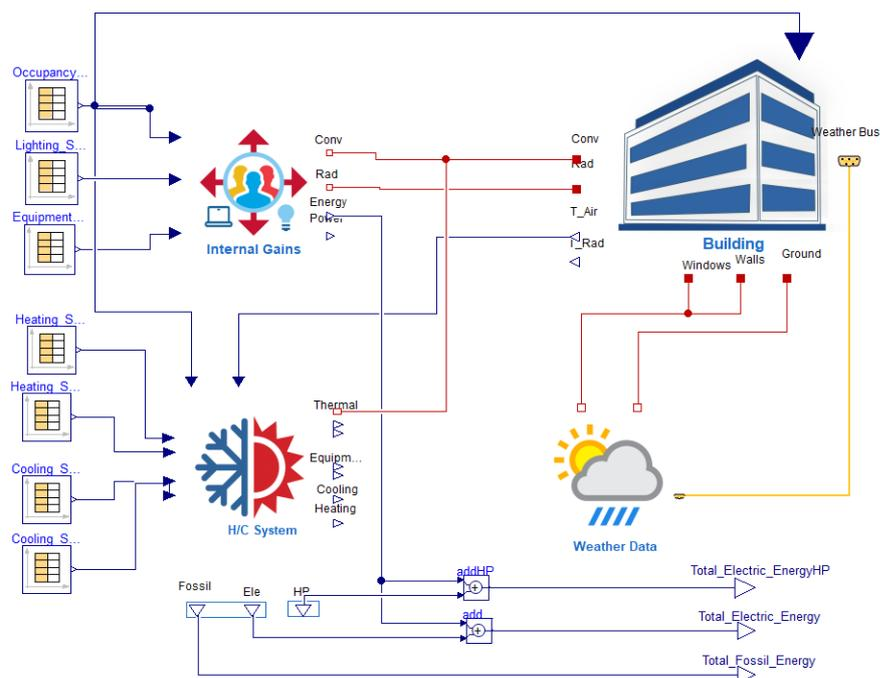


Fig. 11 main components of the ROM

The model consists of 4 main components which are:

- Building component

Some elements from the Modelica library and others from the IBPSIA library were used to model the building. The building component is composed of 4 groups of resistances and capacities which relate the internal and external elements of the building, the first group is used to combine the internal walls of the building and the slabs, the second group is used to combine all the elements of the opaque envelope, the third group represents the transparent elements of the building and the last group the building ground floor. To the groups of resistances and capacities are added a solar radiation component, a natural entilation component and a natural ventilation component and an air infiltration component. All elements have been connected to an element representing the entire volume of the building, modelled using the model library component mixing volume.

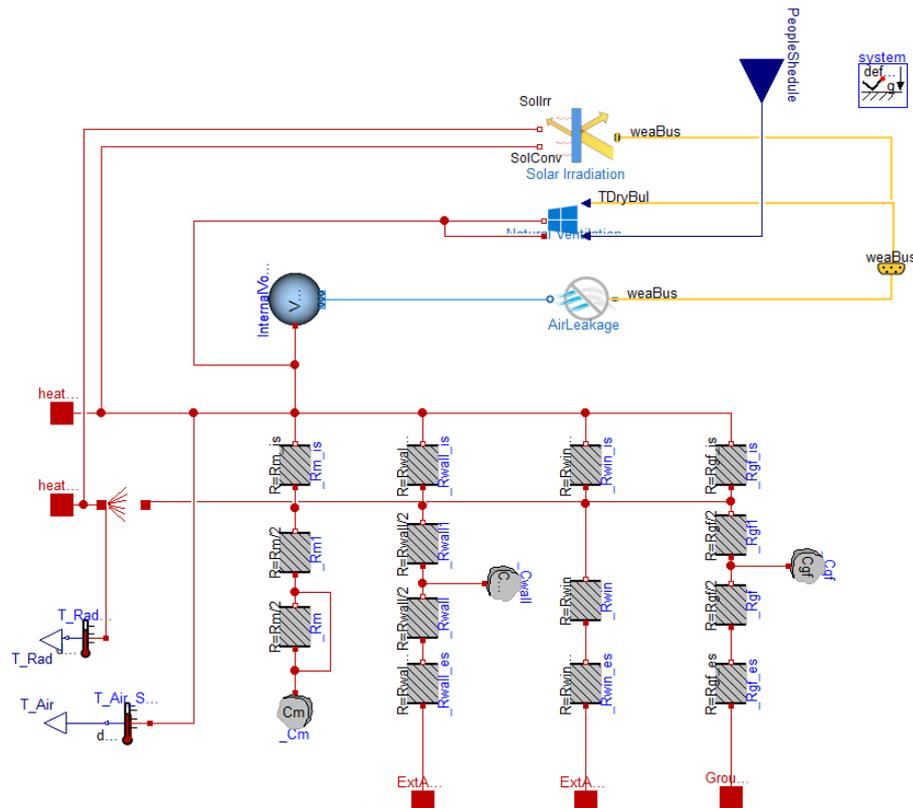


Fig. 12 Building component of the ROM [61]

- Internal gains component

This component takes into account the heat gains from people, lighting and equipment in the building. For the calculation of this component, data were

collected on occupancy hours, activities in the building to include heat gains from people, and information on equipment and lighting. From all these gains is subtracted the share of consumed energy which is estimated by a component of the model library.

- Heating and cooling system component

Through this component, the thermal heat gain of the power system [W] that is generated by the heating and cooling component is estimated. This value is related to the operating time of the system and the set point of cooling and heating, as a thermo-regulated heat gain with an internal control loop. In general, it consists of two parts: one represents the thermoregulated heat gain and the other estimates the heating and cooling energy consumption of the system.

- Weather data component

It's a simple data container. it represents external conditions by data usually on an hourly basis. Obviously, it is linked to the position where the model object is located. Through this component, effects related to the climatic conditions at the site are taken into account. It provides input to the solar irradiation element of the building component and the ground temperature used as input to the heating cooling system component.

3.1.4. SIMULATION AND SCENARIO ANALYSIS

After all input parameters have been calculated, they can be entered into the model and the simulation phase can be started. The results of the simulation can be different according to the desired application. As a result, it is possible obtain estimation of parameters related to the thermal performance of the building such as the temperature or estimation of the energy consumption of the structure. After simulation, the model is usually validated through calibration.

In this case, the model used has already been applied in other case studies. It has already been calibrated follow the method used by Giretti [60],and amply demonstrated how valid the simulations obtained are [61].

Therefore, this step will be omitted, considering the model already calibrated, and the analysis of the results obtained will be carried out. Analyses will be performed in three different scenarios for four different building envelopes. The difference between one

scenario and the other will concern the volumetry of the cell. At the end of the simulations, it will be analysed how much the volume and size of the cell affect air temperature and energy consumption for the same tested envelope.

The results of the simulations will be used as a tool for evaluations during the design of a new BET. Creating an even stronger link between the physical and digital environment as shown in the figure below.

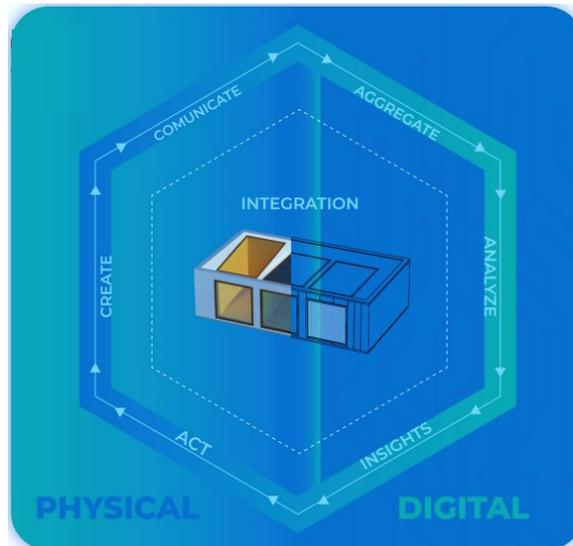


Fig. 13 Exchange of information between the physical BET and its digital twin

3.2. Case study

The case study building is the Building Envelope Testbed (BET) located in Anglet, France. It was designed and built, by Nobatek [62] in 2015, specifically for testing building envelope solutions, as part of EU and industry projects.

The BET consists of three highly isolated and identical cells. The test bench is to be used to evaluate the thermal performance of opaque or transparent and possibly dynamic façade elements. For this reason, the cells are identical in order to have comparable results between them, they have only one south orientated open façade for testing.



Fig. 14 Existing BET in Anglet, France

The cells are in contact with the outside on their south side, through the roof and the floor. On the other sides their vertical components are surrounded by a buffer zone called a guard. The controlled temperature conditions in the common guarded zone enables to greatly reduce the heat transfer in the vertical walls of the cells, while in the horizontal ones (roof and floor) an ample thickness of insulation limits the heat transfer to small values.

The test cells are identical to each other. Since the three cells are identical, only one cell will be studied.

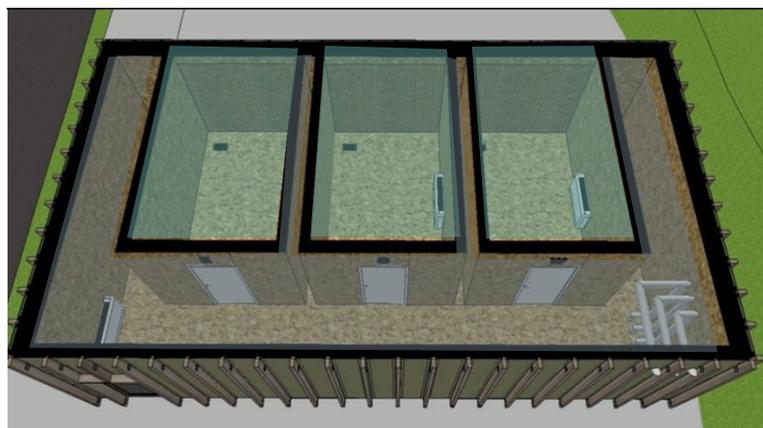


Fig. 15 BET configuration

The presence of sensors and monitors allows easy installation, regulation and environmental and energy verification of building envelope systems. National Instruments hardware and software are used for the monitoring and logging. The hardware installation is identical in the three cells, as shown in Fig. 14.

To take into account the heat dissipated by the monitoring hardware there are these acquisition cards in the cells:

- PT100: 4 entries
- Thermocouples : 16 entries
- Analogic signal: 8 entries
- + some open slots for additional cards such as impulsions, or numerical ones.

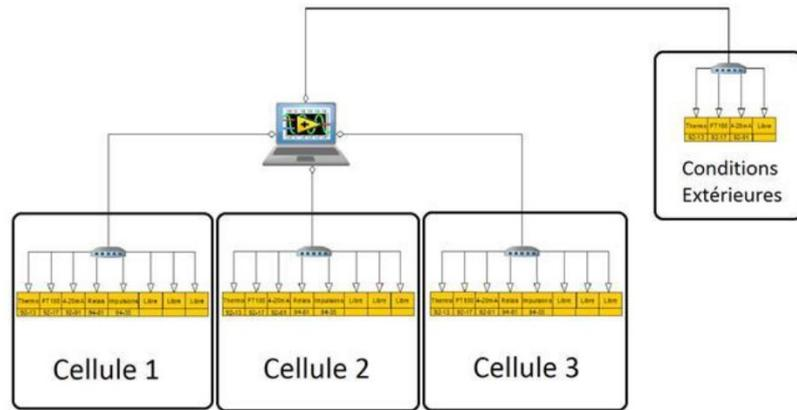


Fig. 16 Architecture of the monitoring of the BET

3.2.1. COLLECTING DATA

In this step, data was collected about the composition of the different cell surfaces, the installation and the location of the test structure. The test cell is made of wood and is highly insulated. In relation to the test cell, the characteristics of the different surface layers are listed in the tables below. The high degree of insulation is achieved through the use of material as EPDM (Ethylene-Propylene Diene Monomer), glass wool, PUR (Polyurethane) and air gaps. The wooden side, on the other hand, consists of wood fiber panels and OBS (Oriented Strand Board).

CEILING CELL

Material (From Ext to Int)	Thickness (m)	Conductivity (W/mK)	Density (Kg/m ³)	Specific Heat Capacity (J/KgK)	Thermal Resistance (m ² K/W)
EPDM_1	0,02	0,05	70	1500	0,4
PU	0,1	0,028	35	1590	3,57
EPDM_2	0,01	0,05	70	1500	0,2
OSB_1	0,012	0,13	650	1700	0,09
GLASS WOOL	0,12	0,038	12	1030	3,15
GLASS WOOL	0,1	0,038	12	1030	2,63
AIR_GAP	0,038	0,211	1,2	1000	0,18
OSB_2	0,012	0,13	650	1700	0,09

Table 1 Properties of the cell ceiling

CELL WALL

Material (From Ext to Int)	Thickness (m)	Conductivity (W/mK)	Density (Kg/m ³)	Specific Heat Capacity (J/KgK)	Thermal Resistance (m ² K/W)
OSB_1	0,012	0,13	640	2000	0,09
AIR_GAP_1	0,038	0,024	1,029	1004	0,15
WOODEN FIBER	0,04	0,038	640	2100	1,05
OSB_2	0,012	0,13	640	2000	0,09
GLASS WOOL	0,12	0,038	20	1030	3,16
AIR_GAP_2	0,012	0,024	1,029	1004	0,15
OSB_3	0,012	0,13	640	2000	0,09

Table 2 Properties of the cell walls

FLOOR CELL

Material (From Ext to Int)	Thickness (m)	Conductivity (W/mK)	Density (Kg/m ³)	Specific Heat Capacity (J/KgK)	Thermal Resistance (m ² K/W)
WOOD PANEL	0,2	2	2450	1000	0,1
PUR	0,12	0,028	35	1590	0,6
OSB	0,022	0,13	650	1700	0,169

Table 3 Properties of the cell floor

In order to control the test conditions, the facility is also equipped with an air cooling and heating system, as well as an illumination system.

The structure is equipped with:

- Convective Electric heating (electric)
- Fan coil (cold water from a Heat Pump), THE MAXIMUM POWER OF THE S
- Air renewal (from 0,2 vol/h to 4 vol/h)
- The maximum power of the heating and cooling systems is 1000W

The dimensions of the test cell are :

- 2,75 m width
- 2,67 m height
- 4,72 m depth
- Cell volume is 34,95 m³

The facility, as mentioned above, is located in Aglet, France, the coordinates of which are: 53.486183718120024, -1.5139608730113714.

In addition to the geometric characteristics of the structure at this stage, information was collected regarding the use of the structure and its occupation. Since it is a test facility, no human activities are carried out within it. Therefore, only those due to the equipment in it and the lighting are considered in terms of internal gains. Using Excel, schedules were created describing the switching on and off of the systems for each day for a year, useful for evaluating consumption and earnings. All data were collected through documents related to the MBLabs project and through consultation with Nobatek personnel.

3.2.2. PARAMETER ESTIMATION

Once all the data had been collected, the input parameters of the reduced-order model were estimated. The RomPar tool was crucial in this transition. This tool makes it possible to automatically calculate the resistances and thermal capacities for each type of surface and also the solar factor for glazed surfaces. All parameters calculated by this tool were then used as input for the component building of the ROM. The parameters calculated with the tool for each surface described above are shown at the following point.

AWinSouth	area of the south windows [m ²]
AWinNorth	area of the north windows [m ²]
AWinWest	area of the west windows [m ²]
AWinEast	area of the east windows [m ²]
AWinRoof	area of the roof windows [m ²]
GtotWSouth	g total factor South - Solar factor of the glass and shaders
GtotWNorth	g total factor North - Solar factor of the glass and shaders
GtotWWest	g total factor West- Solar factor of the glass and shaders
GtotWEast	g total factor East - Solar factor of the glass and shaders
GtotWRoof	g total factor Roof - Solar factor of the glass and shaders
Ratio_m	Ratio between internal partitions surface and the total building surface
Ratio_wall	Ratio between external wall surface and the total building surface
Ratio_win	Ratio between external windows surface and the total building surface

Ratio_gf	Ratio between ground floor surface and the total building surface
Rwall_is	Thermal Resistance - Internal surface of the Exterior Walls, Facades and Slabs [K/W]
Rwall	Thermal Resistance -Exterior Walls, Facades and Slabs [K/W]
Rwall_es	Thermal Resistance - External surface of the Exterior Walls, Facades and Slabs [K/W]
Cwall	Heat Capacity - Exterior Facades and slabs [J/K]
Rwin_is	Thermal Resistance - Internal surface of the Exterior Windows, Facades [K/W]
Rwin	Thermal Resistance - Exterior Windows, Facades [K/W]
Rwin_es	Thermal Resistance - External surface of the Exterior Windows, Facades [K/W]
Rm_is	Thermal Resistance - Internal surface of the Internal Facades and Slabs [K/W]
Rm	Thermal Resistance - Internal Facades and Slabs [K/W]
Cm	Heat Capacity - Internal Facades and slabs [J/K]
Rgf_is	Thermal Resistance - Internal surface of the Ground floor Slab [K/W]
Rgf	Thermal Resistance - Ground floor Slab [K/W]
Rgf_es	Thermal Resistance - External surface of the Ground floor Slab [K/W]
Cgf	Heat Capacity - Ground floor Slab [J/K]

With regard to the internal gains component, the only internal gain considered is that of lighting. A maximum internal gain for lighting of 30 W was estimated. The same switch-on/off schedule was used for lighting as for the heating and cooling system. A continuous use of the systems every day from 8:00 am to 8:00 pm was set. In the schedules the trend goes to 1 when the system is switched on and to zero when it is switched off.

Below is a screenshot of the schedules created by setting the conditions described previously.

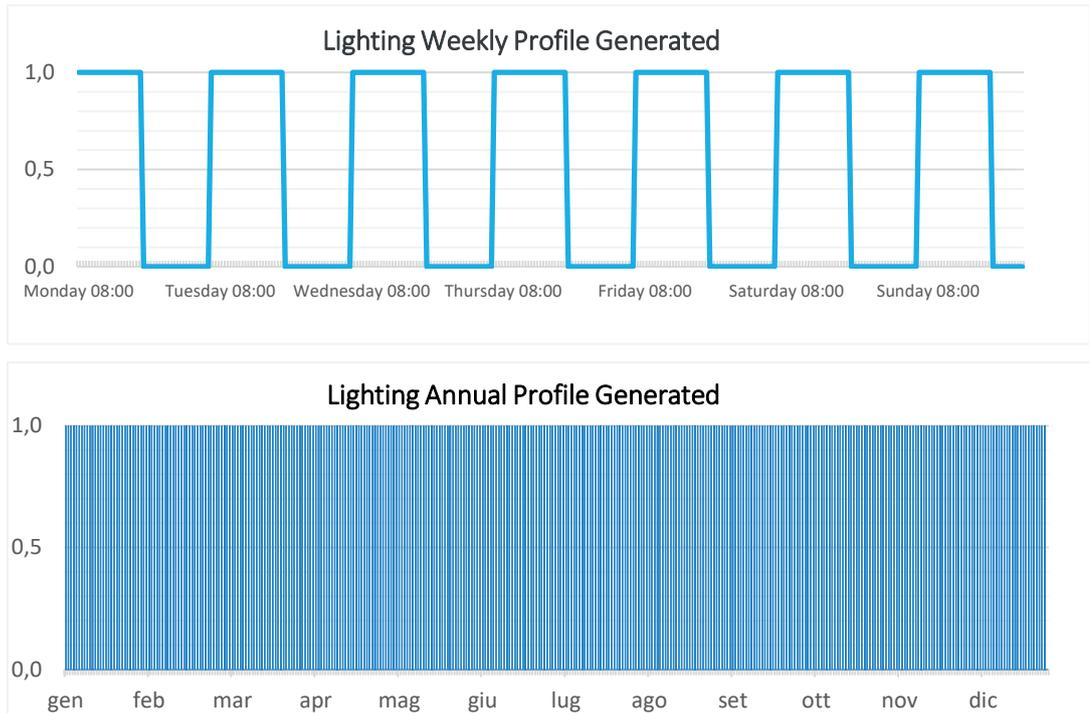
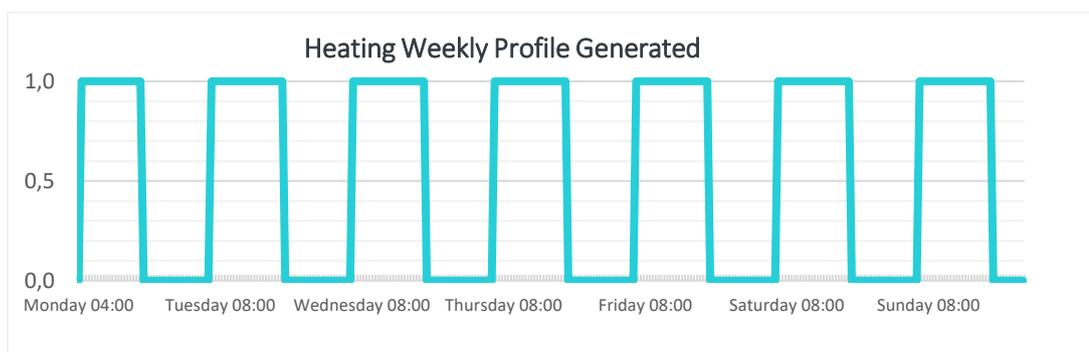


Fig. 17 Weekly and annual lighting profile generated

Turning to the heating and cooling component, the input parameters are related to the maximum power of the systems and their utilization. As mentioned before, the maximum power of heating and cooling systems is 1000 Watt. The operation of the systems is not manually activated, but is automated and linked to the switching on and off time of the system and the set point temperatures. The operation of the system, as for lighting, has been set equal for all days of the year from 8:00 a.m. to 8:00 p.m. the schedules then follow a similar pattern as shown below. The schedules for the cooling system are the same; to avoid repetition, they will not be reported.

The set point temperatures are 20°C for the heating system and 26°C for the cooling system.



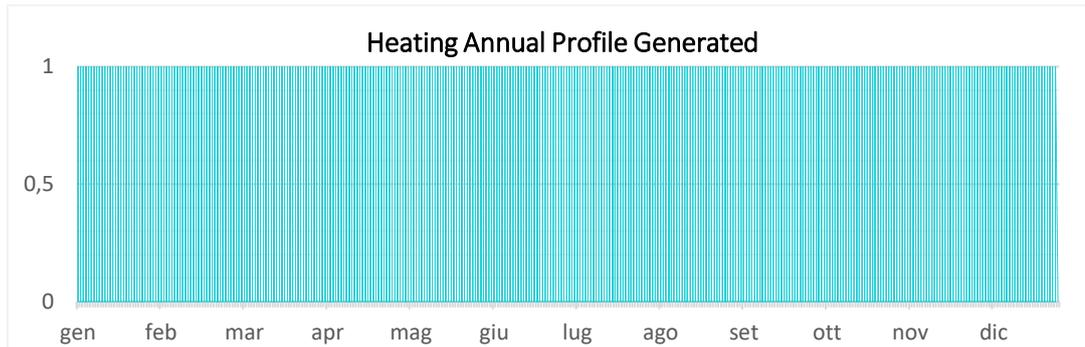


Fig. 18 Weekly and annual heating profile generated

Finally, a “.mos” extension file was created for the weather component as an input into the ROM. The starting point was a file in “.epw” format, the standard format for weather files. The weather file was downloaded from the Energy plus[63] website, which contains files with climatic conditions created specifically for simulations of the thermal behaviour of buildings. The aforementioned website offers weather data for 3,034 locations. Belmulet's weather file was used, a village in the country Mayo in Ireland, the closest place to Galway available. The choice of the weather file for Ireland is related to the fact that the simulations obtained from the ROM will be used to perform scenario analysis for the design of a test facility to be built in Galway, Ireland.

3.2.3. REDUCED ORDER MODELLING

Once all the parameters had been estimated, the actual modelling was carried out. The ROM running on Dymola was used to perform twelve simulations. The thermal response of the test cell was analysed for four different wall samples, two of the heavy type, brick structure, one less insulated and one more insulated, and two of the light type, wooden structure, one less insulated and one more insulated. All the tested samples have dimensions 2.67m*2.75m for a surface area of 7.3425 m². In addition, all headwalls have a minimum glazed area of 3% or an area of 0.220275 m². The glass component is necessary to insert a forcing into the model that would otherwise not give realistic results. The glazed part considered has the same characteristics for all the samples considered, it is a double-glazed window surface with a 16 mm argon cavity.

During the simulations, in order to have a comparable result and to analyse the influence of the cell size on the response, the dimensions of the cell vary but those of the sample tested do not. In general, the walls tested are all made up of a support system on which "coat" type insulation is installed, with high thermal performance and therefore a very

low thermal transmittance[U value]. Where thermal transmittance means the amount of heat that in a defined unit of time passes through an element with a surface area of 1 m² in the presence of a temperature difference of 1 K between the inside and outside. Thermal transmittance is measured in W/m²K. For the calculation of thermal transmittance, the indications provided by the EN ISO 6946:2017 [64] and EN ISO 10077-1:2018[65] standard were used. Where ISO 6946:2017 “provides the method of calculation of the thermal resistance and thermal transmittance of building components and building elements, excluding doors, windows and other glazed units, curtain walling, components which involve heat transfer to the ground, and components through which air is designed to permeate” and ISO 10077-1:2017 “specifies methods for the calculation of the thermal transmittance of windows and pedestrian doors consisting of glazed and/or opaque panels fitted in a frame, with and without shutters”.

Another very important parameter for glazed surfaces is the solar factor (g). This parameter takes into account the amount of solar energy that manages to pass through the glazed surface and reach the interior spaces. The solar factor g is the total solar radiation penetrating through the glazing with in relation to the total incident radiation, and is calculated following the requirements provided by the standard EN ISO 52022-1:2018[66].

It should be specified that in the modelling of the cell, the walls of the cell have been considered as internal walls, since due to the guard zone surrounding the cell, the walls are always kept at the same condition. While the test wall (which is located on the south side of the cell) was modelled as an external wall as it is exposed to the external environment and therefore directly influenced by the weather conditions and solar radiation. The roof surface (ceiling surface) is also exposed to the outside environment, though the ground surface (floor surface) is in contact with the ground and therefore its response is influenced by the ground temperature, which has been set at 20°C. The sample walls are numbered from 1 to 4 as shown below:

- TESTED WALL NUMBER 1 is the least insulated brick wall, with an insulation layer of 14 cm . With a total thickness of 43,4 cm.
- TESTED WALL NUMBER 2 is the most insulated brick wall, with an insulation layer of 18cm. With a total thickness of 47,4 cm.
- TESTED WALL NUMBER 3 is the most insulated cross-laminated timber wall, with a 14 cm insulation layer. With a total thickness of 35,1 cm.

- TESTED WALL NUMBER 4 is the most insulated cross-laminated timber wall, with a 20 cm insulation layer. With a total thickness of 39,1 cm.

For each type of wall, 3 different scenarios were analysed. In each scenario, the parameter that was varied was the size of the cell. For convenience the cell solutions have been named in this way:

- STANDARD CELL: in this scenario the modelled cell has the same dimensions as the real test structure existing in Anglet. The dimension of the cell are:
 - 2,75 m width
 - 2,67 m height
 - 4,72 m depth.
 - Cell volume is 34,95 m³

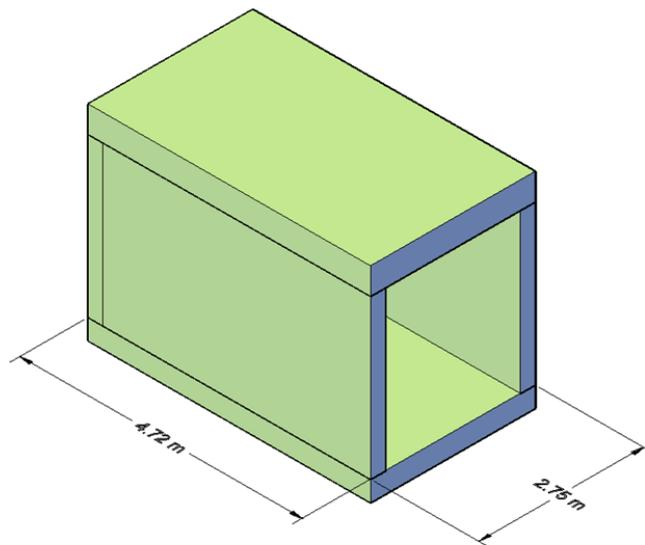


Fig. 19 Representation of the standard cell

- SMALL CELL: in this scenario the cell has a smaller depth than the real one. The dimensions of the cell are:
 - 2,75 m width
 - 2,67 m height
 - 3 m depth
 - Cell volume is 22,0275 m³

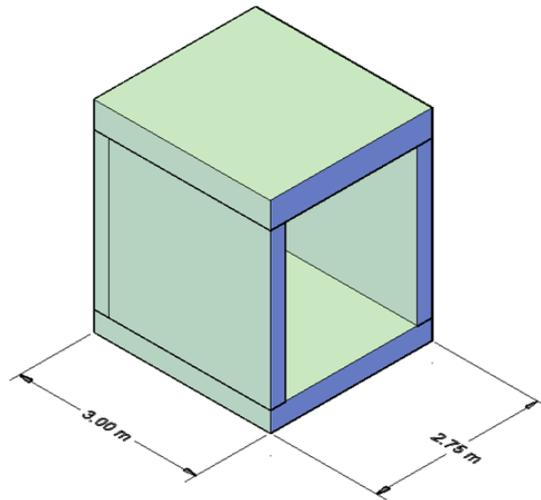


Fig. 20 Representation of the small cell

- LARGE CELL: in this scenario the cell has a greater depth than the real one. The dimensions of the cell are:
 - 2,75 m width
 - 2,67 m height
 - 6 m depth
 - Cell volume is 44,055 m³

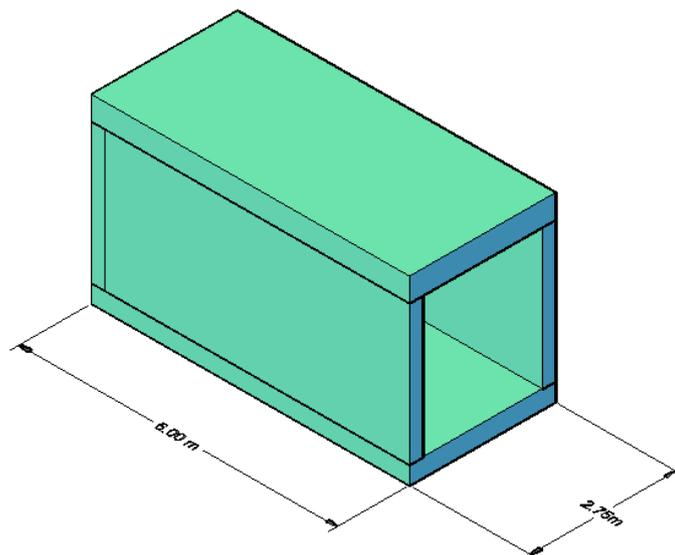


Fig. 21 Representation of the large cell

Subsequently, the input parameters for each tested wall type/cell size combination and the modelling results are given, the modelling outputs that will be evaluated are:

- The air temperature inside the cell(assumed uniform within the cell)
- The mean radiant temperature

- The electricity consumption
- The energy demand for heating/cooling the cell
- The time taken for the simulation.

The modelling is on an annual basis.

3.2.3.1. Tested wall number 1

Material (from int to ext)	Thickness (mm)	Conductivity (W/m.K)	Density (kg/m ³)	Specific heat capacity (J/KgK)
Levelling mortar	15	0,95	1830	1000
Brick	250	0,170	700	850
Mortar for levelling	4	0,95	1830	1000
Mortar for bonding	4	0,32	1400	1100
Eps w30	140	0,035	30	1450
Mortar for bonding with glass fibre mesh	6	0,32	1400	1100
Acrylic plaster	15	0,89	1300	1000

Table 4 Tested wall number 1

Calculated U Value W/m²K 0,1805
 Thermal Capacity kJ/K 517

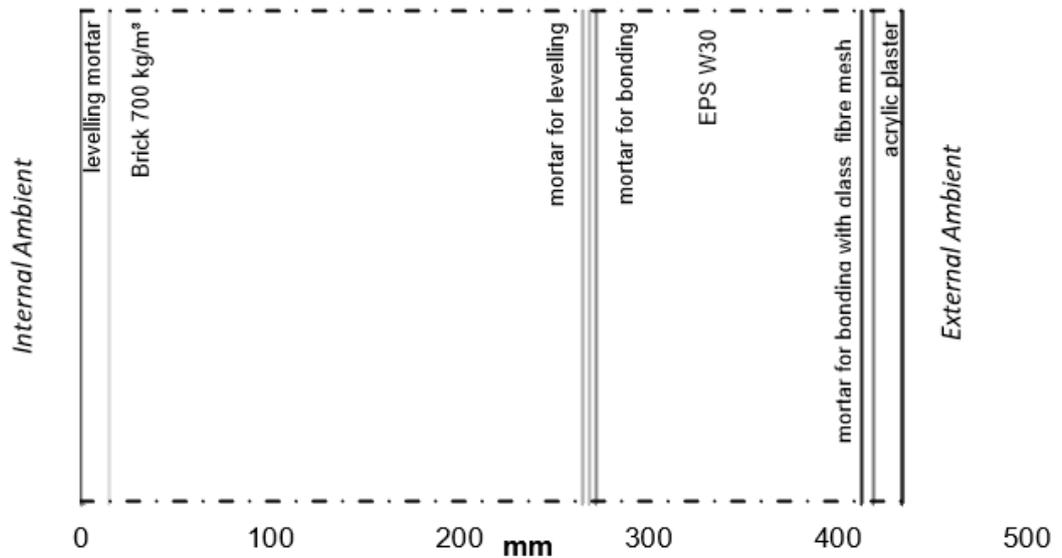


Fig. 22 Tested Wall number 1

3.2.3.1.1. Standard cell

Parameters estimated using the RomPar tool

AWinSouth	0	Ratio_gf	0,19645808
AWinNorth	0	Rwall	0,7855217
AWinWest	0	Rwall_es	0,00196826
AWinEast	0	Cwall	1648464,68
AWinRoof	0	Rwin_is	0,59017138
GtotWSouth	0,63	Rwin	1,74606916
GtotWNorth	0	Rwin_es	0,18159119
GtotWWest	0	Rm_is	0,00199709
GtotWEast	0	Rm	0,22007626
GtotWRoof	0	Cm	3392003,31
Ratio_m	0,49261788	Rgf_is	0,01309707
Ratio_wall	0,30759009	Rgf	0,15791412
Ratio_win	0,00333396	Rgf_es	0,00308166
Rwall_is	0,00639685	Cgf	6762424,24

Simulation results

- **Time for integration** 42.4 seconds
- **Air temperature**
 - 18,62140088 °C average value
 - 1,442064685 standard deviation
 - 15,00184 °C minimum value
 - 22,987167 °C maximum value
- **Mean radiant temperature**
 - 18,63644806 °C average value
 - 1,397778428 standard deviation
 - 15,157363 °C minimum value
 - 22,892231 °C maximum value
- **Electric energy demand**
 - 136,875 kWh maximum value
- **Fossil energy demand**
 - 558,9805 kWh maximum value

Graphical results

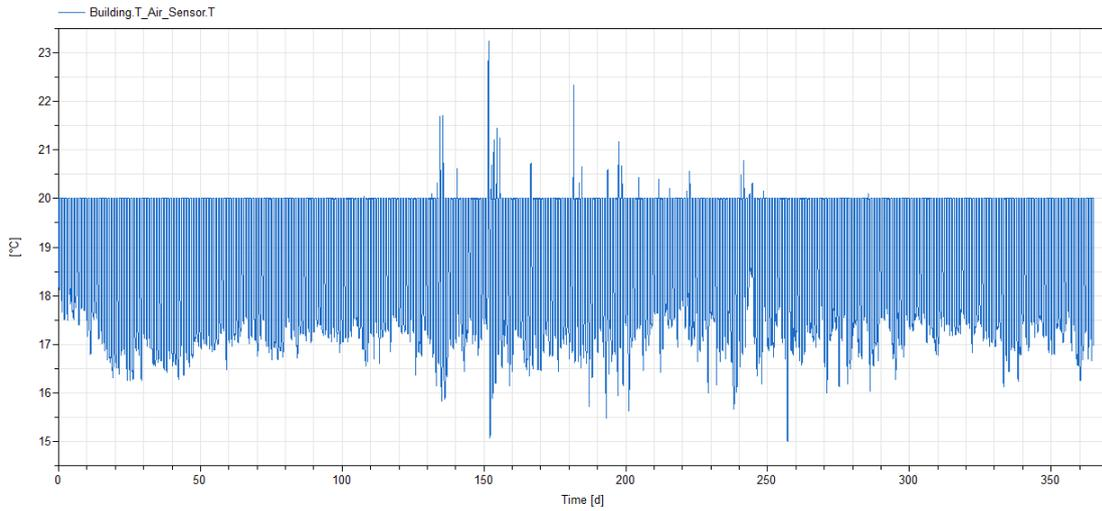


Fig. 22 Annual trend of the Air Temperature

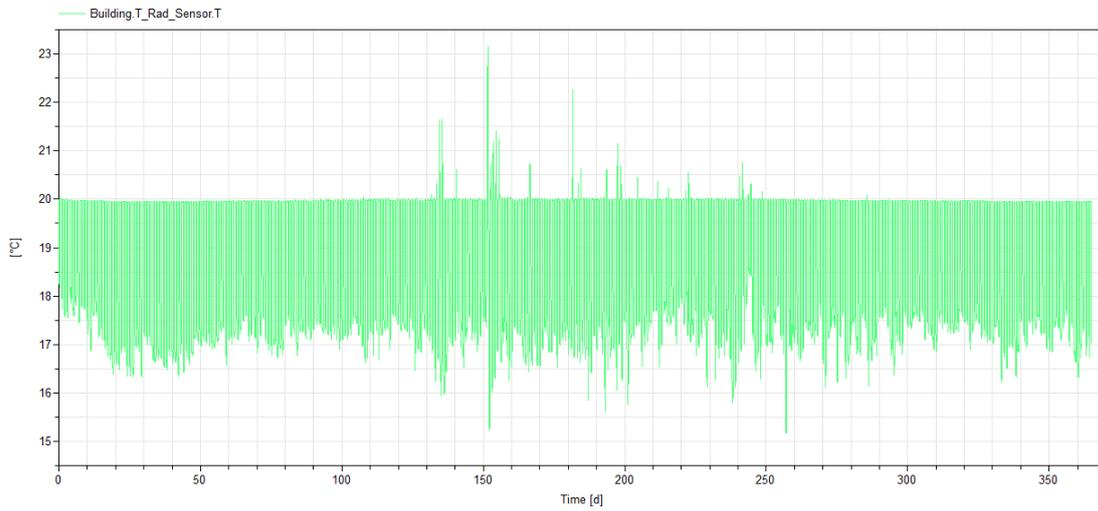


Fig. 23 Annual trend of the Mean radiant temperature

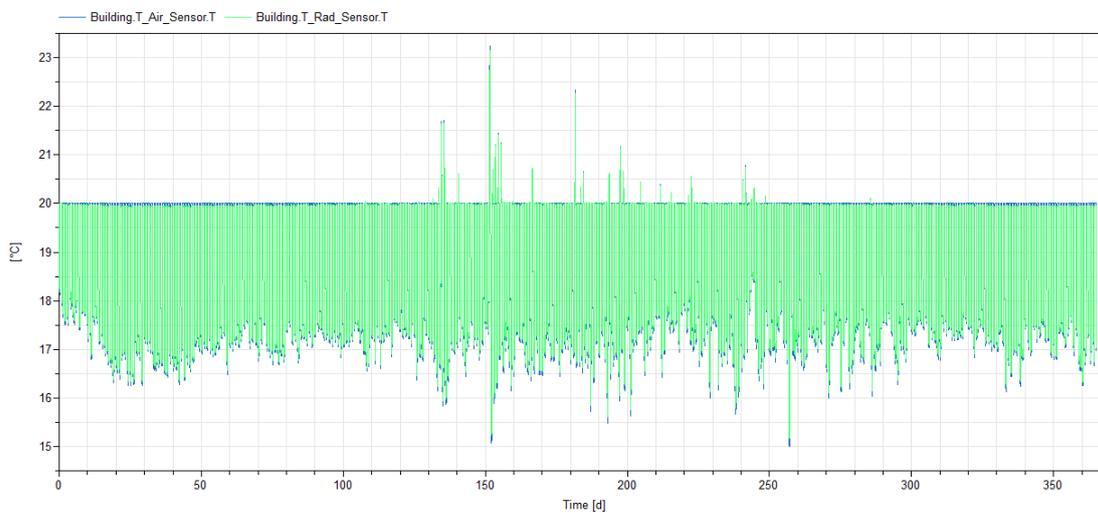


Fig. 23 Comparison between mean radiant temperature and air temperature

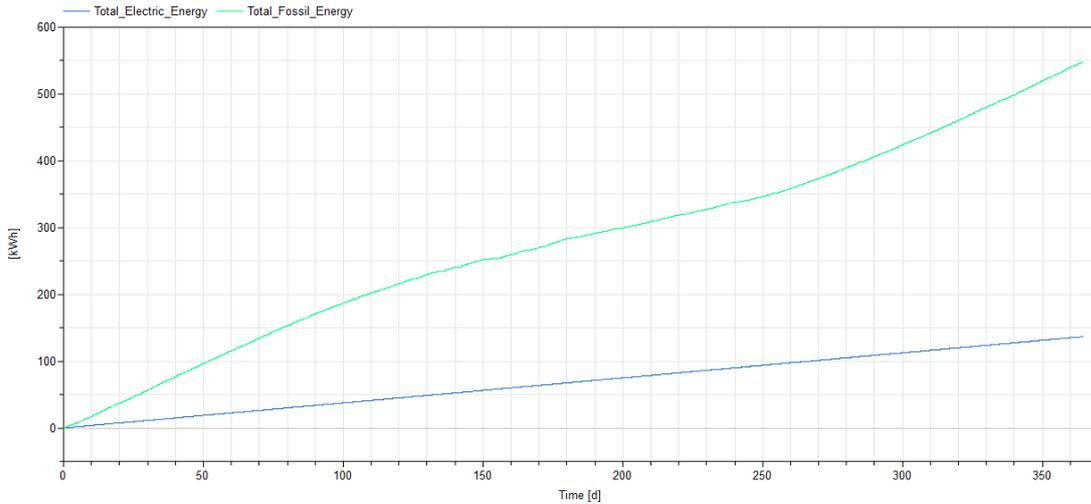


Fig. 24 Annual trends in electricity and fossil energy demand

3.2.3.1.2. Small cell

Parameters estimated using the RomPar tool

AWinSouth	0	Rwall	1,031804
AWinNorth	0	Rwall_es	0,002565
AWinWest	0	Cwall	1648465
AWinEast	0	Rwin_is	0,590171
AWinRoof	0	Rwin	1,746069
GtotWSouth	0,75	Rwin_es	0,181591
GtotWNorth	0	Rm_is	0,002782
GtotWWest	0	Rm	0,306598
GtotWEast	0	Cm	2434785
GtotWRoof	0	Rgf_is	0,020606
Ratio_m	0,492617	Rgf	0,248452
Ratio_wall	0,32878	Rgf_es	0,004848
Ratio_win	0,004645	Cgf	4298151
Ratio_gf	0,173958	Rwall_is	0,008337

Simulation results

- **Time for integration** 45 seconds

- **Air temperature**

18,63591243 °C average value

1,501290905 standard deviation

15,133757 °C minimum value

24,41846 °C maximum value

- Mean radiant temperature**
 18,94300827 °C average value
 1,468635007 standard deviation
 15,556051 °C minimum value
 24,614424 °C maximum value
- Electrical energy demand**
 136,875 kWh maximum value
- Fossil energy demand**
 296,25763 kWh maximum value

Graphical results

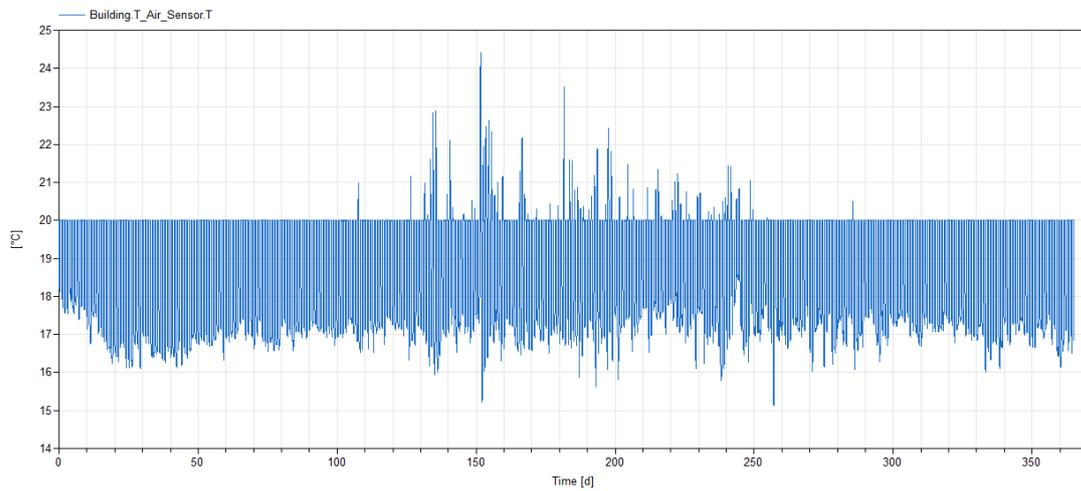


Fig. 25 Annual trend of the Air Temperature

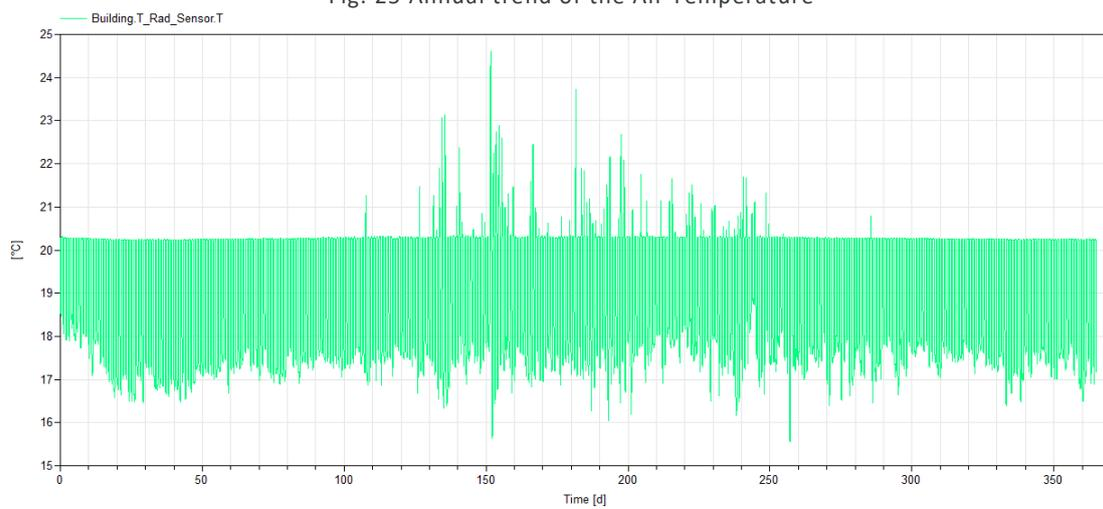


Fig. 26 Annual trend of the Mean radiant temperature

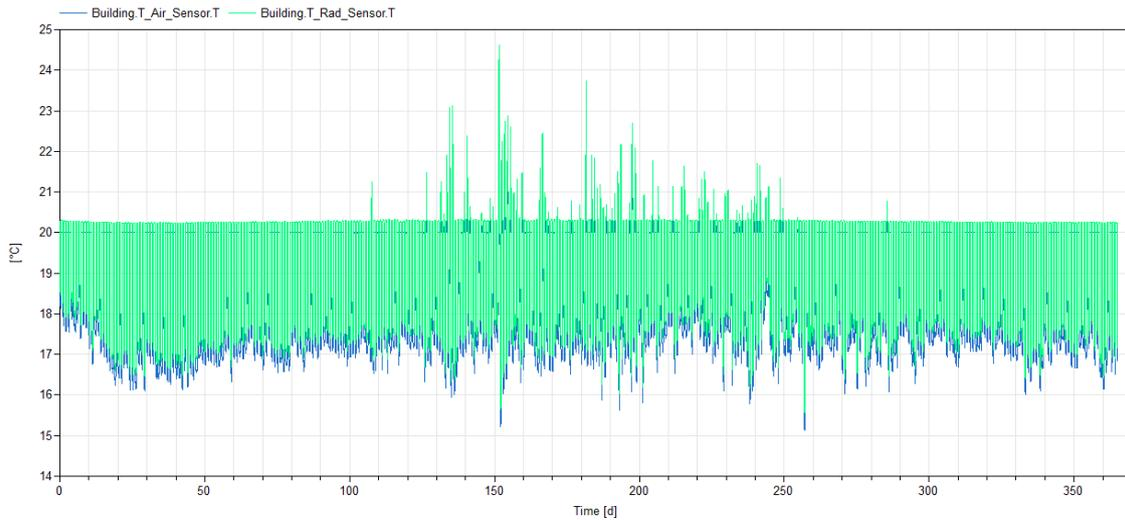


Fig. 27 Comparison between mean radiant temperature and air temperature

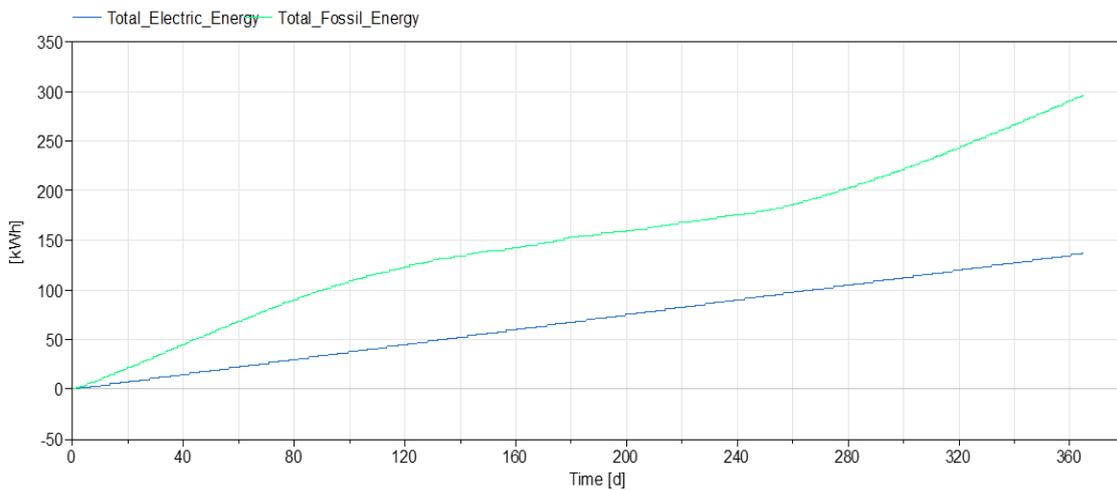


Fig. 28 Annual trends in electricity and fossil energy demand

3.2.3.1.3. Large cell

Parameters estimated using the RomPar tool

AWinSouth	0,220275	Rwall_is	0,005452
AWinNorth	0	Rwall	0,647041
AWinWest	0	Rwall_es	0,001678
AWinEast	0	Cwall	1648465
AWinRoof	0	Rwin_is	0,590171
GtotWSouth	0,63	Rwin	1,746069
GtotWNorth	0	Rwin_es	0,181591
GtotWWest	0	Rm_is	0,00165
GtotWEast	0	Rm	0,18188
GtotWRoof	0	Cm	4104352
Ratio_m	0,492618	Rgf_is	0,010303
Ratio_wall	0,298235	Rgf	0,124226
Ratio_win	0,002755	Rgf_es	0,002424

Ratio_gf 0,206391 Cgf 8596302

Simulation results

- **Time for integration** 45.1 seconds
- **Air temperature**
18,62658392°C average value
1,432440089 standard deviation
14,992492 °C minimum value
22,766052 °C maximum value
- **Mean radiant temperature**
18,6396103 °C average value
1,384300253 standard deviation
15,15466 °C minimum value
22,666376 °C maximum value
- **Electrical energy demand**
136,875 kWh maximum value
- **Fossil energy demand**
736,94275 kWh maximum value

Graphical results

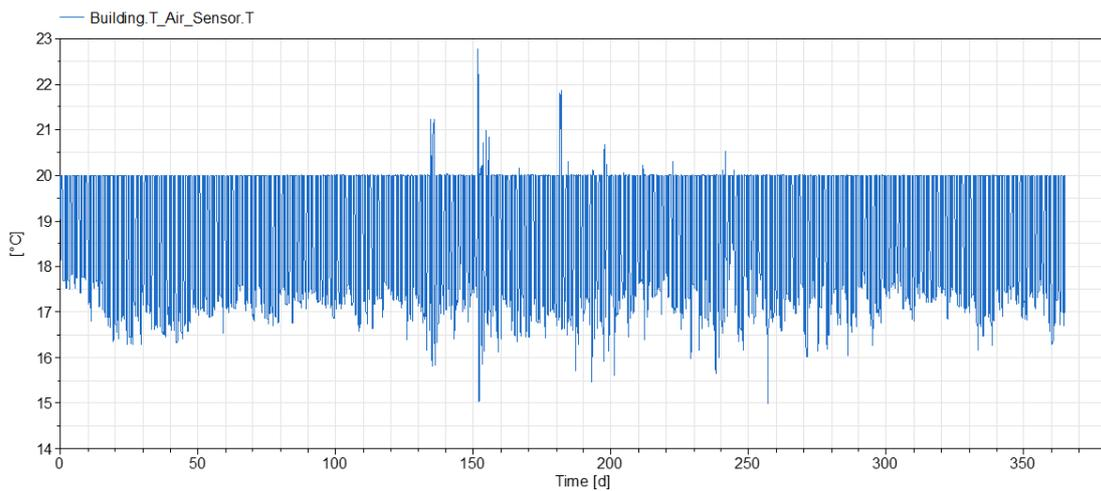


Fig. 29 Annual trend of the Air Temperature

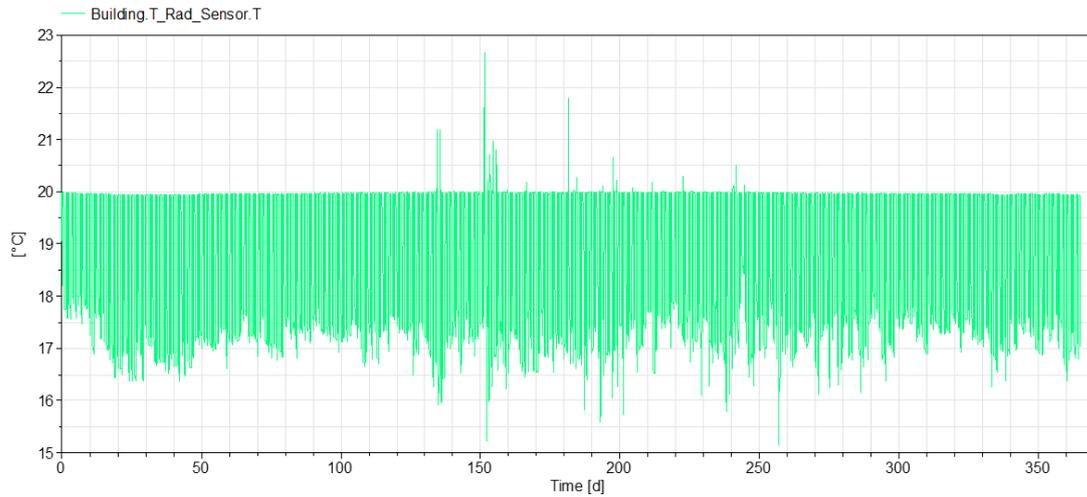


Fig. 30 Annual trend of the Mean radiant temperature

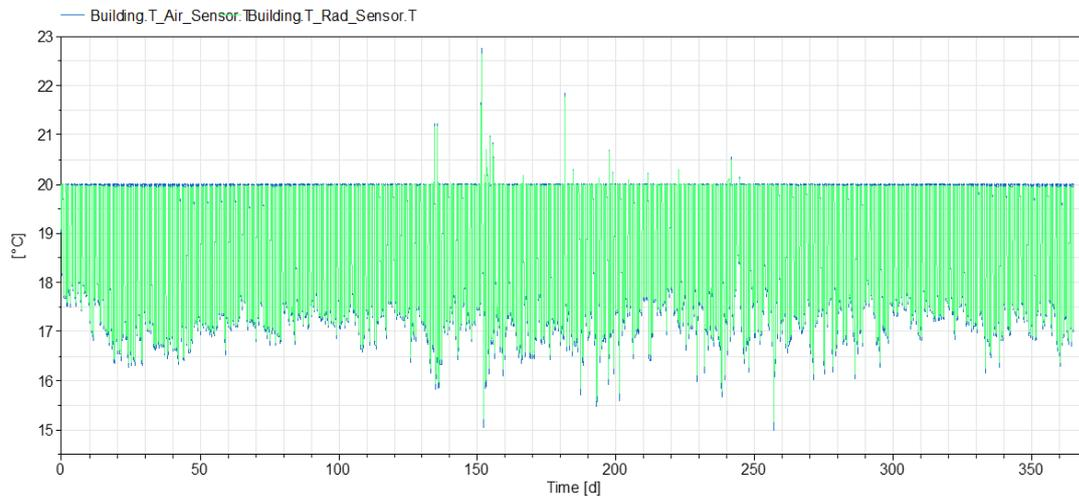


Fig. 31 Comparison between Mean radiant temperature and air temperature

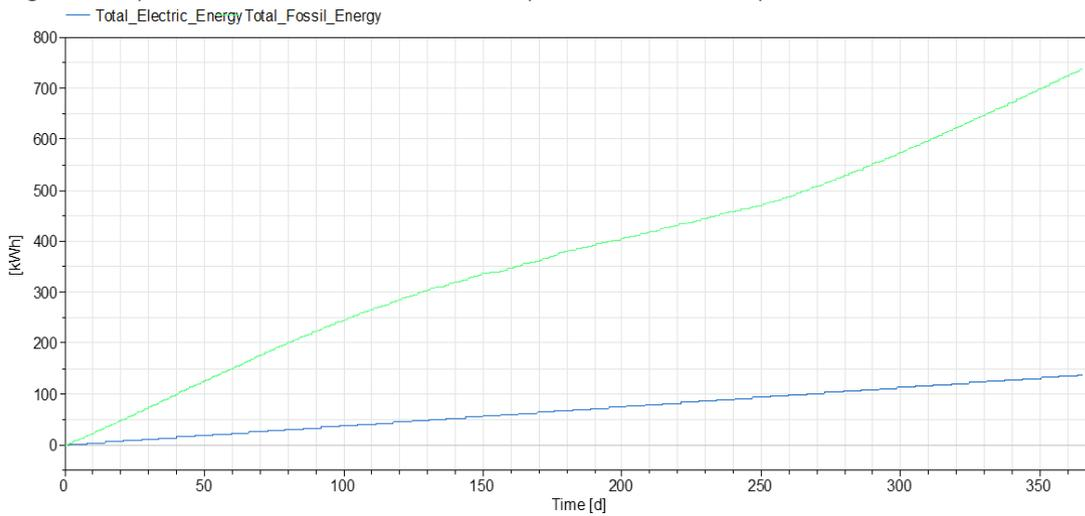


Fig. 32 Annual trends in electricity and fossil energy demand

3.2.3.2. Tested wall number 2

Material (from int to ext)	Thickness (mm)	Conductivity (W/mK)	Density (kg/m ³)	Specific heat capacity (J/KgK)
levelling mortar	15	0,95	1830	1000
brick	250	0,170	700	850
mortar for levelling	4	0,95	1830	1000
mortar for bonding	4	0,32	1400	1100
EPS W30	180	0,035	30	1450
mortar for bonding with glass fibre mesh	6	0,32	1400	1100
acrylic plaster	15	0,89	1300	1000

Calculated U Value W/m²K 0,1497

Thermal Capacity kJ/K 477

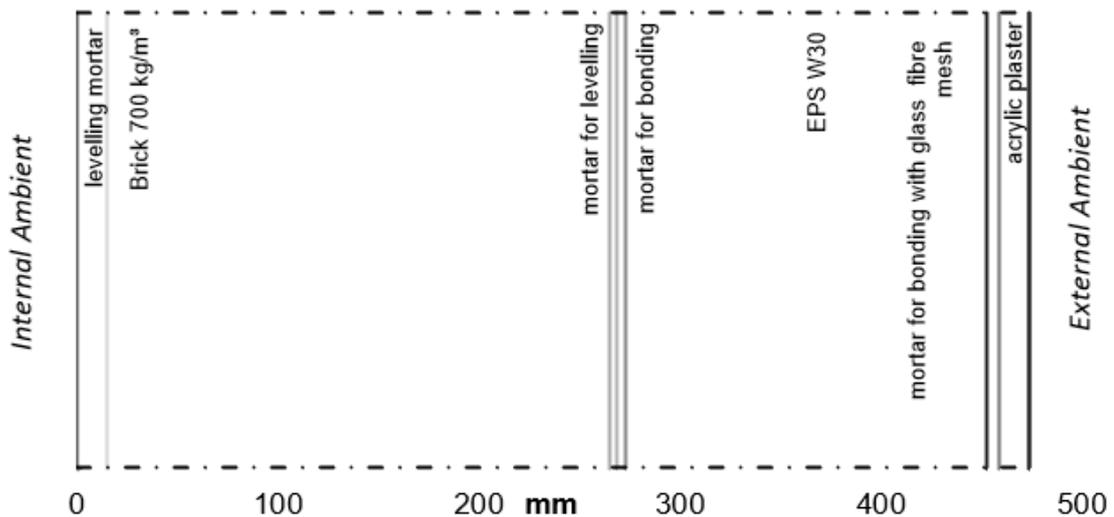


Fig. 33 Tested Wal number 2

3.2.3.2.1. Standard cell

Parameters estimated using the RomPar tool

AWinSouth	0,220275	Rwall_is	0,006397
AWinNorth	0	Rwall	0,823254
AWinWest	0	Rwall_es	0,001968
AWinEast	0	Cwall	1661241
AWinRoof	0	Rwin_is	0,590171
GtotWSouth	0,63	Rwin	1,746069
GtotWNorth	0	Rwin_es	0,181591
GtotWWest	0	Rm_is	0,001997
GtotWEast	0	Rm	0,220076

GtotWRoof	0	Cm	3392003
Ratio_m	0,492618	Rgf_is	0,013097
Ratio_wall	0,30759	Rgf	0,157914
Ratio_win	0,003334	Rgf_es	0,003082
Ratio_gf	0,196458	Cgf	6762424

Simulation results

- **Time for integration** 47 seconds

- **Air temperature**

18,63051765 °C average value
1,440079926 standard deviation
15,0029955 °C minimum value
23,252642 °C maximum value

- **Mean radiant temperature**

18,64672562 °C average value
1,396948971 standard deviation
15,158549°C minimum value
23,156033°C maximum value

- **Electrical energy demand**

136,875 kWh maximum value

- **Fossil energy demand**

547,79834 kWh maximum value

Graphical results

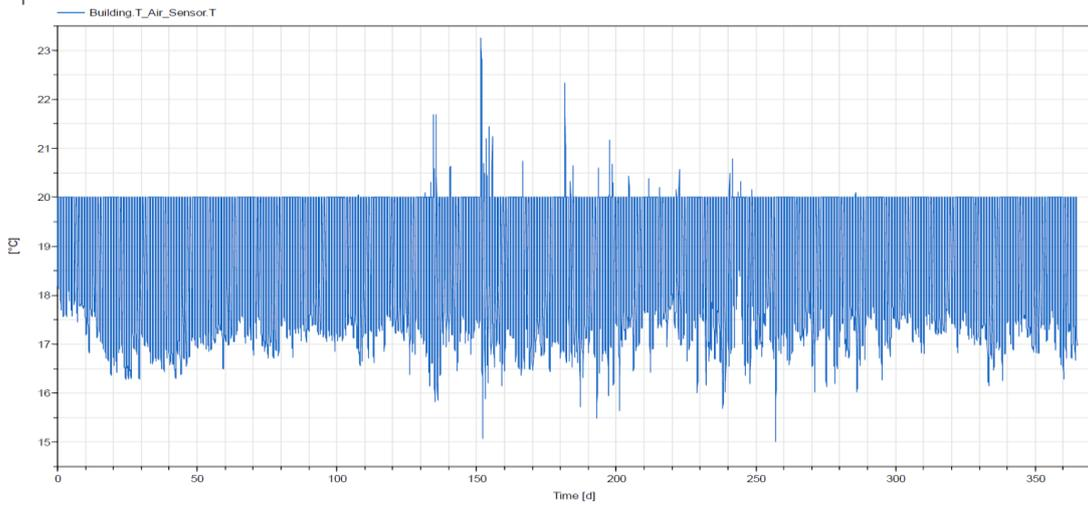


Fig. 34 Annual trend of the Air Temperature

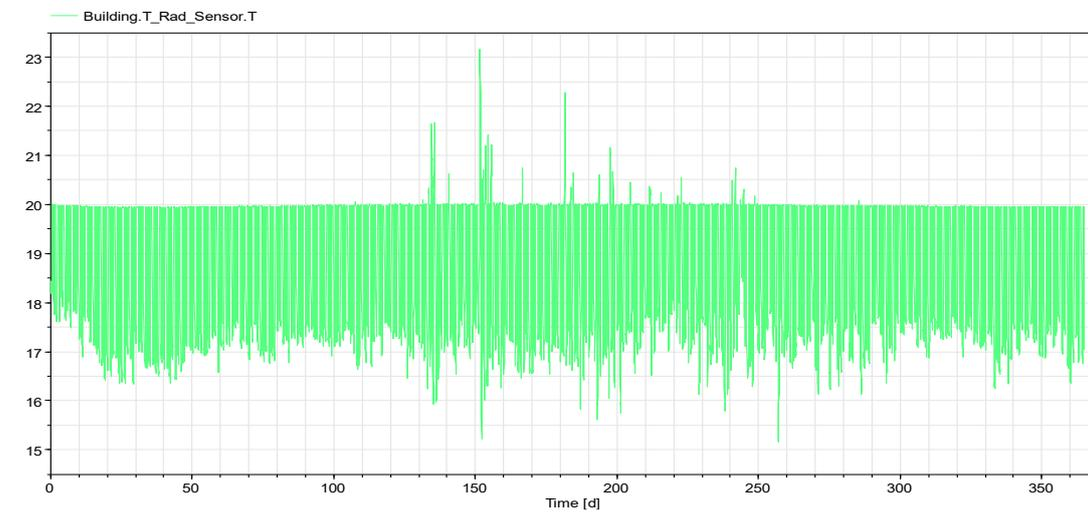


Fig. 35 Annual trend of the Mean radiant temperature

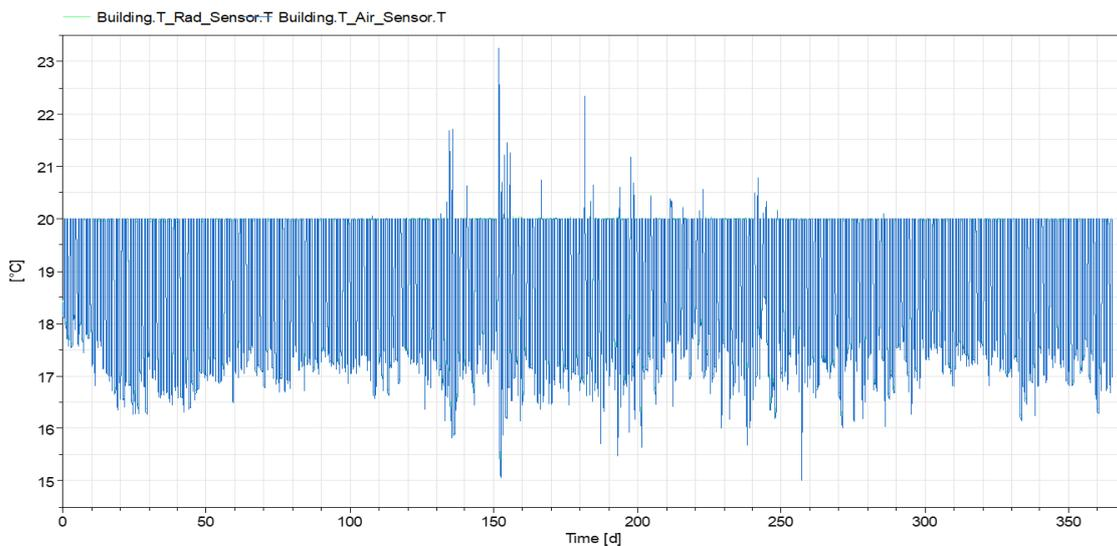


Fig. 36 Comparison between Mean radiant temperature and air temperature

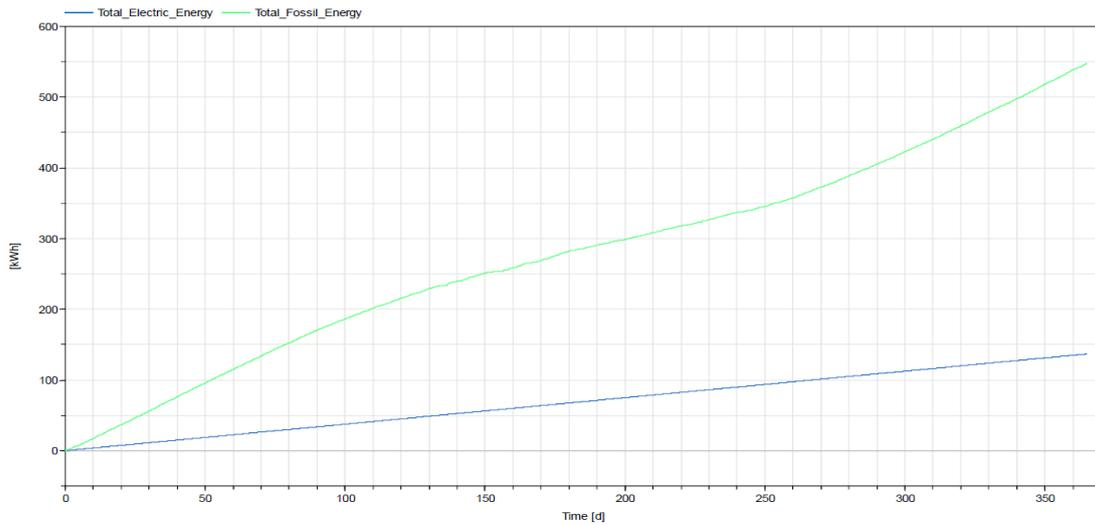


Fig. 37 Annual trends in electricity and fossil energy demand

3.2.3.2.2. Small cell

Parameters estimated using the RomPar tool

AWinSouth	0,220275	Ratio_gf	0,174
AWinNorth	0	Rwall_is	0,008
AWinWest	0	Rwall	1,101
AWinEast	0	Rwall_es	0,002565
AWinRoof	0	Cwall	1661240,62500
GtotWSouth	0,63	Rwin_is	0,590171
GtotWNorth	0	Rwin	1,746069162
GtotWWest	0	Rwin_es	0,181591
GtotWEast	0	Rm_is	0,002782236
GtotWRoof	0	Rm	0,3065977
Ratio_m	0,49261707	Cm	2434784,983628
Ratio_wall	0,328780381	Rgf_is	0,02060606
Ratio_win	0,005	Rgf	0,248451548
Rgf_es	0,004848	Cgf	4298151,000000

Simulation results

- **Time for integration** 48.9 seconds
- **Air temperature**
 - 18,64947003 °C average value
 - 1,490293936 standard deviation
 - 15,1273775 °C minimum value

24,459312 °C maximum value

- **Mean radiant temperature**

18,95769018 °C average value

1,458476697 standard deviation

15,549543 °C minimum value

24,656921 °C maximum value

- **Electrical energy demand**

136,875 kWh maximum value

- **Fossil energy demand**

292,75192 kWh maximum value

Graphical results

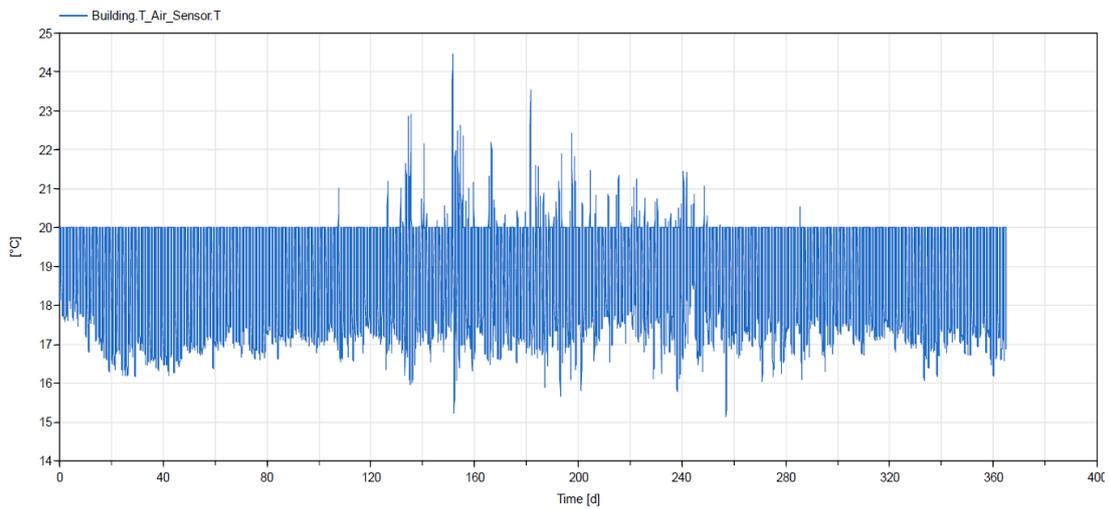


Fig. 38 Annual trend of the Air Temperature

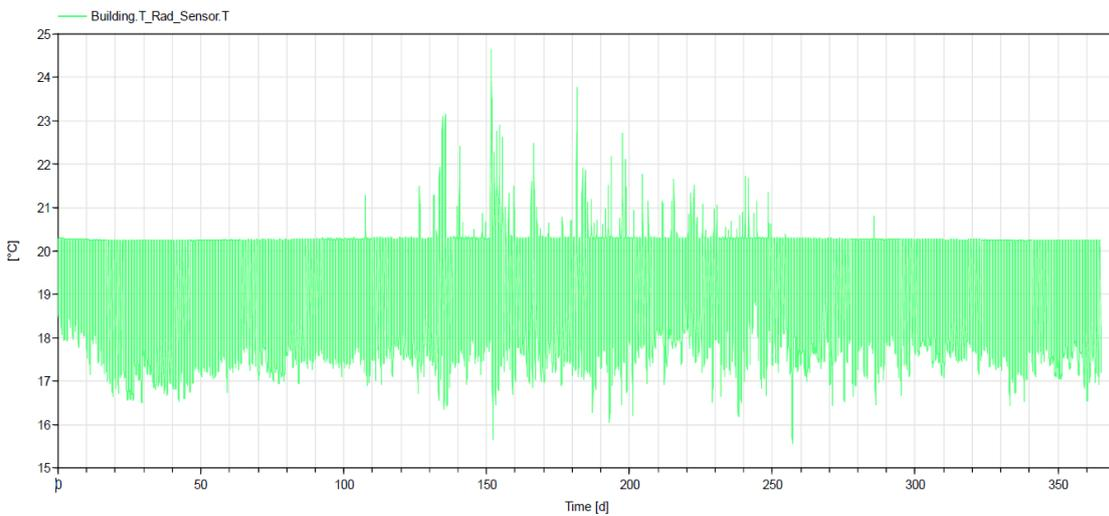


Fig. 39 Annual trend of the main radiant temperature

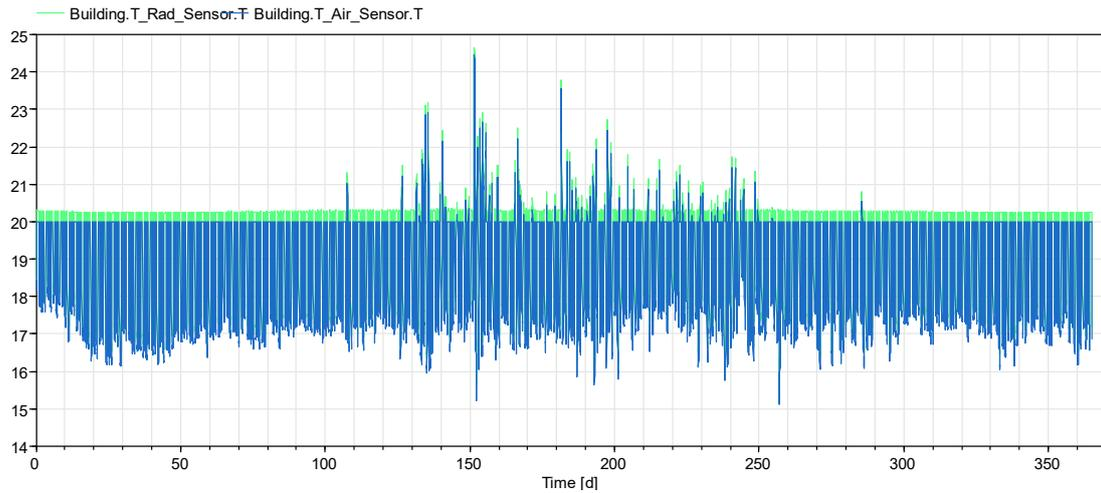


Fig. 40 Comparison between main radiant temperature and air temperature

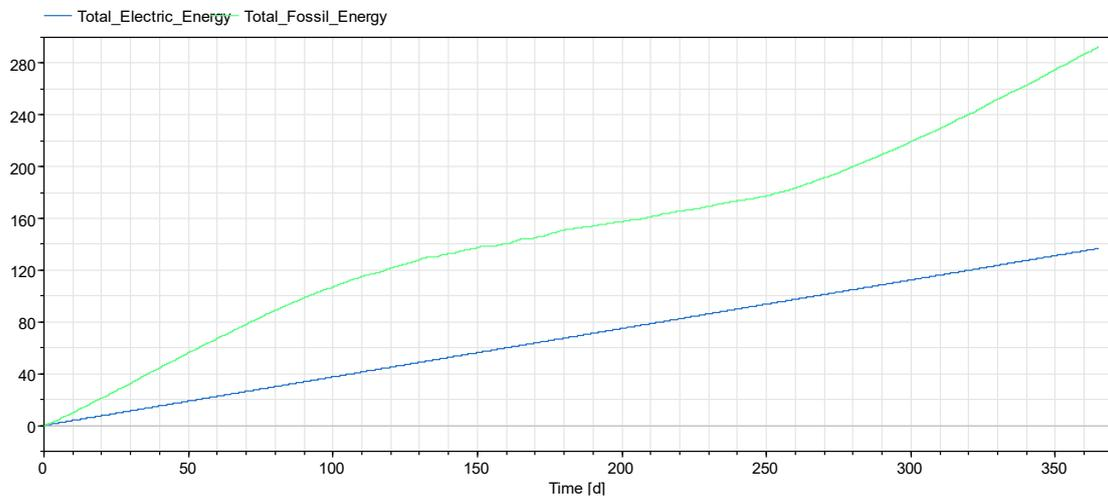


Fig. 41 Annual trends in electricity and fossil energy demand

3.2.3.2.3. Large cell

Parameters estimated using the RomPar tool

AWinSouth	0,220275	Rwall_is	0,005452
AWinNorth	0	Rwall	0,672769
AWinWest	0	Rwall_es	0,001678
AWinEast	0	Cwall	1661241
AWinRoof	0	Rwin_is	0,590171
GtotWSouth	0,63	Rwin	1,746069
GtotWNorth	0	Rwin_es	0,181591
GtotWWest	0	Rm_is	0,00165
GtotWEast	0	Rm	0,18188
GtotWRoof	0	Cm	4104352
Ratio_m	0,492618	Rgf_is	0,010303
Ratio_wall	0,298235	Rgf	0,124226
Ratio_win	0,002755	Rgf_es	0,002424
Ratio_gf	0,206391	Cgf	8596302

Simulation results

- **Time for integration** 41.6 seconds
- **Air temperature**
 - 18,63336892°C average value
 - 1,426177298 standard deviation
 - 14,989054°C minimum value
 - 22,781431°C maximum value
- **Mean radiant temperature**
 - 18,64703996 °C average value
 - 1,378541781 standard deviation
 - 15,151159°C minimum value
 - 22,682812°C maximum value
- **Electrical energy demand**
 - 136,875 kWh maximum value
- **Fossil energy demand**
 - 733,4357 kWh maximum value

Graphical results

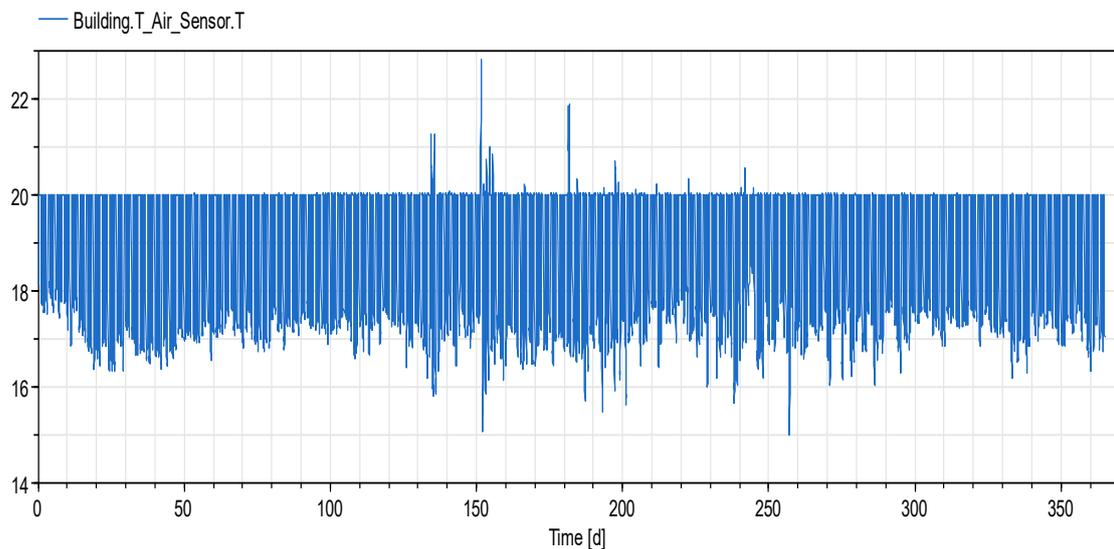


Fig. 42 Annual trend of the Air Temperature

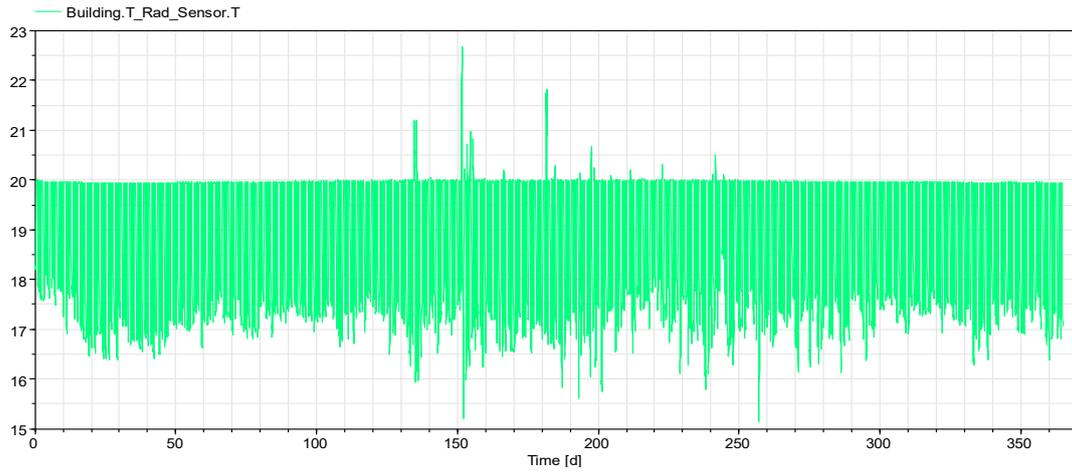


Fig. 43 Annual trend of the main radiant temperature

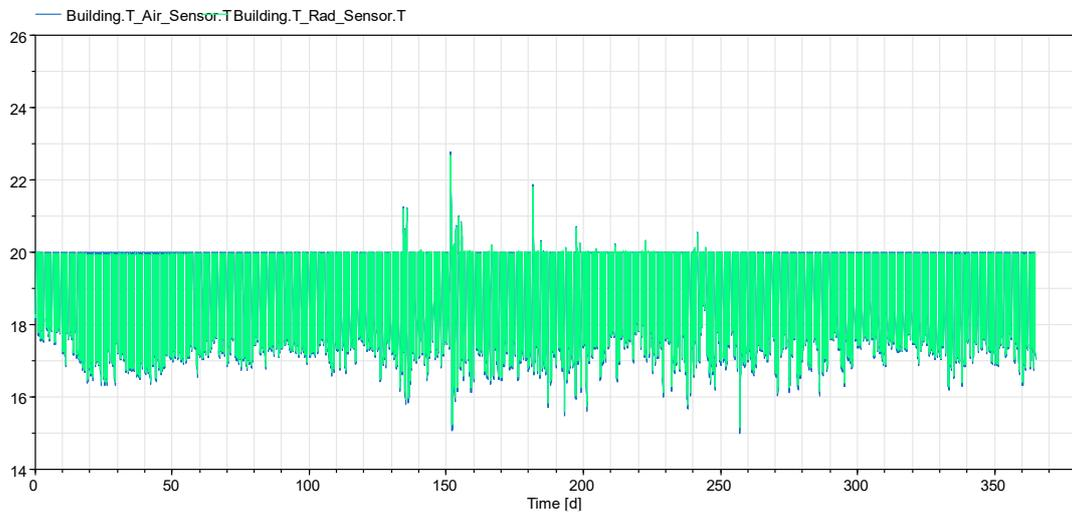


Fig. 44 Comparison between mean radiant temperature and air temperature

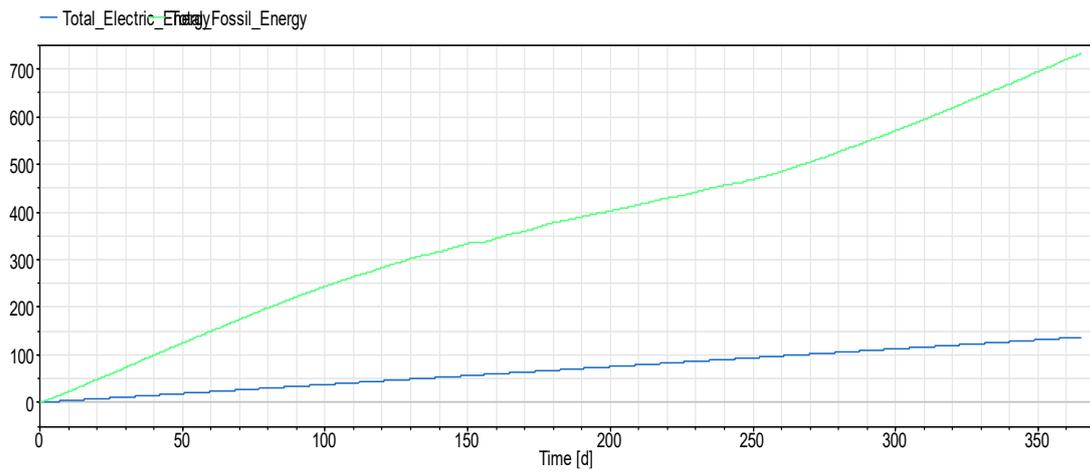


Fig. 45 Annual trends in electricity and fossil energy demand

3.2.3.3. Tested wall number 3

Material (from int to ext)	Thickness (mm)	Conductivity (W/m.K)	Density (kg/m ³)	Specific heat capacity (J/KgK)
plasterboard	13	0,21	900	1050
gypsum fibre	13	0,36	1180	1000
rock wool	50	0,033	70	1030
multilayer wood panel	100	0,13	500	1600
rock wool	160	0,036	90	1030
lime plaster	15	0,68	1620	1000

Calculated U Value W/m²K 0,1413

Thermal Capacity kJ/K 414

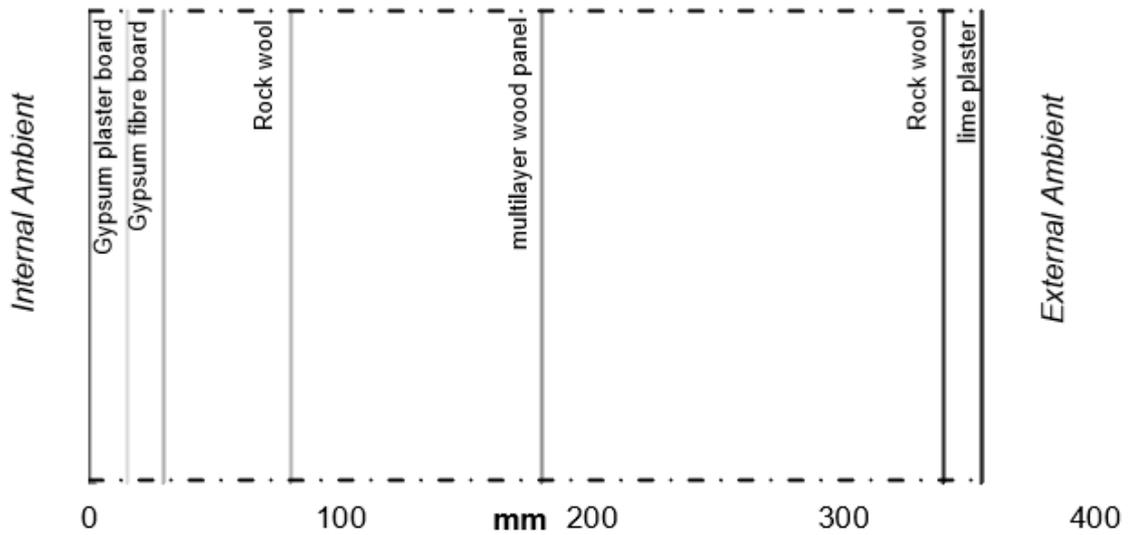


Fig. 46 Tested wall number 3

3.2.3.3.1. Standard cell

Parameters estimated using the RomPar tool

AWinSouth	0,220275	Rwall_is	0,006397
AWinNorth	0	Rwall	0,8363
AWinWest	0	Rwall_es	0,001968
AWinEast	0	Cwall	1080177
AWinRoof	0	Rwin_is	0,590171
GtotWSouth	0,63	Rwin	1,746069
GtotWNorth	0	Rwin_es	0,181591
GtotWWest	0	Rm_is	0,001997
GtotWEast	0	Rm	0,220076
GtotWRoof	0	Cm	3392003
Ratio_m	0,492618	Rgf_is	0,013097
Ratio_wall	0,30759	Rgf	0,157914

Ratio_win	0,003334	Rgf_es	0,003082
Ratio_gf	0,196458	Cgf	6762424

Simulation results

- **Time for integration** 42.4 seconds
- **Air temperature**
 - 18,63160049°C average value
 - 1,439571394 standard deviation
 - 14,99505 °C minimum value
 - 23,274782 °C maximum value
- **Mean radiant temperature**
 - 18,64795931 °C average value
 - 1,396568059 standard deviation
 - 15,150392 °C minimum value
 - 23,17923 °C maximum value
- **Electrical energy demand**
 - 136,875 kWh maximum value
- **Fossil energy demand**
 - 547,1965 kWh maximum value

Graphical results

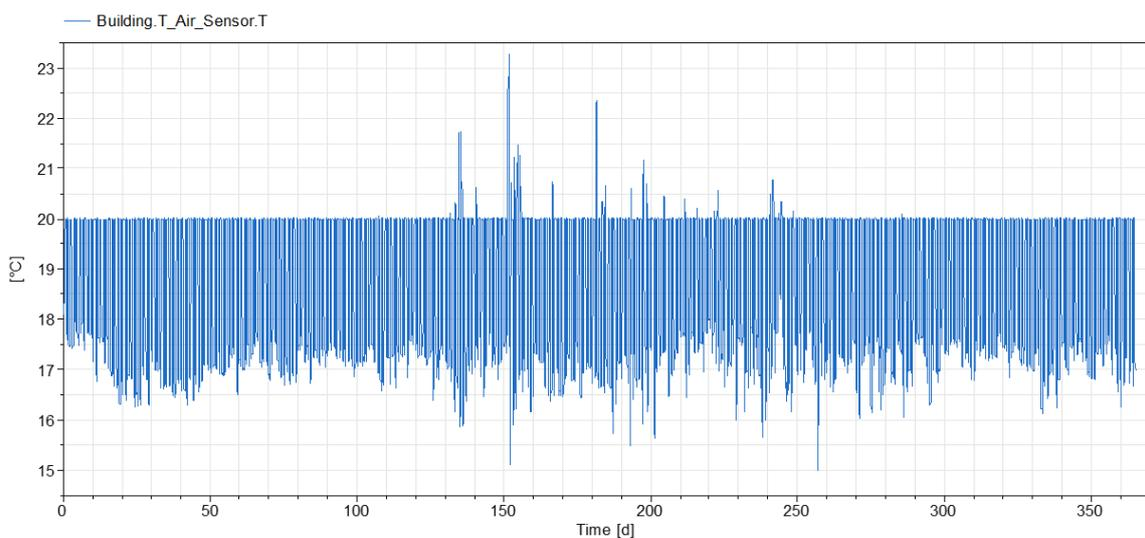


Fig. 47 Annual trends of the air temperature

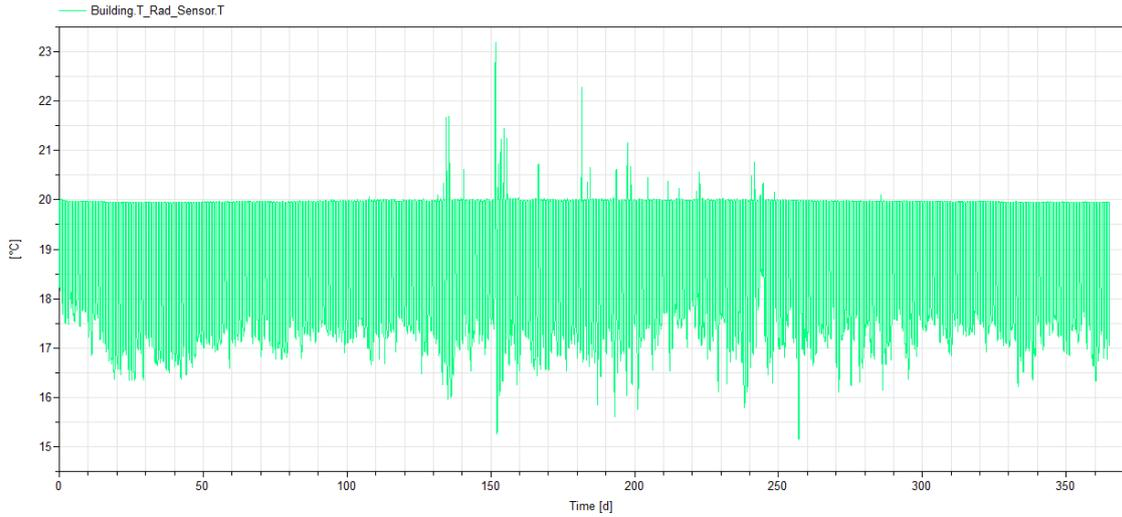


Fig. 48 Annual trends of the main radiant temperature

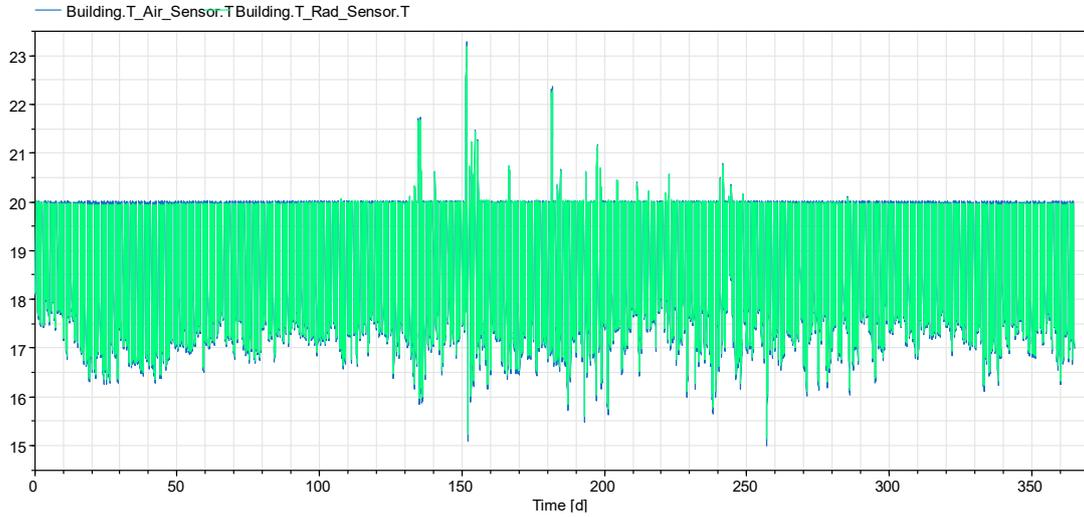


Fig. 49 Comparison between the main radiant temperature and the air temperature

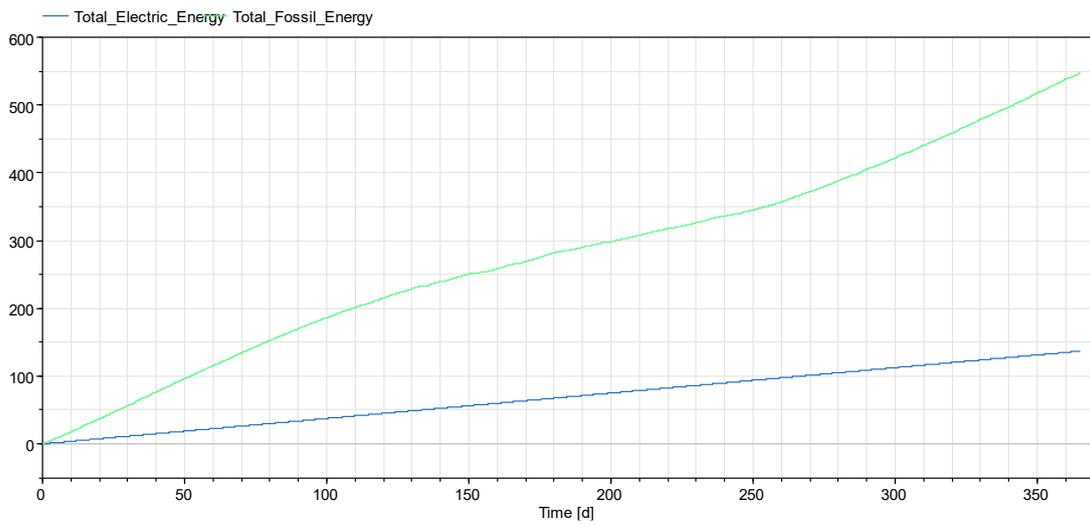


Fig. 50 Annual trends in electricity and fossil energy demand

3.2.3.3.2. Small cell

Parameters estimated using the RomPar tool

AWinSouth	0,220275	Rwall	1,124387
AWinNorth	0	Rwall_es	0,002565
AWinWest	0	Cwall	1080177
AWinEast	0	Rwin_is	0,590171
AWinRoof	0	Rwin	1,746069
GtotWSouth	0,63	Rwin_es	0,181591
GtotWNorth	0	Rm_is	0,002782
GtotWWest	0	Rm	0,306598
GtotWEast	0	Cm	2434785
GtotWRoof	0	Rgf_is	0,020606
Ratio_m	0,492617	Rgf	0,248452
Ratio_wall	0,32878	Rgf_es	0,004848
Ratio_win	0,004645	Ratio_gf	0,173958
Rwall_is	0,008337	Cgf	4298151

Simulation results

- **Time for integration** 46.6 seconds
- **Air temperature**
 - 18,65145913 °C average value
 - 1,489829027 standard deviation
 - 15,119817 °C minimum value
 - 24,484861 °C maximum value
- **Mean radiant temperature**
 - 18,95989459 °C average value
 - 1,458206232 standard deviation
 - 15,541793 °C minimum value
 - 24,683569 °C maximum value
- **Electrical energy demand**
 - 136,875 kWh maximum value
- **Fossil energy demand**
 - 292,15802 kWh maximum value

Graphical results

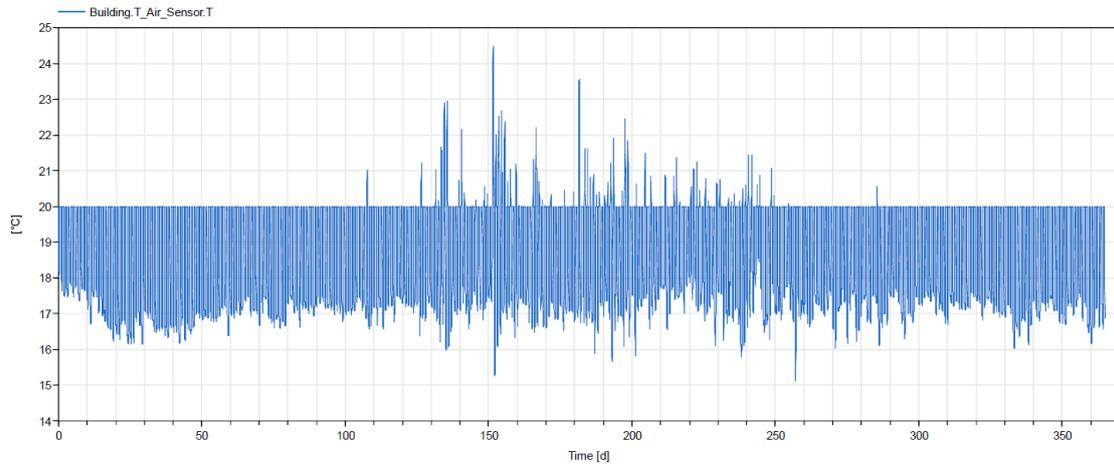


Fig. 51 Annual trend of the Air Temperature

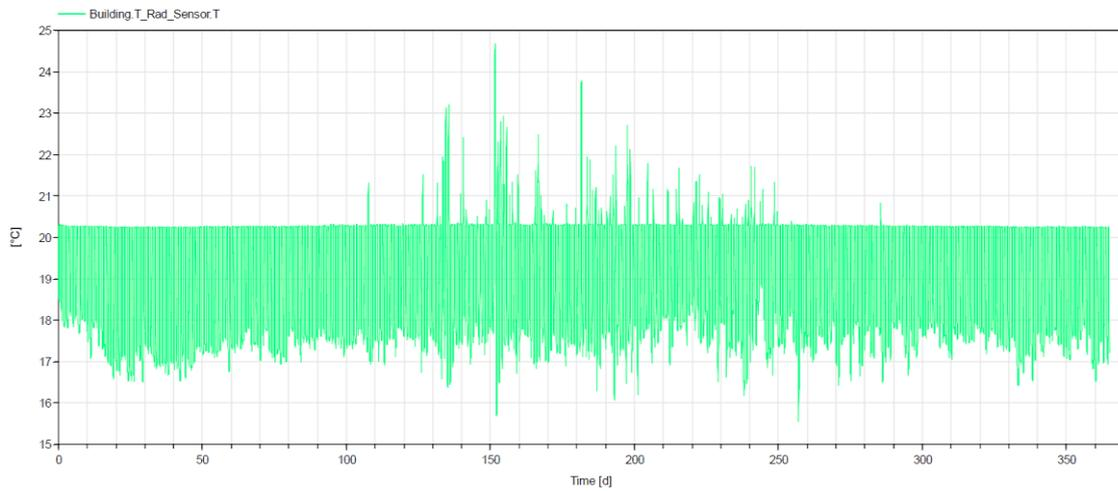


Fig. 52 Annual trend of the main radiant temperature

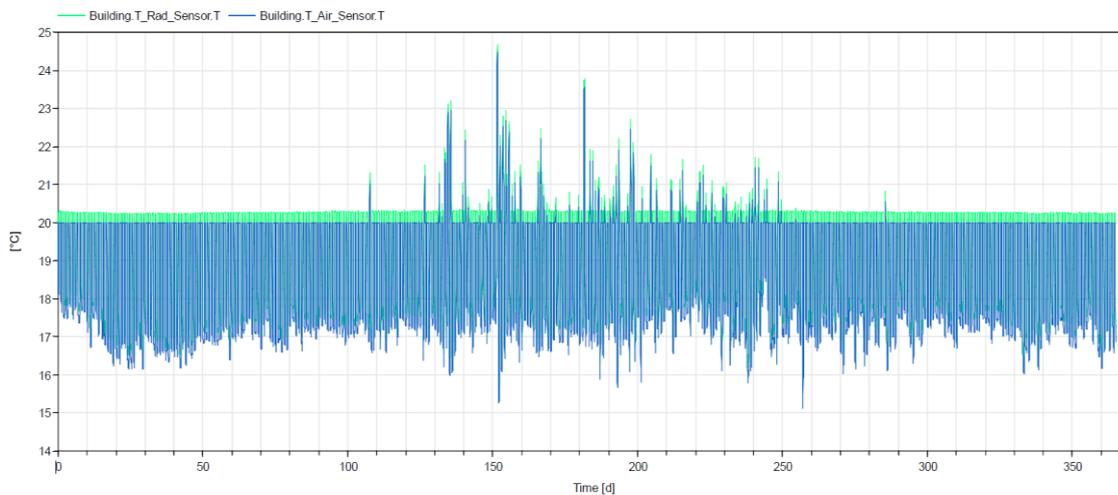


Fig. 53 Comparison between mean radiant temperature and air temperature

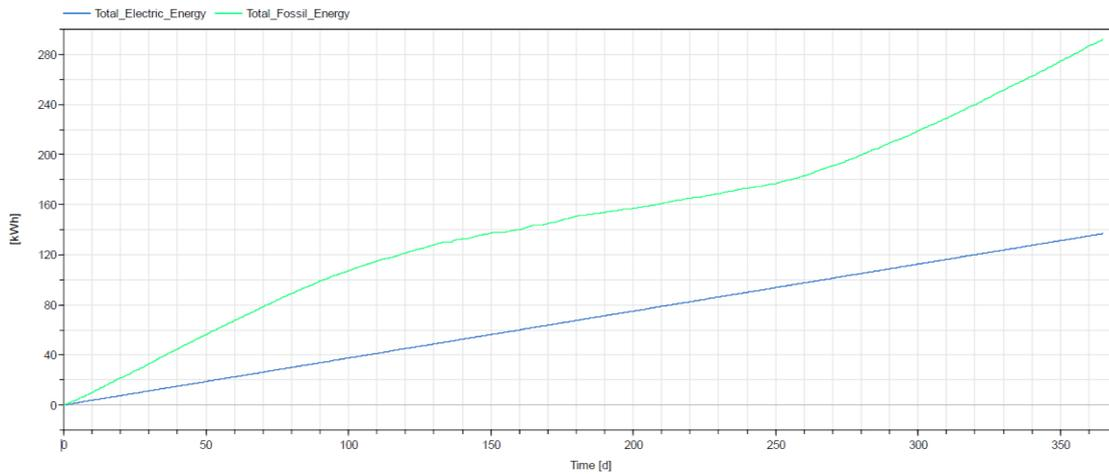


Fig. 54 Annual trends in electricity and fossil energy demand

3.2.3.3.3. Large cell

Parameters estimated using the RomPar tool

AWinSouth	0,220275	Ratio_gf	0,206391184
AWinNorth	0	Rwall_is	0,005452448
AWinWest	0	Rwall	0,681664276
AWinEast	0	Rwall_es	0,001677676
AWinRoof	0	Cwall	1080177,203
GtotWSouth	0,63	Rwin_is	0,590171377
GtotWNorth	0	Rwin	1,746069162
GtotWWest	0	Rwin_es	0,181591193
GtotWEast	0	Rm_is	0,001650479
GtotWRoof	0	Rm	0,181879972
Ratio_m	0,492618232	Cm	4104351,83
Ratio_wall	0,298235262	Rgf_is	0,01030303
Ratio_win	0,002755322	Rgf	0,124225774
Rgf_es	0,002424242	Cgf	8596302

Simulation results

- **Time for integration** 47.9 seconds
- **Air temperature**
 - 18,63424343 °C average value
 - 1,425824356 standard deviation

14,979618 °C minimum value

22,80638 °C maximum value

- **Mean radiant temperature**

18,64804314 °C average value

1,378299677 standard deviation

15,141467 °C minimum value

22,707676 °C maximum value

- **Electrical energy demand**

136,875 kWh maximum value

- **Fossil energy demand**

732,80774 kWh maximum value

Graphical results

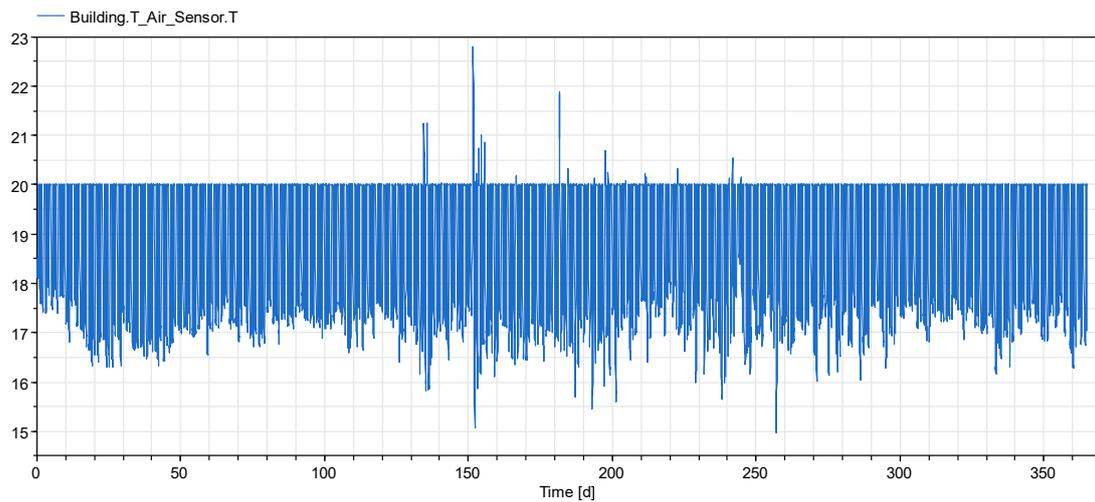


Fig. 55 Annual trend of the Air Temperature

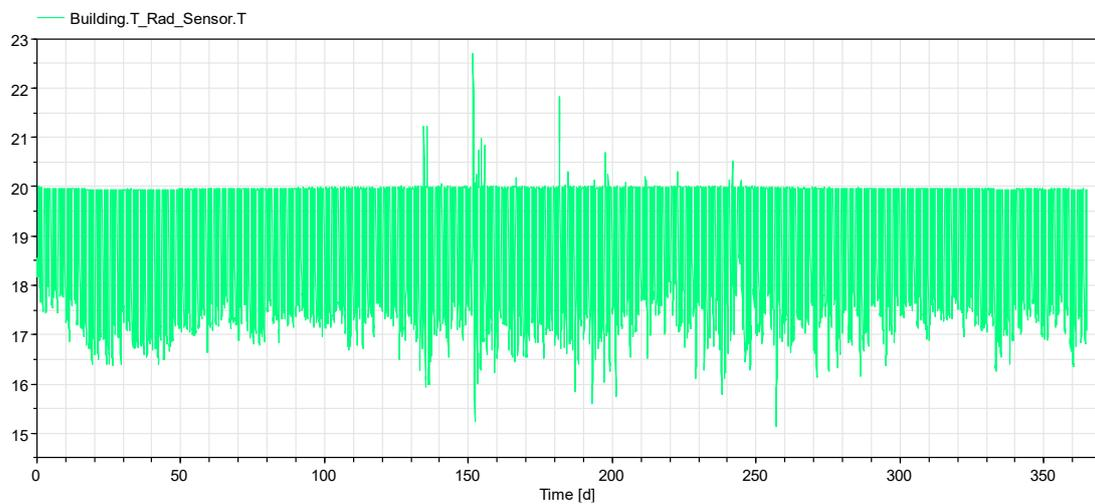


Fig. 56 Annual trend of the main radiant temperature

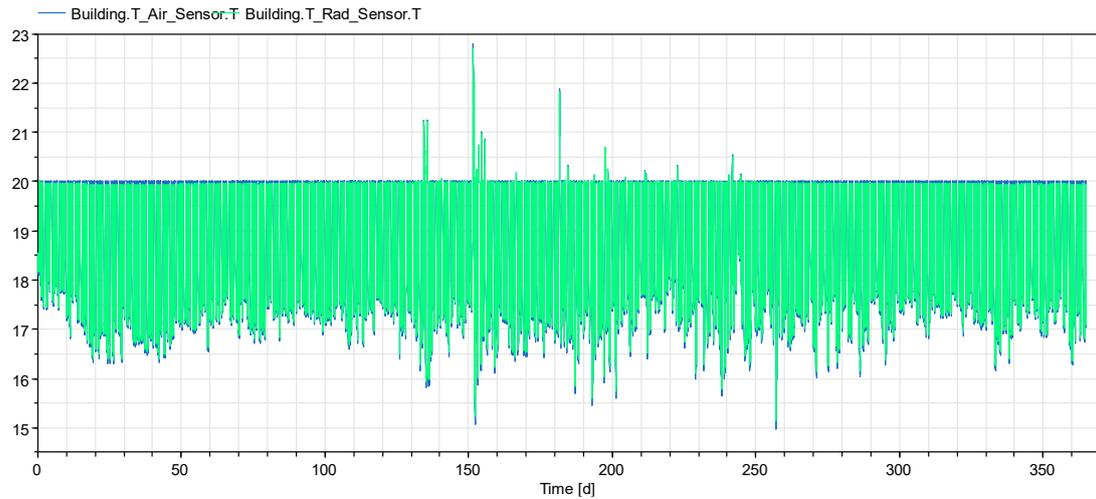


Fig. 57 Comparison between mean radiant temperature and air temperature

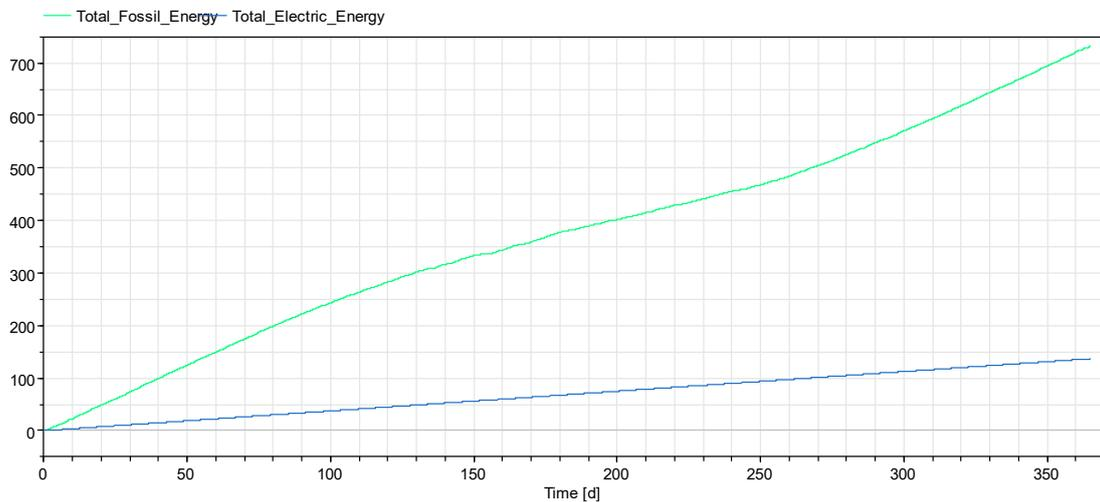


Fig. 58 Annual trends in electricity and fossil energy demand

3.2.3.4. Tested wall number 4

Material (from int to ext)	Thickness (mm)	Conductivity (W/mK)	Density (kg/m ³)	Specific heat capacity (J/KgK)
Plasterboard	13	0,21	900	1050
Gypsum fibre	13	0,360	1180	1000
Rock wool	50	0,033	70	1030
Multilayer wood panel	100	0,13	500	1600
Rock wool	200	0,036	90	1030
Lime plaster	15	0,68	1620	1000

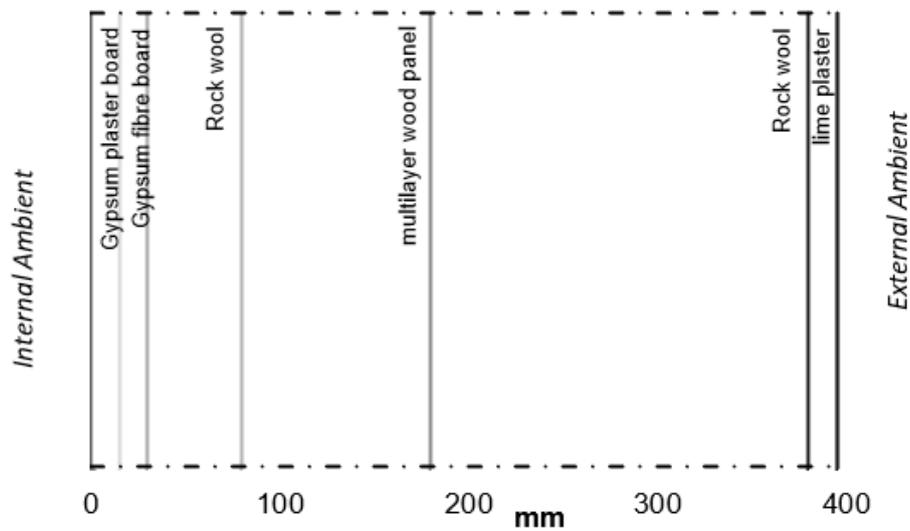


Fig. 59 Tested wall number 4

Calculated U Value	W/m ² K	0,1212
Thermal Capacity	kJ/K	379

3.2.3.4.1. Standard cell

Parameters estimated using the RomPar tool

AWinSouth	0,220275	Rwall	0,875142333
AWinNorth	0	Rwall_es	0,001968262
AWinWest	0	Cwall	1098327,863
AWinEast	0	Rwin_is	0,590171377
AWinRoof	0	Rwin	1,746069162
GtotWSouth	0,63	Rwin_es	0,181591193
GtotWNorth	0	Rm_is	0,001997093
GtotWWest	0	Rm	0,220076258
GtotWEast	0	Cm	3392003,309
GtotWRoof	0	Rgf_is	0,013097072
Ratio_m	0,492617876	Rgf	0,15791412
Ratio_wall	0,307590085	Rgf_es	0,003081664
Ratio_win	0,00333396	Cgf	6762424,24
Ratio_gf	0,196458079	Rwall	0,875142333

Simulation results

- **Time for integration** 45 seconds
- **Air temperature**
 18,63932159 °C average value
 1,432556175 standard deviation

14,991656 °C minimum value

23,292877 °C maximum value

- **Mean radiant temperature**

18,65638705°C average value

1,390098405 standard deviation

15,146937°C minimum value

23,198118°C maximum value

- **Electrical energy demand**

136,875 kWh maximum value

- **Fossil energy demand**

544,03973kWh maximum value

Graphical results

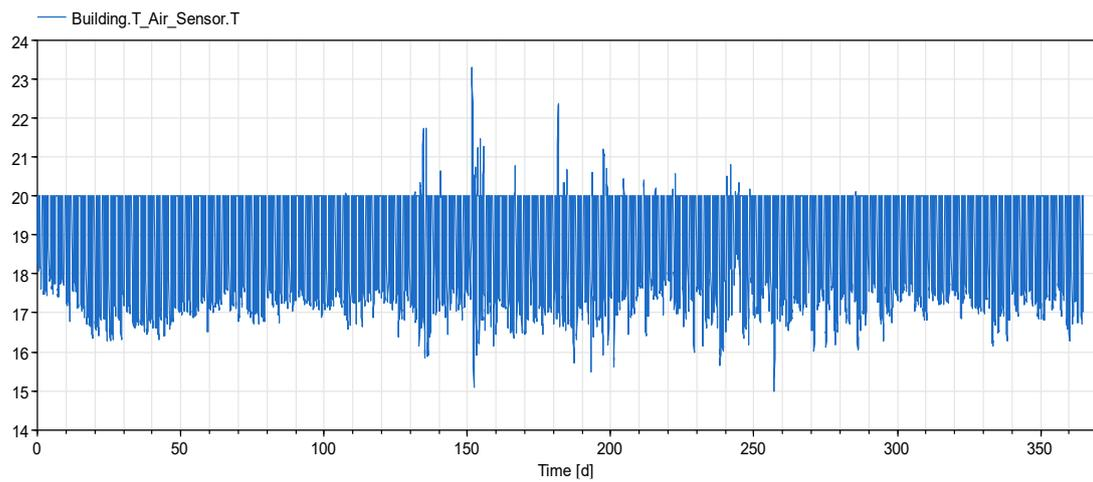


Fig. 60 Annual trend of the Air Temperature

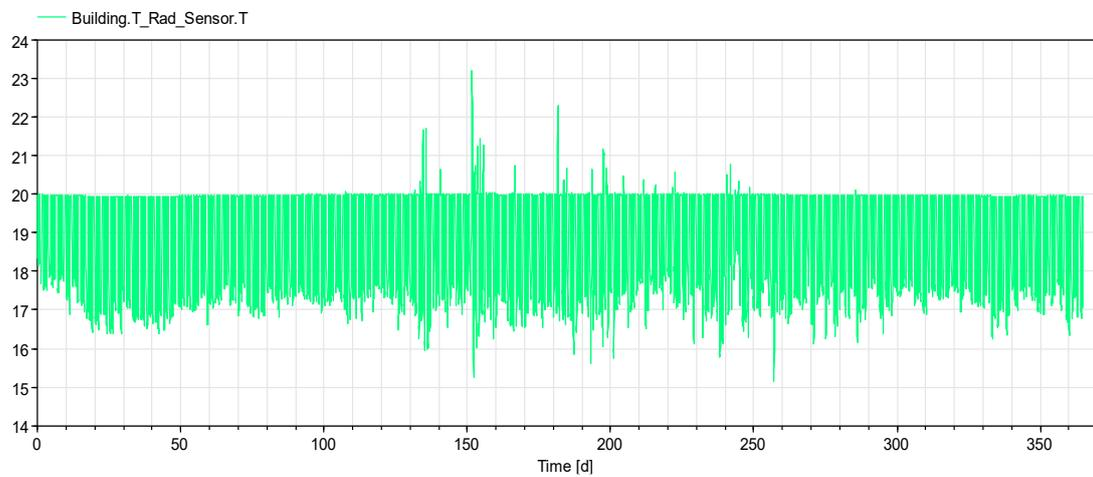


Fig. 61 Annual trend of the main radiant temperature

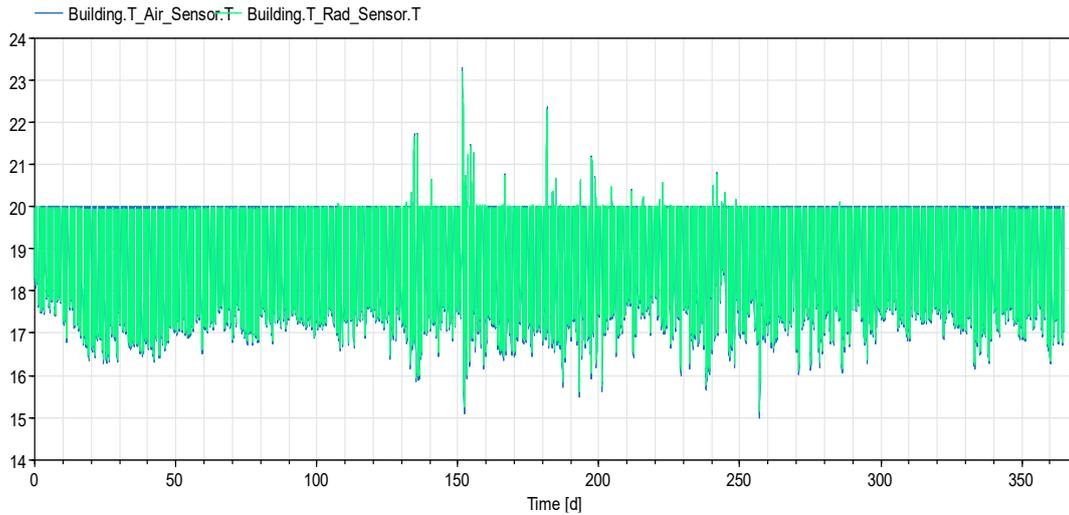


Fig. 62 Comparison between mean radiant temperature and air temperature

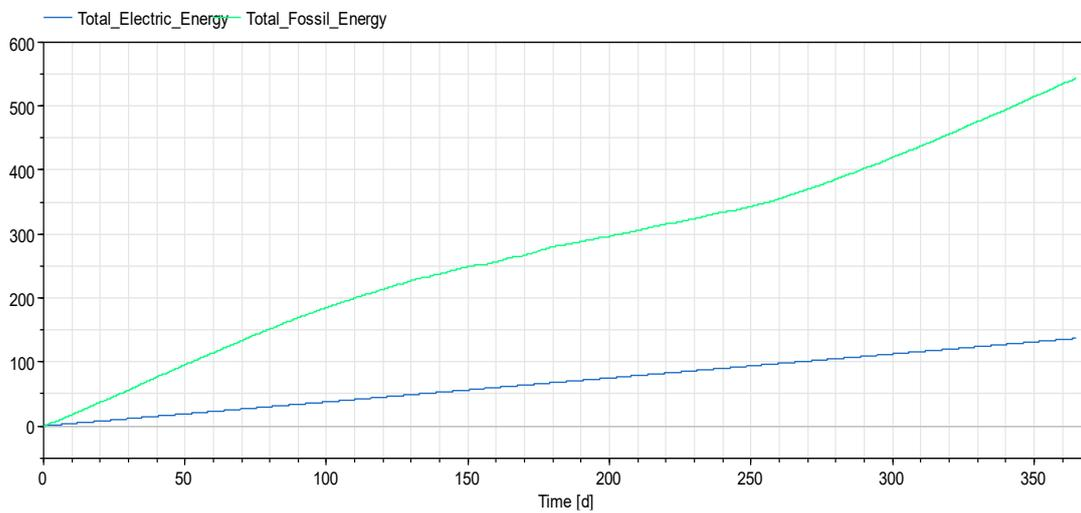


Fig. 63 Annual trends in electricity and fossil energy demand

3.2.3.4.2. Small cell

Parameters estimated using the RomPar tool

AWinSouth	0,220275	Rwall	1,195207
AWinNorth	0	Rwall_es	0,002565
AWinWest	0	Cwall	1098328
AWinEast	0	Rwin_is	0,590171
AWinRoof	0	Rwin	1,746069
GtotWSouth	0,63	Rwin_es	0,181591
GtotWNorth	0	Rm_is	0,002782
GtotWWest	0	Rm	0,306598
GtotWEast	0	Cm	2434785
GtotWRoof	0	Rgf_is	0,020606
Ratio_m	0,492617	Rgf	0,248452
Ratio_wall	0,32878	Rgf_es	0,004848

Ratio_win	0,004645	Cgf	4298151
Ratio_gf	0,173958	Rwall_is	0,008337342

Simulation results

- **Time for integration** 45.8 seconds
- **Air temperature**
18,66350359 °C average value
1,480129014 standard deviation
15,11479 °C minimum value
24,51932 °C maximum value
- **Mean radiant temperature**
18,97292201 °C average value
1,449235511 standard deviation
15,53667 °C minimum value
24,719406 °C maximum value
- **Electrical energy demand**
136,875 kWh maximum value
- **Fossil energy demand**
289,09296 kWh maximum value

Graphical results

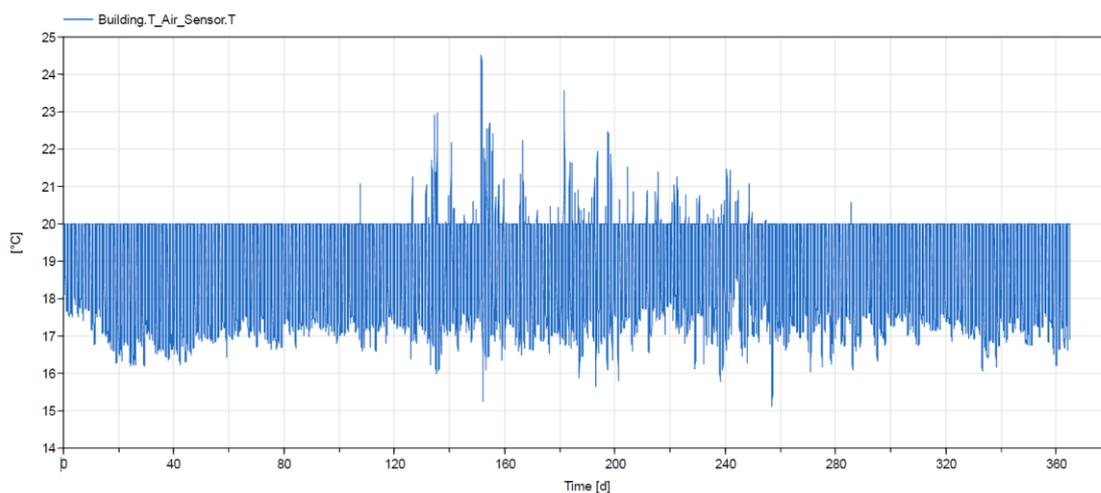


Fig. 64 Annual trend of the Air Temperature

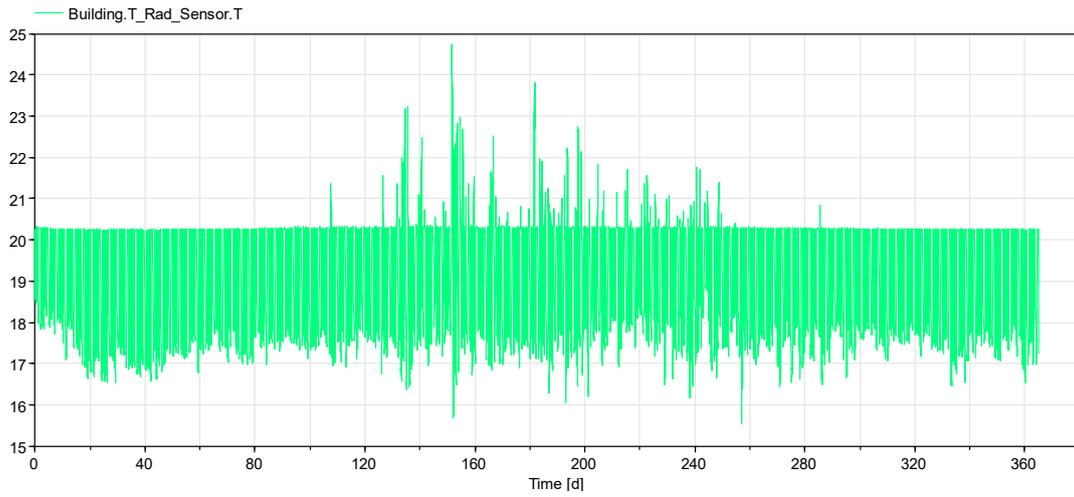


Fig. 65 Annual trend of the main radiant temperature

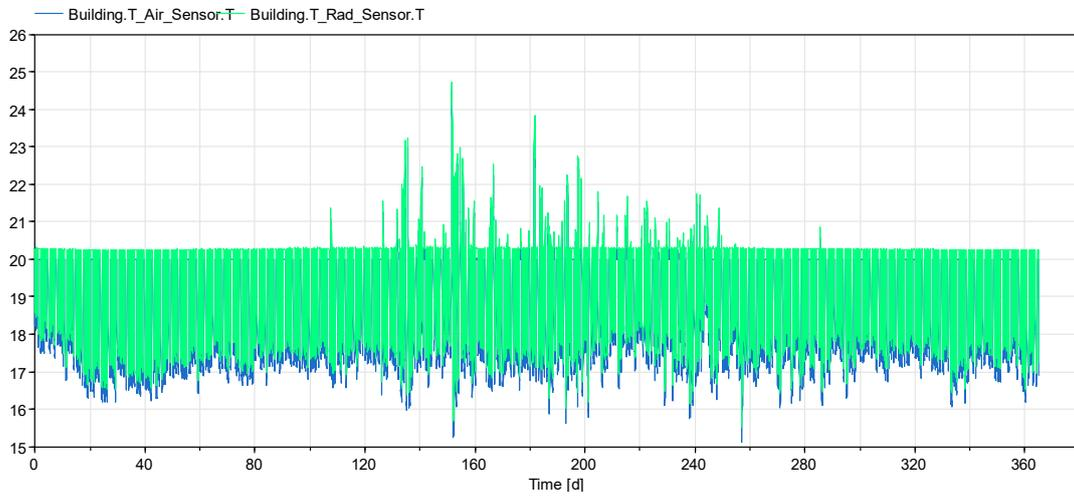


Fig. 66 Comparison between mean radiant temperature and air temperature

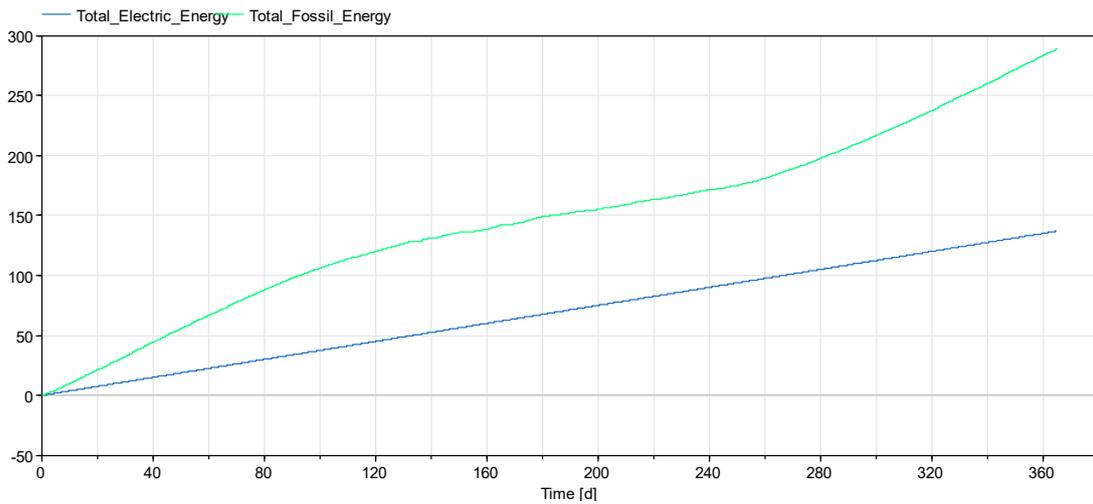


Fig. 67 Annual trends in electricity and fossil energy demand

3.2.3.4.3. Large cell

Parameters estimated using the RomPar tool

AWinSouth	0,220275	Ratio_win	0,002755
AWinNorth	0	Ratio_gf	0,206391
AWinWest	0	Rwall_is	0,005452
AWinEast	0	Rwall	0,708149
AWinRoof	0	Rwall_es	0,001678
GtotWSouth	0,63	Cwall	1098328
GtotWNorth	0	Rwin_is	0,590171
GtotWWest	0	Rwin	1,746069
GtotWEast	0	Rwin_es	0,181591
GtotWRoof	0	Rm_is	0,00165
Ratio_m	0,492618	Rm	0,18188
Ratio_wall	0,298235	Cm	4104352
Rgf_is	0,010303	Rgf_es	0,002424
Rgf	0,124226	Cgf	8596302

Simulation results

- **Time for integration** 46.9 seconds
- **Air temperature**
 - 18,64062419 °C average value
 - 1,419914463 standard deviation
 - 14,977287 °C minimum value
 - 22,819023 °C maximum value
- **Mean radiant temperature**
 - 18,65502431 °C average value
 - 1,372857622 standard deviation
 - 15,1391 °C minimum value
 - 22,72088 °C maximum value
- **Electrical energy demand**
 - 136,875 kWh maximum value
- **Fossil energy demand**
 - 729,53827 kWh maximum value

Graphical results

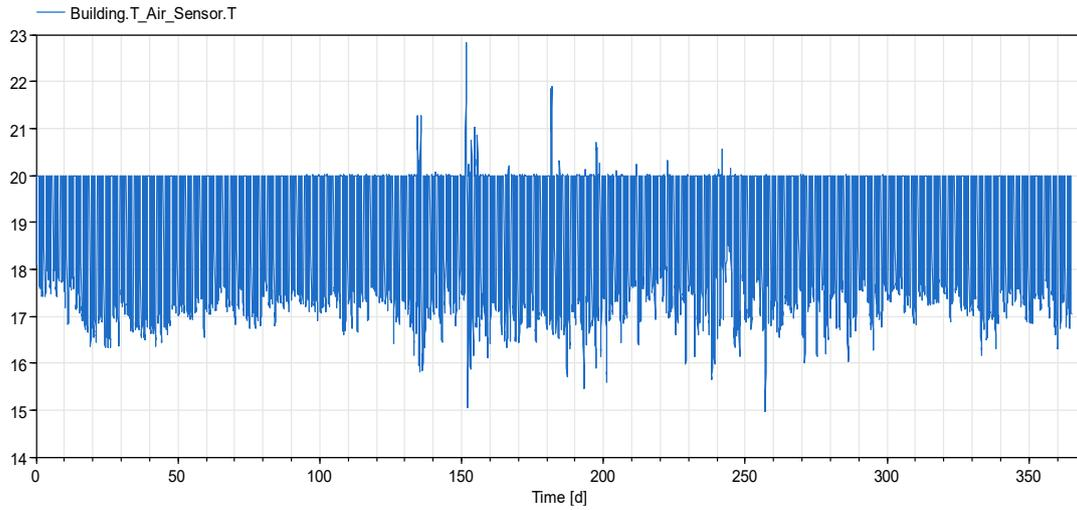


Fig. 68 Annual trend of the Air Temperature

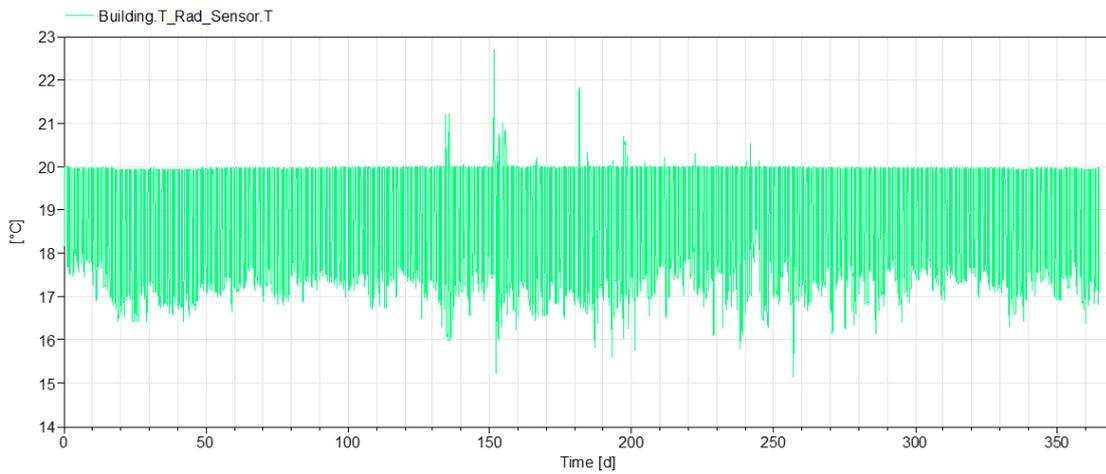


Fig. 69 Annual trend of the main radiant temperature

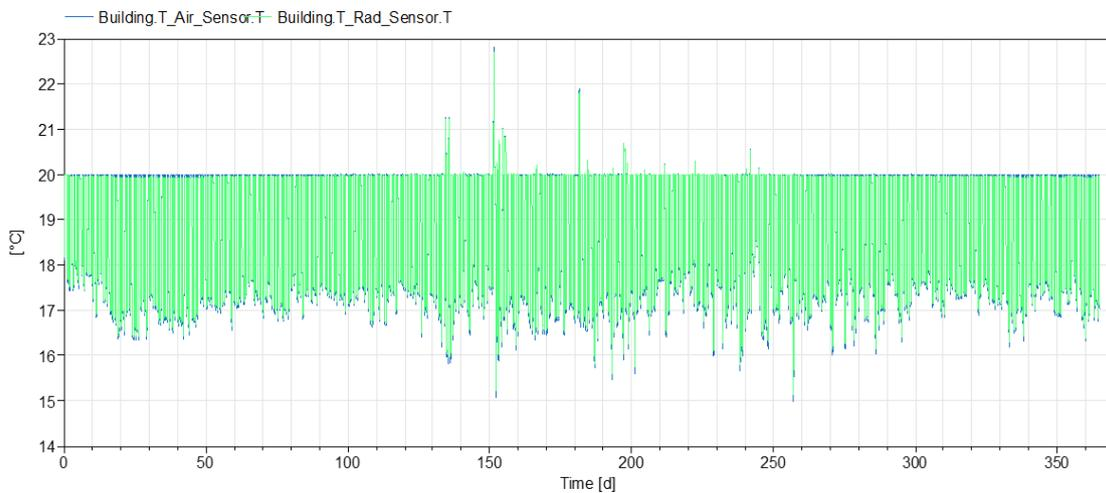


Fig. 70 Comparison between mean radiant temperature and air temperature

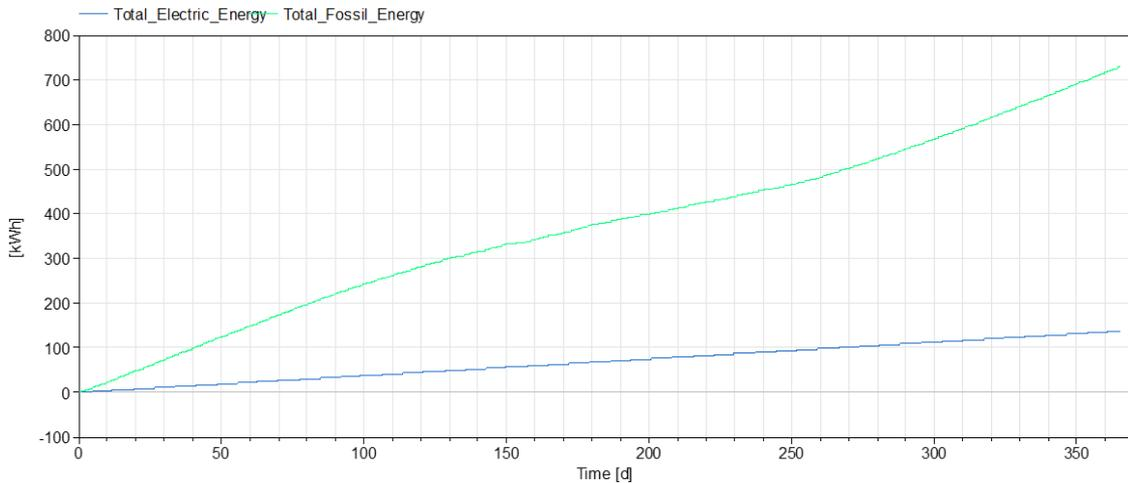


Fig. 71 Annual trends in electricity and fossil energy demand

3.2.4. SIMULATION AND SCENARIO ANALYSIS

Once all the simulations were completed, analysis of the results was carried out. The data taken into account in the scenario analyses are the air temperature, the average radiant temperature and the electricity and fossil energy demand for heating. In relation to the temperatures, the mean value and standard deviation were also measured in order to analyse the fluctuation of the measurement and to quantify the sensitivity of the instrument. The data analysed are on an annual basis. Below is a table of the final results obtained, which constitute the starting point for the analyses carried out.

Cell type	Type of wall	Time for simulation	Maximum T Air	Minimum T air	Average T air	Standard deviation T air	Maximum T Rad	Minimum T Rad	Average T Rad	Standard deviation T Rad	Demand for electrical energy	Demand for fossil energy
		seconds	°C	°C	°C	°C	°C	°C	°C	°C	kWh	kWh
Standard	Number 1	42,4	22,987167	15,00184	18,621401	1,442064685	22,892231	15,157363	18,63644806	1,397778428	136,875	558,9805
Small		45	24,41846	15,133757	18,635912	1,501290905	24,614424	15,556051	18,94300827	1,468635007	136,875	296,2576
Large		45,1	22,766052	14,992492	18,626584	1,432440089	22,666376	15,15466	18,6396103	1,432440089	136,875	736,9428
Standard	Number 2	47	23,252642	15,0029955	18,630518	1,440079926	23,156033	15,158549	18,64672562	1,396948971	136,875	547,7983
Small		48,9	24,459312	15,1273775	18,64947	1,490293936	24,656921	15,549543	18,95769018	1,458476697	136,875	292,7519
Large		41,6	22,781431	14,989054	18,633369	1,426177298	22,682812	15,151159	18,64703996	1,378541781	136,875	733,4357
Standard	Number 3	42,4	23,274782	14,99505	18,6316	1,439571394	23,17923	15,150392	18,64795931	1,396568059	136,875	547,1965
Small		46,6	24,484861	15,119817	18,651459	1,489829027	24,683569	15,541793	18,95989459	1,458206232	136,875	292,158
Large		47,9	22,80638	14,979618	18,634243	1,425824356	22,707676	15,141467	18,64804314	1,378299677	136,875	732,8077
Standard	Number 4	45	23,292877	14,991656	18,639322	1,425824356	23,198118	15,146937	18,65638705	1,390098405	136,875	544,0397
Small		45,8	24,51932	15,11479	18,663504	1,480129014	24,719406	15,53667	18,97292201	1,449235511	136,875	289,093
Large		46,9	22,819023	14,977287	18,640624	1,419914463	22,72088	15,1391	18,65502431	1,372857622	136,875	729,5383

Table 5 Modelling output

To move on to the scenario analysis, the cell size was set as an independent variable. As explained previously, each scenario corresponds to a different cell size, standard, small, large. The data for the different analysis scenarios are shown below.

Scenario number 1, standard cell size

In the first scenario, the thermal response of the model is analysed considering the standard cell size, the variables that change concern the different walls tested. In the table below, the simulation outputs for the different walls can be found.

Cell type	Type of wall	Time for simulation	Maximum T Air	Minimum T air	Average T air	Standard deviation T air	Maximum T Rad	Minimum T Rad	Average T Rad	Standard deviation T Rad	Demand for electrical energy	Demand for fossil energy
		seconds	°C	°C	°C	°C	°C	°C	°C	°C	kWh	kWh
standard	Number 1	42,4	22,98717	15,00184	18,6214	1,4420647	22,89223	15,15736	18,63645	1,3977784	136,875	558,9805
	Number 2	47	23,25264	15,003	18,63052	1,4400799	23,15603	15,15855	18,64673	1,396949	136,875	547,79834
	Number 3	42,4	23,27478	14,99505	18,6316	1,4395714	23,17923	15,15039	18,64796	1,3965681	136,875	547,1965
	Number 4	45	23,29288	14,99166	18,63932	1,4258244	23,19812	15,14694	18,65639	1,3900984	136,875	544,03973

Table 6 Modelling results for scenario number 1

Using MatLab[67], a programming and numeric computing platform, the air temperature and mean radiant temperature trends were analysed, always considering standard cell dimensions and all wall samples tested. In the trend analysis, the maximum value, minimum value, mean value, standard deviation, mean and median were highlighted. This operation was repeated for all scenarios.

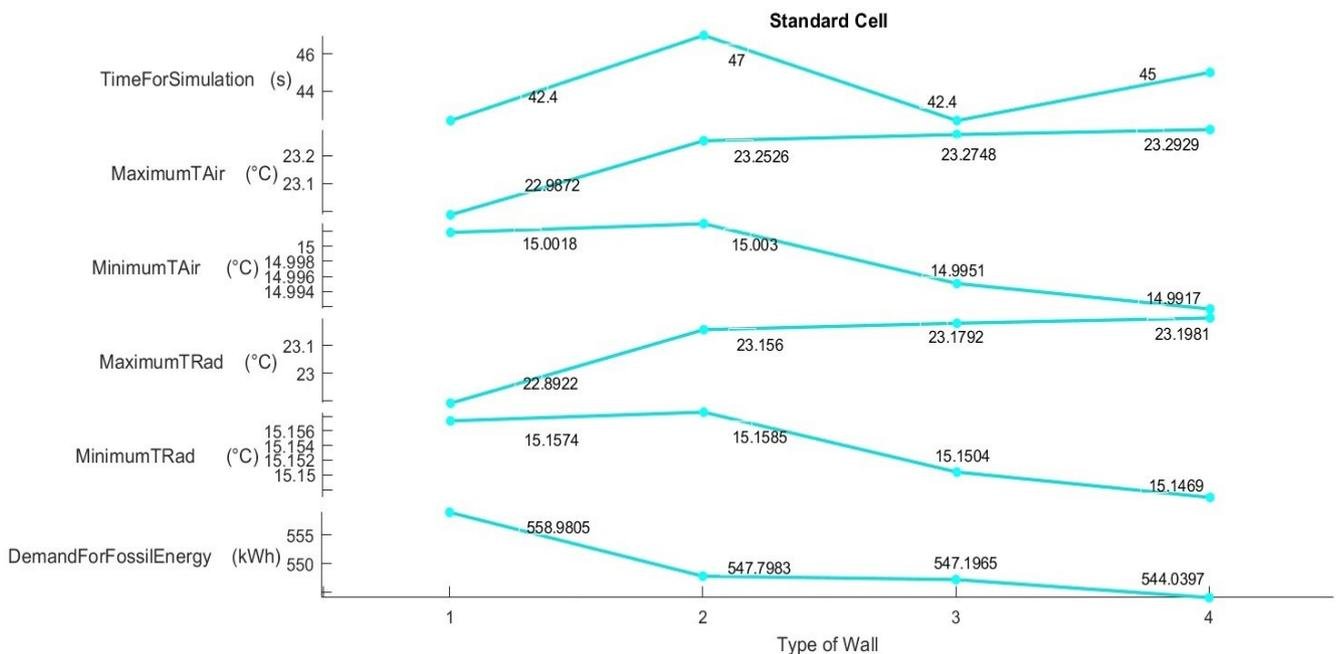


Fig. 72 statistical analysis of results for the standard cell

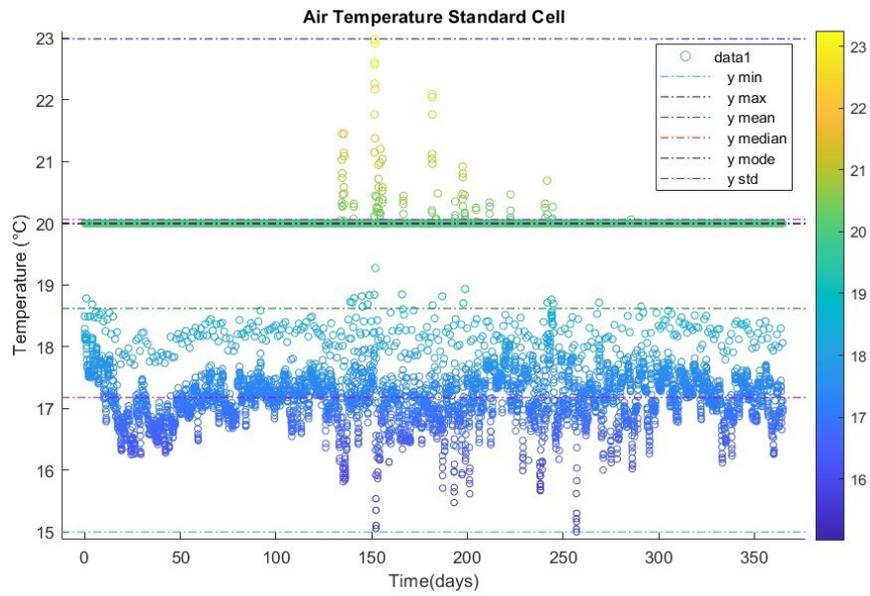


Fig. 73 Air temperature trend

Value	Air temperature (°C)
Min	15
Max	22.99
Mean	18.62
Median	19.99
Mode	20
Standard deviation	1.442

Table 7 Air temperature reference parameters

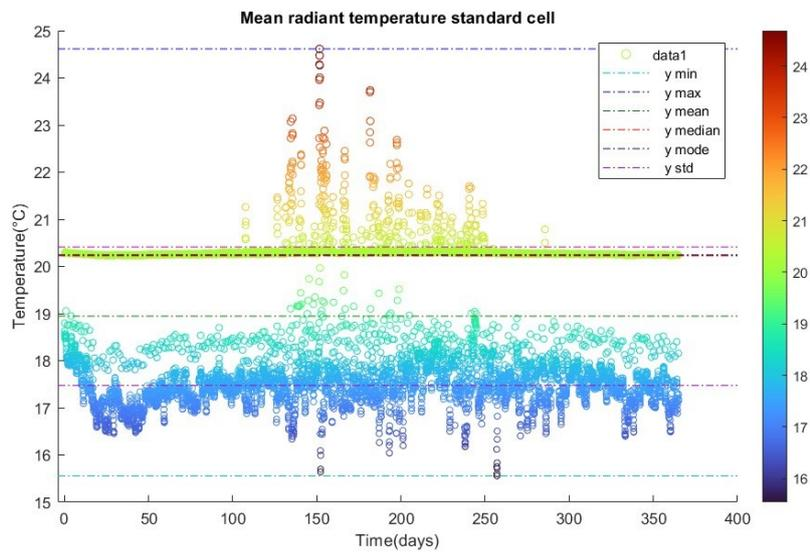


Fig. 74 Mean radiant temperature trend

Value	Mean radiant temperature (°C)
Min	15.65
Max	24.61
Mean	18.94

Median	20.23
Mode	20.24
Standard deviation	1.469

Table 8 Mean radiant temperature reference parameters

Scenario number 2, small cell size

In the scenario number 2, the thermal response of the model is analysed considering the small cell size.

Cell type	Type of wall	Time for simulation	Maximum T Air	Minimum T air	Average T air	Standard deviation T air	Maximum T Rad	Minimum T Rad	Average T Rad	Standard deviation T Rad	Demand for electrical energy	Demand for fossil energy
		seconds	°C	°C	°C	°C	°C	°C	°C	°C	kWh	kWh
small	Number 1	45	24,41846	15,13376	18,63591	1,5012909	24,61442	15,55605	18,94301	1,468635	136,875	296,25763
	Number 2	48,9	24,45931	15,12738	18,64947	1,4902939	24,65692	15,54954	18,95769	1,4584767	136,875	292,75192
	Number 3	46,6	24,48486	15,11982	18,65146	1,489829	24,68357	15,54179	18,95989	1,4582062	136,875	292,15802
	Number 4	45,8	24,51932	15,11479	18,6635	1,480129	24,71941	15,53667	18,97292	1,4492355	136,875	289,09296

Table 9 Modelling results for scenario number 2

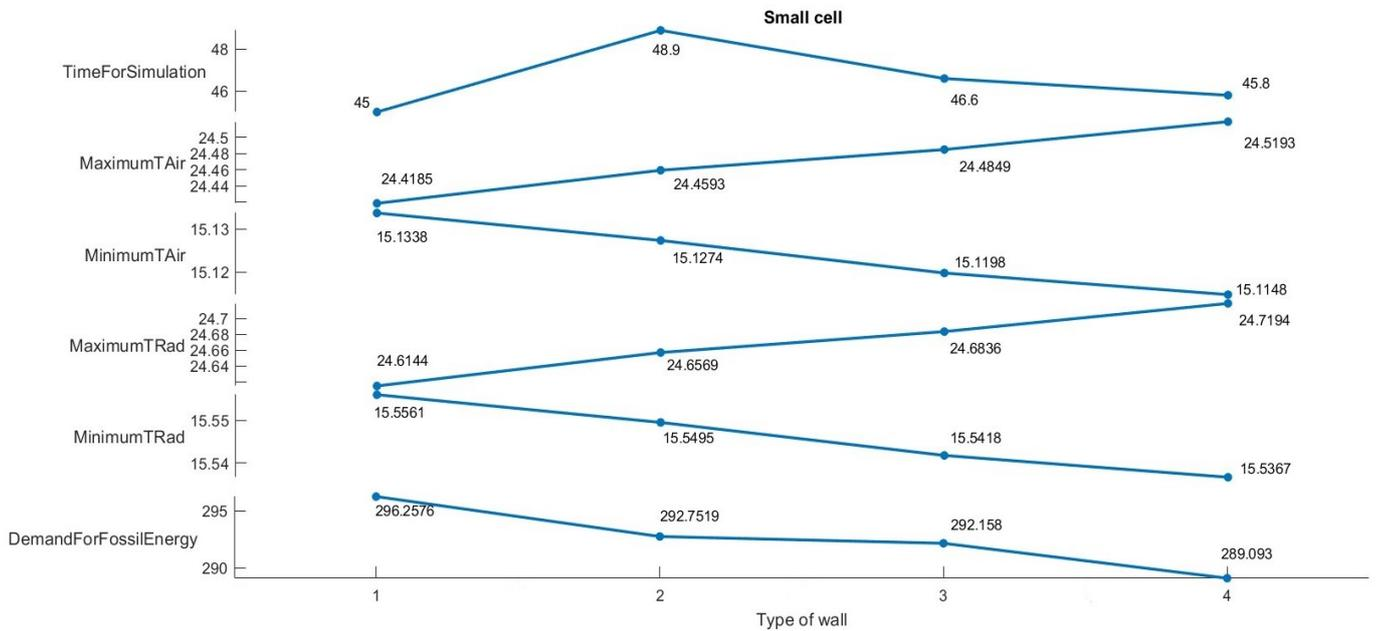


Fig. 75 Statistical analysis of results for the small cell

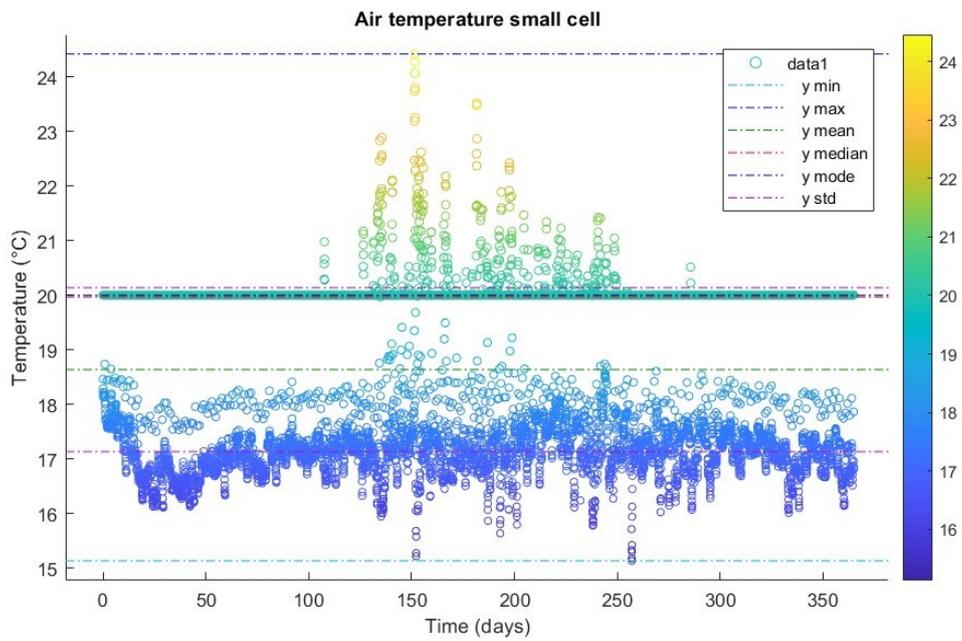


Fig. 76 Air temperature trend

Value	Air temperature (°C)
Min	15.13
Max	24.42
Mean	18.64
Median	19.97
Mode	20
Standard deviation	1.501

Table 10 Air temperature reference parameters

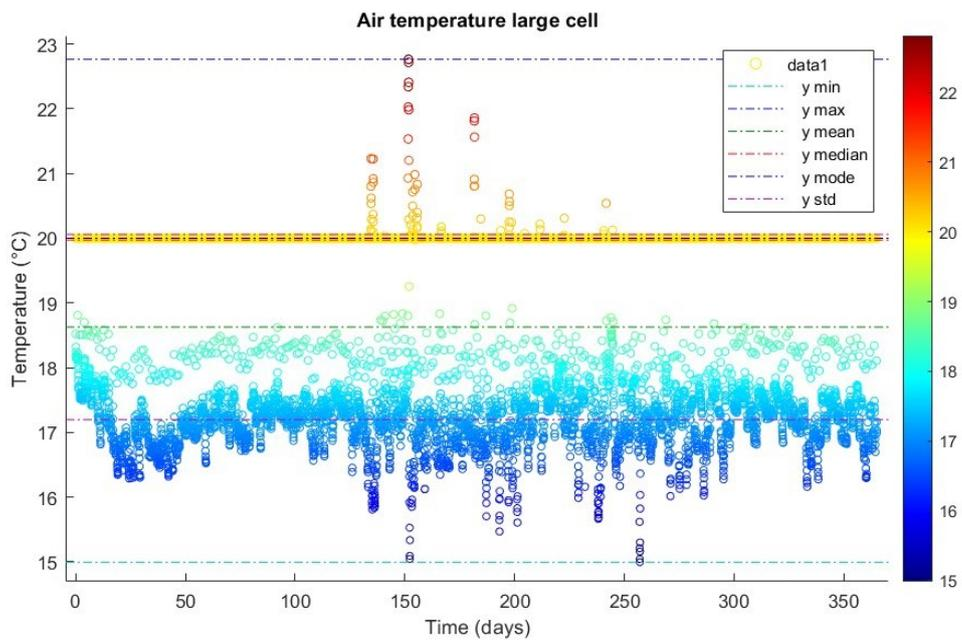


Fig. 77 Mean radiant temperature trend

Value	Mean radiant temperature (°C)
Min	14.99
Max	22.77
Mean	18.63
Median	19.97
Mode	20
Standard deviation	1.432

Table 11 Mean radiant temperature reference parameters

Scenario number 3, large cell size

In the scenario number 3, the thermal response of the model is analysed considering the large cell size.

Cell type	Type of wall	Time for simulation	Maximum T Air	Minimum T air	Average T air	Standard deviation T air	Maximum T Rad	Minimum T Rad	Average T Rad	Standard deviation T Rad	Demand for electrical energy	Demand for fossil energy
		seconds	°C	°C	°C	°C	°C	°C	°C	°C	kWh	kWh
large	Number 1	45,1	22,76605	14,99249	18,62658	1,4324401	22,66638	15,15466	18,63961	1,4324401	136,875	736,94275
	Number 2	41,6	22,78143	14,98905	18,63337	1,4261773	22,68281	15,15116	18,64704	1,3785418	136,875	733,4357
	Number 3	47,9	22,80638	14,97962	18,63424	1,4258244	22,70768	15,14147	18,64804	1,3782997	136,875	732,80774
	Number 4	46,9	22,81902	14,97729	18,64062	1,4199145	22,72088	15,1391	18,65502	1,3728576	136,875	729,53827

Table 12 Modelling results for scenario number 3

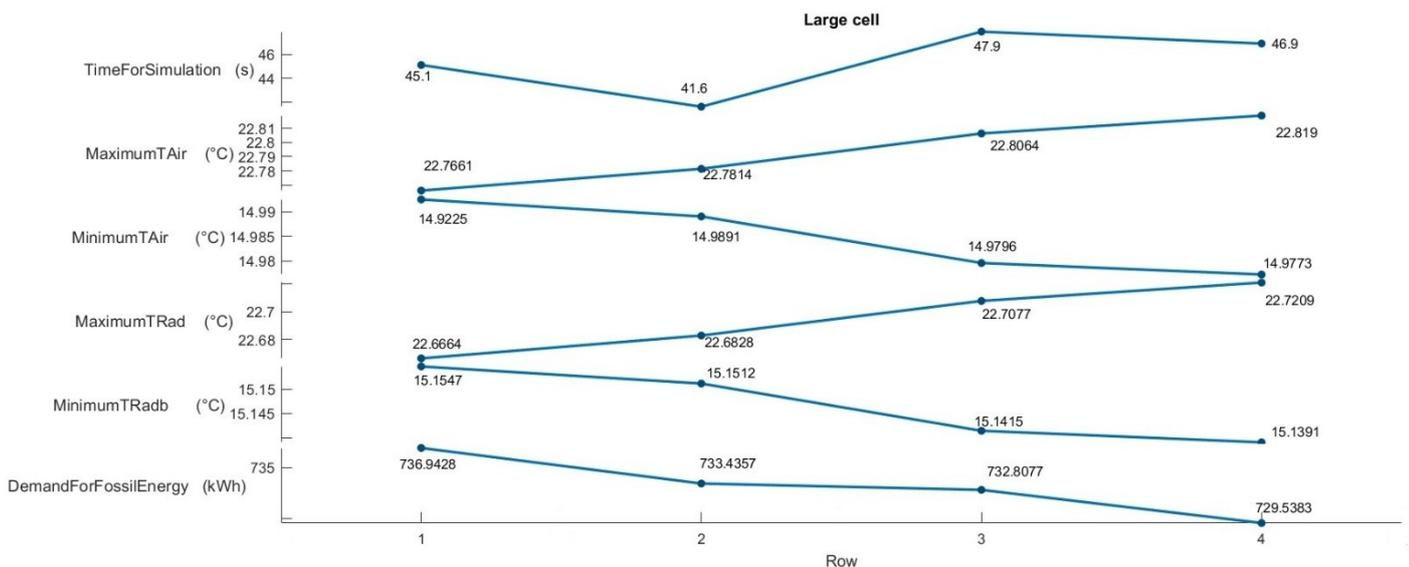


Fig. 78 statistical analysis of results for the large cell

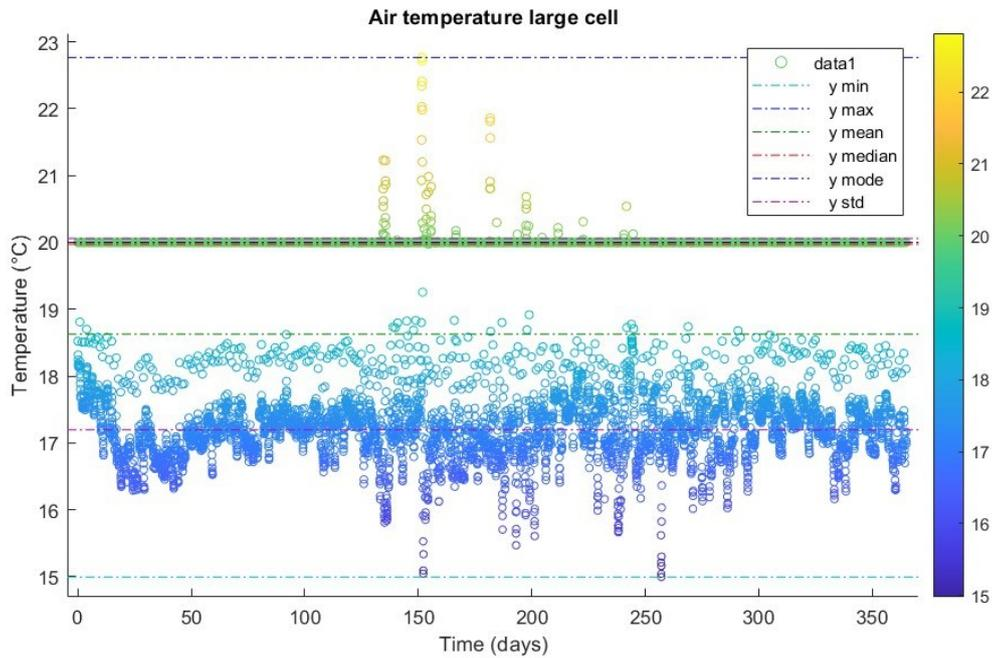


Fig. 79 Air temperature trend

Value	Air temperature (°C)
Min	14.99
Max	22.77
Mean	18.63
Median	19.97
Mode	20
Standard deviation	1.432

Table 13 Air temperature reference parameters

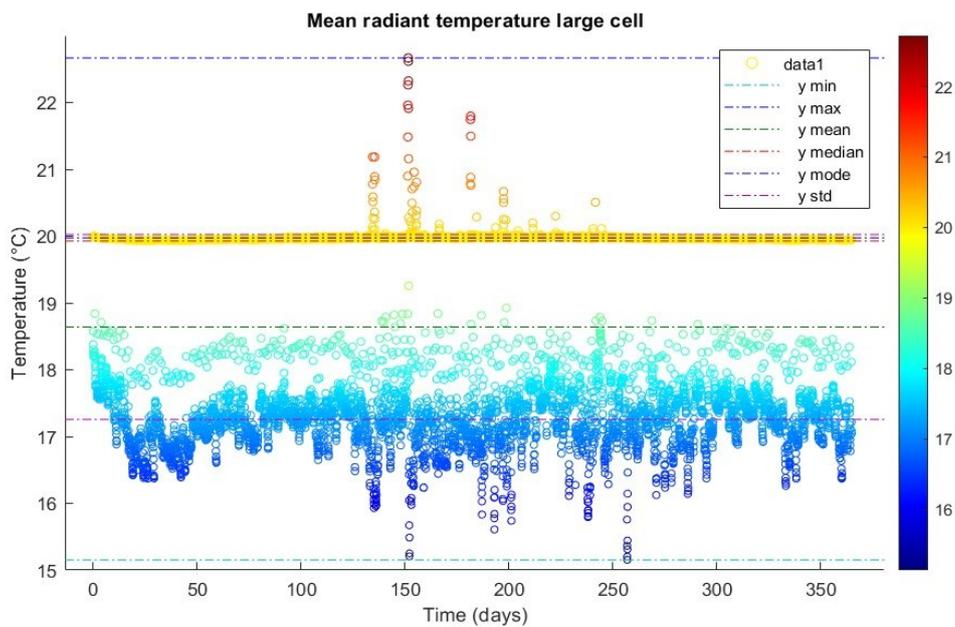


Fig. 80 Mean radiant temperature trend

<i>Value</i>	<i>Mean radiant temperature (°C)</i>
<i>Min</i>	15.15
<i>Max</i>	22.67
<i>Mean</i>	18.64
<i>Median</i>	19.93
<i>Mode</i>	19.97
<i>Standard deviation</i>	1.384

Table 14 Mean radiant temperature reference parameters

In relation to electricity energy demand, it is related to the power of the installed lighting equipment. The conditions of the lighting system do not change in the scenarios analysed and consequently the value of the total electrical energy required does not vary and is in no way influenced by the type of wall tested or the size of the cell.

This is not the position for the total demand for fossil energy. Once again it is highlighted that fossil energy includes the energy demand due to the heating of the facility alone. There is a cooling system in the structure, but it is never activated because of not reaching the activation set point, given the climatic conditions in Ireland. The heating conditions (type of system and maximum system power) do not vary in the different scenarios, so the results obtained are relative to the same input conditions. An analysis of consumption per square metre was also carried out, the results of which are described in the graph below(Fig.81).

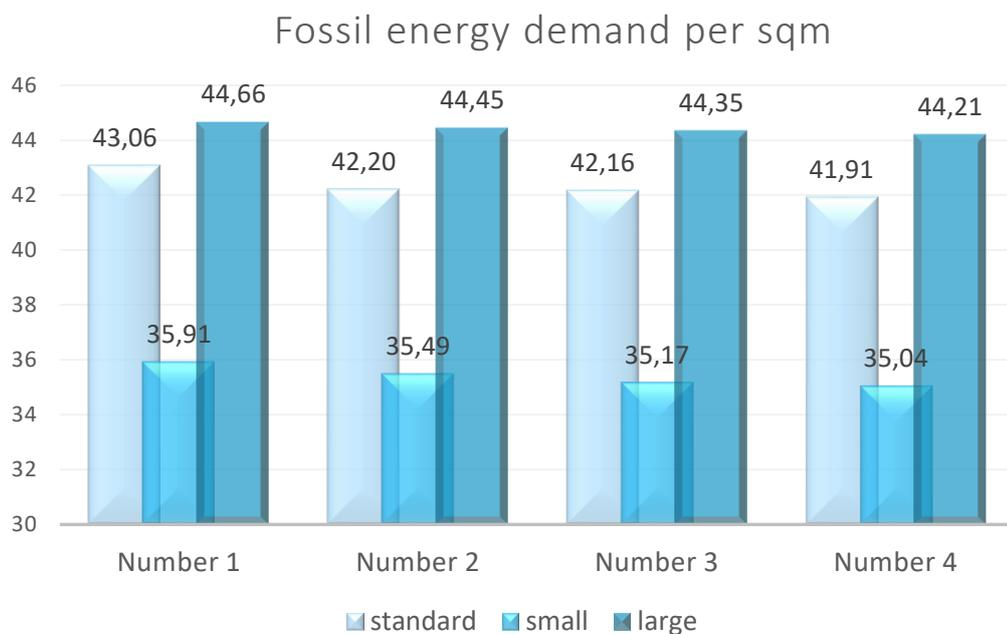


Fig. 81 Fossil energy demand per sqm.

4. RESULT AND DISCUSSION

This chapter will summarise and comment on the final results obtained from the various simulations supported. Starting with the latest reported results, thus discussing consumption, the first result that jumps out is that electricity demand is constant, not varying in any of the three scenarios analysed and for none of the sample walls tested. The constant maximum value of electrical energy required is 136,875 kWh. With regard to the demand for fossil energy, the energy used for heating spaces, on the other hand, the variations are different. It should be specified that reference is always made only to space heating and never to space cooling. Obviously, the energy demand for heating increases as the size of the cell increases. Bigger space requires more energy. However, the analysis focuses on the variation of energy required in the same scenario as the tested wall changes. In general, simulations conducted with the *tested wall number 1* have a higher fossil energy demand as an output. Better results are obtained when the lightest insulated wall, *tested wall number 4*, is tested. But the difference between the *tested wall number 4* (the wall for which less energy is required) and the *tested wall number 1* in *scenario 1*, the standard cell, is twice as much as in the other scenarios. This leads us to hypothesise that the difference in energy demand required for space heating for different tested samples is influenced by the size of the cell. Turning instead to the analysis of the results obtained for the temperatures, obviously the minimum and maximum air temperature values are relative at the lightest insulated wall, the *tested wall number 4*.

Respectively the maximum for *scenario number 2*(small cell) and the minimum for *scenario number 3*(large cell). Whereas with regard to the maximum temperature difference recorded for the different types of wall, the minimum variation in maximum temperature between the different walls tested is recorded in *scenario number 3*, for the large cell.

Thus, as the depth of the cell increases, the variation between the maximum temperature peaks recorded in the different tests decreases. In *scenario number 2*, small cell, on the contrary, the gap between the minimum peaks is greater. Where the minimum peaks represent the temperature reached when the heating system shuts down. The results just described are also valid for the mean radiant temperature trend. When comparing the simulated mean radiant temperature values with those of the air temperature, it can be seen that the largest deviation between the two measurements

occurs for *scenario number 2*, for the small cell. Where the deviation between the maximum recorded values reaches approximately 0.2 °C and 0.4°C for the minimum ones. On the other hand, similar values of discrepancy are reached for scenarios 1 and 3. In general, the temperature trend is quite similar for all scenarios and for all tested walls, the standard deviation for the temperature measurement has a low value ranging from 1.3 to 1.5. It should be noted that the value of the standard deviation decreases as the cell size increases.

The last aspect that stands out, which is fundamental, concerns the time taken for the simulation. A minimum time was taken for each simulation carried out, all of which took less than one minute. The range of seconds taken to complete the simulations is from 42 to 49 seconds. Times that would have been unthinkable if the simulations had been carried out with a white-box type model; of course, it must also be remembered that the behaviour of a single cell was simulated, hence a very small entity.

The objective of this thesis, after the application of ROM for the thermal simulation of BET, is above all the evaluation of ROM as a measurement and simulation tool, with a view to its use for the optimisation of the design phase of other test structures. Then, for both fossil energy consumption and temperature, a percentage variation analysis was carried out to assess how cell size (input parameter that is varied in each scenario) affects the results obtained. The final result is a comparison, made by scenarios, in which it is defined which scenario allows for a better discretisation of the results obtained with the different types of wall tested. Three comparisons were made for each analysed scenario. The first comparison for the analysis of the percentage variation of the results obtained is made in relation to the first two walls tested (wall no. 1 and 2), thus relating to a heavy wall system, the second was made in relation to the light wall system (wall no. 3 and 4), the third is a percentage analysis that takes into account the minimum and maximum value reached, general. The results obtained for the percentage variance analysis of fossil energy demand are shown below (Fig.81).

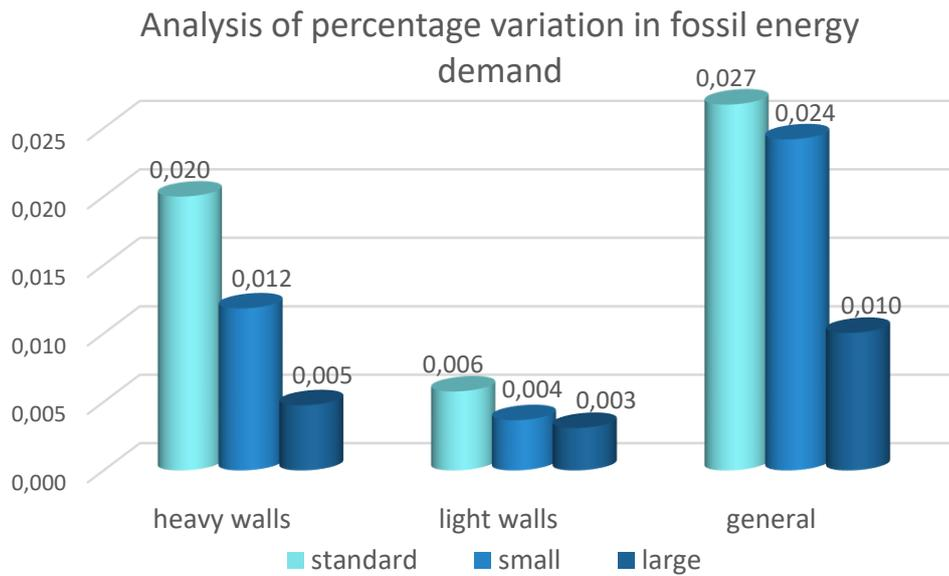


Fig. 82 Analysis of percentage variation in fossil energy demand

For the analysis of fossil energy consumption, the results obtained reflect the analyses done previously, first and foremost the fact that the results for light-weight walls perform better than those obtained for heavy-weight walls. With regard to the effect of varying cell size, however, it can be seen from the graph that the standard-sized cell is better able to discretize the results obtained with the different walls tested. It should be remembered that all tests were carried out in relation to the same heating system, with the same power and the same switch-on and switch-off times.

Analysis of percentage variation in standard deviation of main radiant temperature

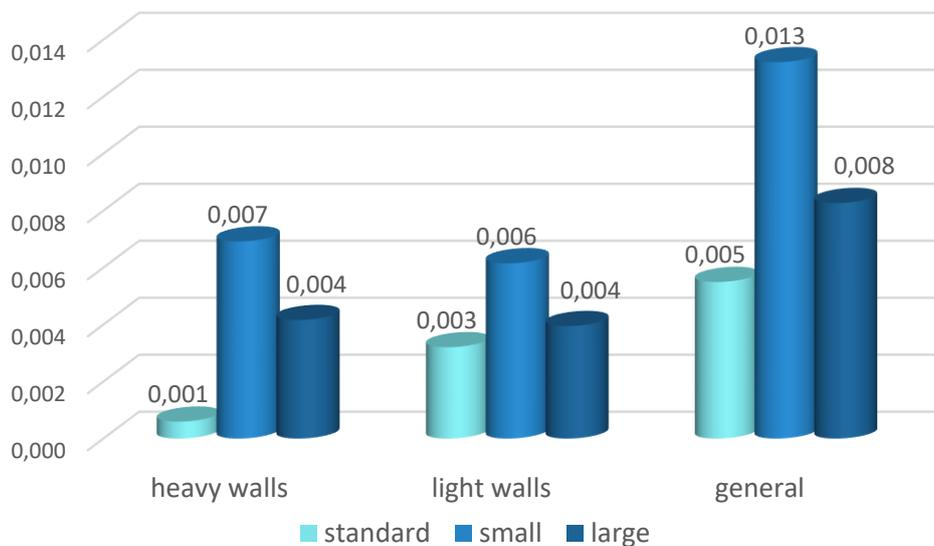


Fig. 83 Analysis of percentage variation in standard deviation of main radiant temperature

Analysis of percentage variation in standard deviation of air temperature

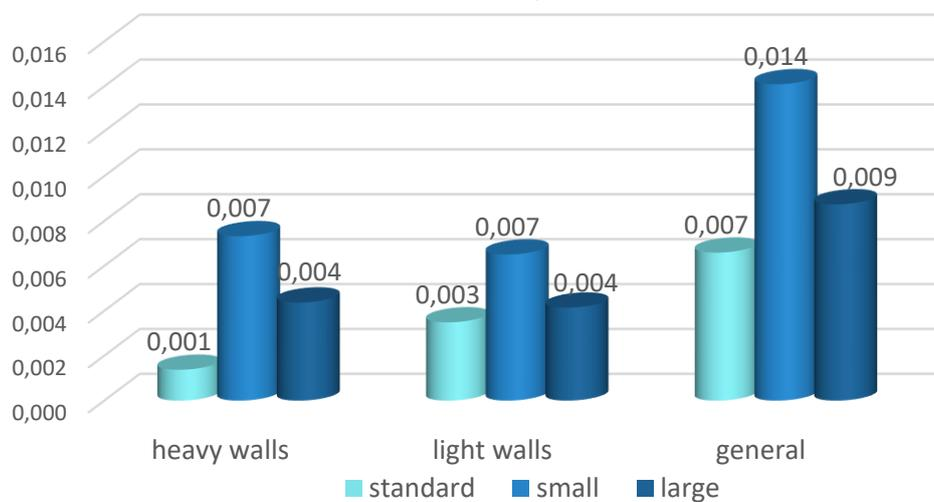


Fig. 84 Analysis of percentage variation in standard deviation of air temperature

For temperatures, the same technique was used, but the standard deviation, the width of the distribution, was taken as a reference. From the results, it can be seen that walls with a higher mass (heavy walls), which have a more pronounced behaviour, tend to compress the amplitude of the standard deviation. In addition, for massive systems, the gap between the results obtained in the different scenarios is greater than for the other systems tested, so for this type of wall, the results are more influenced by the size of the cell.

The analysis conducted for lightweight systems, on the other hand, is less sensitive to the variation in cell size and thus to the variation in the input parameter. In general, there is less variation for all the situations considered in scenario number 1, that of the standard cell size. The results obtained for the analysis of air temperature and mean radiant temperature are similar. The analyses are shown in the graphs above (Fig.82 and Fig.83). For both, the analysis was conducted with reference to the standard deviation. In contrast to fossil energy consumption, for temperature it is not the standard cell that best discretises the results obtained. In general, it can therefore be said that, with reference to both temperature and fossil energy demand, the percentage of variation in the results between the different types of wall tested is very low, always for the large cell, scenario number 3. A better discretisation of the results is obtained for the standard and small cells, depending on whether consumption or temperatures are considered, thus scenario number 1 and 2.

5. CONCLUSIONS

In this work, a reduced-order model is applied for the simulation of the thermal behaviour of a building envelope test structure. The aim of the thesis is to study ROM as a tool for the preliminary design of another test structure. Considering ROM as an analysis tool to be used during the decision-making phase of the preliminary design process, as a digital twin. The idea is to use data from an existing structure to improve the performance of the entire life cycle of another structure, thus also considering design and realisation, use the results obtained from an existent asset to improve an asset to be realised. In this case it is a scenario analysis that can be useful for the design phase. But in order to carry out this process, it must first be ensured that a suitable tool is available. In this case, the performance of a reduced-order model is analysed.

The thermal response obtained using this model is examined, as well as the variation in the results obtained. This is done in order to perform a sensitivity analysis of the model to the input parameters. Three different scenarios are analysed in which the input that is varied is the cell size. For each scenario, the thermal response is simulated for four different wall types tested. The test is performed on different walls to verify that the variations in the behaviour of the experimental cells are significantly different depending on the type of wall being tested. At the end of the work, a discrepancy analysis of the results obtained is carried out in order to assess the performance of ROM as a tool for measuring and evaluating the scenarios tested. Comparative experimental analyses can then be carried out with these cells.

It is a reduced, very simple model, which consequently requires very short simulation times. The risk of simplification lies in also simplifying the response obtained and thus increasing the margin of error. The model in question has already been used for several case studies and consequently also calibrated. But in order to be sure of the margin of error, it is advisable to model the entire structure and then calibrate the model using the data recorded by the sensors located inside the structure.

The method developed in this work and the test protocol established can be the basis for further studies. To confirm these preliminary results obtained, the method must be iterated several times. By increasing the tested walls or repeating the tests under different conditions, the boundary conditions that may have changed may be different. In this work, the depth of the cell was chosen as the variation input for each scenario,

other inputs could be other cell dimensions (height, width, stratigraphy) or plant characteristics.

The energy consumption of buildings and their impact on the environment is no longer negligible, every tool that can reduce their environmental footprint must be considered and utilised.

Energy modelling is certainly one of the ways we can improve building performance and their environmental impact. Furthermore, the use of digital twins in the design phase would allow the construction sector, which is still behind in terms of automation, to catch up with the times and what they require.

REFERENCES

- [1] Globalabc ,2021,“Global Status Report for Buildings and Construction”, Global alliance for building and construction available online at <https://globalabc.org/resources/publications/2021-global-status-report-buildings-and-construction>
- [2] IEA,2021,“Global energy use and energy-related CO2 emissions by sector, 2020” available online at <https://www.iea.org/data-and-statistics/charts/global-energy-use-and-energy-related-co2-emissions-by-sector-2020>, International Energy Agency
- [3] IEA, 2019,“Shares of residential energy consumption by end use in selected IEA countries, 2019” available online at <https://www.iea.org/data-and-statistics/charts/shares-of-residential-energy-consumption-by-end-use-in-selected-iea-countries-2019> ,International Energy Agency
- [4] OpenLearn,Open University, 2019,“Energy in buildings”, section 2.4.1,available online at <https://www.open.edu/openlearn/nature-environment/energy-buildings/content-section-2.4.1>
- [5] M. Barozzi, J. Lienhard, A. Zanelli, and C. Monticelli, “The Sustainability of Adaptive Envelopes: Developments of Kinetic Architecture,” *Procedia Engineering*, vol. 155, pp. 275–284, Jan. 2016, doi: 10.1016/J.PROENG.2016.08.029.
- [6] IEA,2021 ,“Perspectives for the Clean Energy Transition” available online at <https://www.iea.org/reports/the-critical-role-of-buildings>, International Energy Agency
- [7] M. Santamouris and K. Vasilakopoulou, “Present and future energy consumption of buildings: Challenges and opportunities towards decarbonisation,” *e-Prime - Advances in Electrical Engineering, Electronics and Energy*, vol. 1, p. 100002, Jan. 2021, doi: 10.1016/J.PRIME.2021.100002.
- [8] United Nations,1992 “UNITED NATIONS FRAMEWORK CONVENTION ON CLIMATE CHANGE UNITED NATIONS”.
- [9] Unite Nations, 1997, “Kyoto protocol to the United Nations framework convention on climate change”
- [10] UNFCCC,2015,“The Paris Agreement” available online at <https://unfccc.int/process-and-meetings/the-paris-agreement/the-paris-agreement> , United Nations Framework Convention on Climate Change
- [11] European Parliament and of the Council,2010,““Directive 2010/31/EU of the European Parliament and of the Council of 19 May 2010 on the energy performance of buildings”.

- [12] European Parliament ,Directive 2012/27/EU amended in 2018 “Energy efficiency directive” available online at https://energy.ec.europa.eu/topics/energy-efficiency/energy-efficiency-targets-directive-and-rules/energy-efficiency-directive_en
- [13] Ireland government, “Project Ireland 2040” available online at <https://www.gov.ie/en/campaigns/09022006-project-ireland-2040/>.
- [14] Metabuilding,2020,“innovation Funding and Support for SMEs of the Built Environment Sector” available online at <http://www.metabuilding-project.eu/>
- [15] IEA,2021, “Tracking Buildings” available online at <https://www.iea.org/topics/buildings>
- [16] L. G. Swan and V. I. Ugursal, “Modeling of end-use energy consumption in the residential sector: A review of modeling techniques,” *Renewable and Sustainable Energy Reviews*, vol. 13, no. 8, pp. 1819–1835, Oct. 2009, doi: 10.1016/J.RSER.2008.09.033.
- [17] T. Hong, Y. Chen, X. Luo, N. Luo, and S. H. Lee, “Ten questions on urban building energy modeling,” *Building and Environment*, vol. 168, p. 106508, Jan. 2020, doi: 10.1016/J.BUILDENV.2019.106508.
- [18] L. G. Swan and V. I. Ugursal, “Modeling of end-use energy consumption in the residential sector: A review of modeling techniques,” *Renewable and Sustainable Energy Reviews*, vol. 13, no. 8, pp. 1819–1835, Oct. 2009, doi: 10.1016/J.RSER.2008.09.033.
- [19] C. Deb and A. Schlueter, “Review of data-driven energy modelling techniques for building retrofit,” *Renewable and Sustainable Energy Reviews*, vol. 144, p. 110990, Jul. 2021, doi: 10.1016/J.RSER.2021.110990.
- [20] Usman Ali, Mohammad Haris Shamsi, Cathal Hoare, Eleni Mangina, James O’Donnell,“Review of urban building energy modeling (UBEM) approaches, methods and tools using qualitative and quantitative analysis,Energy and Buildings, Volume 246,2021,111073,ISSN 0378-7788,<https://doi.org/10.1016/j.enbuild.2021.111073>
- [21] U.S. Department of energy, “About Building Energy Modeling”, available online at <https://www.energy.gov/eere/buildings/about-building-energy-modeling>
- [22] Y. Chen, M. Guo, Z. Chen, Z. Chen, and Y. Ji, “Physical energy and data-driven models in building energy prediction: A review,” *Energy Reports*, vol. 8, pp. 2656–2671, Nov. 2022, doi: 10.1016/J.EGYR.2022.01.162.
- [23] A. Fouquier, S. Robert, F. Suard, L. Stéphan, and A. Jay, “State of the art in building modelling and energy performances prediction: A review,” *Renewable and Sustainable Energy Reviews*, vol. 23, pp. 272–288, Jul. 2013, doi: 10.1016/J.RSER.2013.03.004.

- [24] C. Boje, A. Guerriero, S. Kubicki, and Y. Rezgui, "Towards a semantic Construction Digital Twin: Directions for future research," *Automation in Construction*, vol. 114, p. 103179, Jun. 2020, doi: 10.1016/J.AUTCON.2020.103179.
- [25] F. Johari, G. Peronato, P. Sadeghian, X. Zhao, and J. WidEn, "Urban building energy modeling: State of the art and future prospects," *Renewable and Sustainable Energy Reviews*, vol. 128, p. 109902, 2020, doi: 10.1016/j.rser.2020.109902.
- [26] U. Ali, M. H. Shamsi, C. Hoare, E. Mangina, and J. O'Donnell, "A data-driven approach for multi-scale building archetypes development," *Energy and Buildings*, vol. 202, p. 109364, Nov. 2019, doi: 10.1016/J.ENBUILD.2019.109364.
- [27] B. Dong, Z. O'Neill, D. Luo, and T. Bailey, "Development and calibration of an online energy model for campus buildings," *Energy and Buildings*, vol. 76, pp. 316–327, Jun. 2014, doi: 10.1016/J.ENBUILD.2014.02.064.
- [28] T. Berthou, P. Stabat, R. Salvazet, and D. Marchio, "Development and validation of a gray box model to predict thermal behavior of occupied office buildings," *Energy and Buildings*, vol. 74, pp. 91–100, May 2014, doi: 10.1016/J.ENBUILD.2014.01.038.
- [29] H. Fu, J. C. Baltazar, and D. E. Claridge, "Review of developments in whole-building statistical energy consumption models for commercial buildings," *Renewable and Sustainable Energy Reviews*, vol. 147, p. 111248, Sep. 2021, doi: 10.1016/J.RSER.2021.111248.
- [30] M. Musy, F. Winkelmann, E. Wurtz, and A. Sergent, "Automatically generated zonal models for building air row simulation: principles and applications," *Building and Environment*, vol. 37, pp. 873–881, 2002, Accessed: May 03, 2022. [Online]. Available online at www.elsevier.com/locate/buildenv
- [31] S. F. Fux, A. Ashouri, M. J. Benz, and L. Guzzella, "EKF based self-adaptive thermal model for a passive house," *Energy and Buildings*, vol. 68, no. PART C, pp. 811–817, Jan. 2014, doi: 10.1016/J.ENBUILD.2012.06.016.
- [32] T. Wüest, P. Schuetz, and A. Luible, "Outdoor Test Cell Modelling with Modelica," *Buildings* 2019, Vol. 9, Page 209, vol. 9, no. 10, p. 209, Sep. 2019, doi: 10.3390/BUILDINGS9100209.
- [33] S. Goyal and P. Barooah, "A method for model-reduction of non-linear thermal dynamics of multi-zone buildings," *Energy and Buildings*, vol. 47, pp. 332–340, Apr. 2012, doi: 10.1016/J.ENBUILD.2011.12.005.
- [34] R. Bruno, G. Pizzuti, and N. Arcuri, "The Prediction of Thermal Loads in Building by Means of the EN ISO 13790 Dynamic Model: A Comparison with TRNSYS," *Energy Procedia*, vol. 101, pp. 192–199, Nov. 2016, doi: 10.1016/J.EGYPRO.2016.11.025.

- [35] N. M. Mateus, A. Pinto, and G. C. da Graça, "Validation of EnergyPlus thermal simulation of a double skin naturally and mechanically ventilated test cell," *Energy and Buildings*, vol. 75, pp. 511–522, Jun. 2014, doi: 10.1016/J.ENBUILD.2014.02.043.
- [36] M. D. Murphy, P. D. O'sullivan, G. Carrilho Da Graça, and A. O'donovan, "Development, Calibration and Validation of an Internal Air Temperature Model for a Naturally Ventilated Nearly Zero Energy Building: Comparison of Model Types and Calibration Methods," 2021, doi: 10.3390/en14040871.
- [37] D. Tuhus-Dubrow and M. Krarti, "Genetic-algorithm based approach to optimize building envelope design for residential buildings," *Building and Environment*, vol. 45, no. 7, pp. 1574–1581, Jul. 2010, doi: 10.1016/J.BUILDENV.2010.01.005.
- [38] O. T. Ogunsola and L. Song, "Application of a simplified thermal network model for real-time thermal load estimation," *Energy and Buildings*, vol. 96, pp. 309–318, Jun. 2015, doi: 10.1016/J.ENBUILD.2015.03.044.
- [39] O. Mejri, E. Palomo Del Barrio, and N. Ghrab-Morcos, "Energy performance assessment of occupied buildings using model identification techniques," *Energy and Buildings*, vol. 43, no. 2–3, pp. 285–299, Feb. 2011, doi: 10.1016/J.ENBUILD.2010.09.010.
- [40] Y. Li, Z. O'Neill, L. Zhang, J. Chen, P. Im, and J. DeGraw, "Grey-box modeling and application for building energy simulations - A critical review," *Renewable and Sustainable Energy Reviews*, vol. 146, Aug. 2021, doi: 10.1016/J.RSER.2021.111174.
- [41] L. Vanfretti et al., "RaPid: A modular and extensible toolbox for parameter estimation of Modelica and FMI compliant models," *SoftwareX*, vol. 5, pp. 144–149, Jan. 2016, doi: 10.1016/J.SOFTX.2016.07.004.
- [42] Python,2022, *Python programming language*, available online at <https://www.python.org/>
- [43] K. Arendt, M. Jradi, M. Wetter, and C. T. Veje, "ModestPy: An Open-Source Python Tool for Parameter Estimation in Functional Mock-up Units," *Proceedings of The American Modelica Conference 2018, October 9-10, Somberg Conference Center, Cambridge MA, USA*, vol. 154, pp. 121–130, Feb. 2019, doi: 10.3384/ECP18154121.
- [44] M. H. Shamsi, U. Ali, E. Mangina, and J. O'Donnell, "Feature assessment frameworks to evaluate reduced-order grey-box building energy models," *Applied Energy*, vol. 298, p. 117174, Sep. 2021, doi: 10.1016/J.APENERGY.2021.117174.
- [45] Matlab,2022,"What Is MATLAB? - MATLAB & Simulink",available online at <https://uk.mathworks.com/discovery/what-is-matlab.html>
- [46] Modelica Association,2022,"Modelica Language" available online at <https://modelica.org/modelicalanguage.html>

- [47] A. Piccinini, M. Hajdukiewicz, and M. M. Keane, "A novel reduced order model technology framework to support the estimation of the energy savings in building retrofits," *Energy and Buildings*, vol. 244, Aug. 2021, doi: 10.1016/J.ENBUILD.2021.110896.
- [48] Y. Li, Z. O'Neill, L. Zhang, J. Chen, P. Im, and J. DeGraw, "Grey-box modeling and application for building energy simulations - A critical review," *Renewable and Sustainable Energy Reviews*, vol. 146, p. 111174, Aug. 2021, doi: 10.1016/J.RSER.2021.111174.
- [49] D. W. U. Perera, D. Winkler, and N. O. Skeie, "Multi-floor building heating models in MATLAB and Modelica environments," *Applied Energy*, vol. 171, pp. 46–57, Jun. 2016, doi: 10.1016/J.APENERGY.2016.02.143.
- [50] R. Sterling et al., "A virtual test-bed for building Model Predictive Control developments," *Proceedings of the 13th International Modelica Conference, Regensburg, Germany, March 4–6, 2019*, vol. 157, pp. 17–24, Feb. 2019, doi: 10.3384/ECP1915717.
- [51] F. Bellalouna, "Case study for design optimization using the digital twin approach," *Procedia CIRP*, vol. 100, pp. 595–600, Jan. 2021, doi: 10.1016/J.PROCIR.2021.05.129.
- [52] F. Bellalouna, "Case study for design optimization using the digital twin approach," *Procedia CIRP*, vol. 100, pp. 595–600, Jan. 2021, doi: 10.1016/J.PROCIR.2021.05.129.
- [53] M. Zhang, F. Sui, A. Liu, F. Tao, and A. Y. C. Nee, "Digital twin driven smart product design framework," *Digital Twin Driven Smart Design*, pp. 3–32, Jan. 2020, doi: 10.1016/B978-0-12-818918-4.00001-4.
- [54] H. Zhang, Q. Liu, X. Chen, D. Zhang, and J. Leng, "A Digital Twin-Based Approach for Designing and Multi-Objective Optimization of Hollow Glass Production Line," *IEEE Access*, vol. 5, pp. 26901–26911, Oct. 2017, doi: 10.1109/ACCESS.2017.2766453.
- [55] F. Jiang, L. Ma, T. Broyd, and K. Chen, "Digital twin and its implementations in the civil engineering sector," *Automation in Construction*, vol. 130, p. 103838, Oct. 2021, doi: 10.1016/J.AUTCON.2021.103838.
- [56] C. Vite and R. Morbiducci, "Optimizing the Sustainable Aspects of the Design Process through Building Information Modeling," *Sustainability 2021*, Vol. 13, Page 3041, vol. 13, no. 6, p. 3041, Mar. 2021, doi: 10.3390/SU13063041.
- [57] G. Chaudhary, J. New, J. Sanyal, P. Im, Z. O'Neill, and V. Garg, "Evaluation of 'Autotune' calibration against manual calibration of building energy models," *Applied Energy*, vol. 182, pp. 115–134, Nov. 2016, doi: 10.1016/J.APENERGY.2016.08.073.
- [58] D. Coakley, P. Raftery, and M. Keane, "A review of methods to match building energy simulation models to measured data," *Renewable and Sustainable Energy Reviews*, vol. 37, pp. 123–141, Sep. 2014, doi: 10.1016/J.RSER.2014.05.007.

- [59] P. Bacher and H. Madsen, "Identifying suitable models for the heat dynamics of buildings," *Energy and Buildings*, vol. 43, no. 7, pp. 1511–1522, Jul. 2011, doi: 10.1016/J.ENBUILD.2011.02.005.
- [60] A. Giretti, M. Vaccarini, M. Casals, M. Macarulla, A. Fuertes, and R. v. Jones, "Reduced-order modeling for energy performance contracting," *Energy and Buildings*, vol. 167, pp. 216–230, May 2018, doi: 10.1016/J.ENBUILD.2018.02.049.
- [61] A. Piccinini et al., "Development of a reduced order model for standard-based measurement and verification to support ECM," *Building Simulation Conference Proceedings*, vol. 6, pp. 4180–4187, 2019, doi: 10.26868/25222708.2019.210482.
- [62] Nobatek, website, "Accueil NOBATEK/INEF4", available online at <https://www.nobatek.inef4.com>.
- [63] Weather, "EnergyPlus", available online at <https://energyplus.net/weather>
- [64] EN ISO, 2017, "EN ISO 6946:2017"
- [65] EN ISO, 2018, "UNI EN ISO 10077-1:2018"
- [66] EN ISO, 2018, "EN ISO 52022-1:2018"
- [67] MathWorks, "MathWorks - MATLAB & Simulink", available online at <https://uk.mathworks.com/products/matlab.html>